Fusion Proteins as Selective Inducers of Constitutive Activity and Tools to Discriminate the Biased Signaling Profile of β_2 Adrenoceptor Ligands

By
Emilio Yaroslav Lucero García Rojas

A dissertation submitted to the Department of Pharmacological and Pharmaceutical Sciences,
College of Pharmacy.

in partial fulfillment of the requirements for the degree of

Doctor of Philosophy

in Pharmacology

Chair of Committee: Richard A. Bond

Co-Chair of Committee: Bradley K. McConnell

Committee Member: Kehe Ruan

Committee Member: Brian Knoll

Committee Member: Richard Dixon

Committee Member: Yu Liu

University of Houston
December 2021

Dedication

In loving memory of Raul Alejandro Lucero Aviña.

- Perception and vitality fade but the wisdom and genes remain -

Acknowledgments

I believe that only a couple of sentences to thank the people that have helped and supported me on my doctoral journey is not enough to show my infinite appreciation for their intentional or unintentional actions. Nevertheless, I am confident that my succinct and honest words will remind them how much I value them.

I am very grateful for having Richard Bond as a mentor and as a friend. He has radically affected my scientific and philosophical perspective about life. I will always cherish our fruitful discussions and in-depth conversations about this plane of existence.

I also want to thank Bradley McConnell. His mentoring, based on empathy, optimism, modesty, and sincere engagement, has had an anxiolytic effect on me and has constantly reminded me that even during hard times, there is another day to shine.

My gratitude also goes to all my committee members for their intellectual support and constructive critiques to develop my project.

I am forever grateful to my beloved Tasha Womack, for her constant emotional support and for slowly sharing her humanity with me. Her kindness and sensitivity have been like a warm and protective hug in the middle of a cold and ruthless blizzard.

Of course, this would not have been possible without my dearest ‘moma’ Marcela Julieta Garcia Rojas de Lucero (she loves to have her full name on paper). She has always been a source of ‘unconditional’ love and inspiration on the realm of persistence, tolerance, and justice.

Many thanks to my lab mates, particularly to Hanan Qasim and Aram Reyes. Your friendship, although ignited by mere chance (what are the odds?), liberated me from the burden of isolation and loneliness I was experiencing in the research environment. Thanks again for making research even more enjoyable.

I also feel very grateful to all my friends, especially Luis Menez, Cleva Villanueva, Pavel Govyadinov, Jordan Gonzalez, Eric Meindl, Dylan Walther, Anton Fatin, Chadi Cherradi, and the bohemian group ‘the warriors’. Thank you for sharing some of your time with me. It makes my life more nuanced, exciting, and entertaining.

I also want to show my appreciation to my brothers Bruno, Orlando, and Raul. Despite our inefficient verbal communication, ‘the call of blood’ makes me feel fortunate to have you “around”.

Abstract

The β_2AR is the prototypical G protein coupled receptor (GPCR) known to orchestrate different cellular responses by the stimulation of specific signaling pathways. The best-established signaling pathways for the β_2AR are the canonical Gs pathway and the alternative β arrestin 2 (βarr2) pathway. Exploring each pathway separately remains a challenging task due to the dynamic nature of the receptor. Here, we fused the β_2AR with its cognate transducers, Gαs and βarr2, using short linkers as a novel approach for restricting the conformation of the receptor and preferentially activating one of its two signaling pathways. We characterized the behavior of our fusion proteins β_2AR-Gαs and β_2AR-βarr2 in HEK293 cells by measuring their constitutive activity, transducer recruitment, and pharmacologic modulation. Our fusion proteins show (a) steric hindrance from the reciprocal endogenous transducers, (b) constitutive activity of the β_2AR for the signaling pathway activated by the tethered transducer, and (c) pharmacologic modulation by β_2AR ligands. Since both fusion proteins remained functional to ligand stimuli, we quantified the pharmacological properties of affinity, efficacy, and potency for cAMP accumulation and ERK1/2 phosphorylation as surrogates of the Gs and βarr2 pathways, respectively, in selected β_2AR ligands. Using these pharmacological parameters, we developed a mathematical method for direct ligand bias quantification based on the well-known transduction coefficient ratios formula ($\Delta\Delta \log(\tau/K_A)$). Our method has the advantage of quantifying an 'absolute' value of signaling bias for any ligand that shows negative or positive efficacy at any signaling pathway. The term absolute is used here to highlight that a reference ligand is not required in our method as each ligand becomes its own

reference. Regarding the isolated constitutive activity observed for each fusion protein, we used this feature to induce a gain-of-function mechanism in the human lung non-tumorigenic epithelial cell line, BEAS-2B cells. This immortalized human bronchial epithelial cell line has immunomodulatory properties through cytokine release mediated by β_2AR stimulation. Our findings suggest that each signaling pathway of the β_2AR is biased towards either the Th1 or Th2 inflammatory response regulating the immune phenotype of respiratory diseases. Our data implies our fusion proteins can be used as tools to isolate the function elicited by a unique signaling pathway in physiologically relevant cell types.

Table of Contents

List of Tables

List of Figures

List of Abbreviations

GPCR	G protein coupled receptors
7TMR	7 transmembrane domain receptors
β_2AR	beta 2 adrenergic receptor
βarr2	β-arrestin 2
Gαs	Alpha subunit of protein Gs
HEK	Human embryonic kidney
BEAS	Bronchial epithelial cells
ICL/ECL	Intra/extracellular loop
TMD	Transmembrane domains
K_A	Equilibrium association constant/ Functional affinity
K_D	Equilibrium dissociation constant
IC/EC_{50}	Inhibitory/effective concentration 50
pA_2	Apparent Affinity
Emax	Maximal Response
cAMP	Cyclic adenosine monophosphate
GDP	Guanosine diphosphate
GTP	Guanosine triphosphate
PKA	Protein Kinase A
EPAC	Exchange proteins directly activated by cAMP
POPDC	Popeye domain containing
GRKs	G protein-coupled receptor kinases
ERK1/2	Extracellular signal-regulated kinase 1 and 2
MAPK	Mitogen-activated protein kinases
USP33	Ubiquitin-specific protease 33
HF	Heart Failure
LV	Left ventricle
hiPSC-CMs	Human induced pluripotent stem cell-derived cardiomyocytes

CaMKII	Calcium calmodulin-dependent kinase II
MLP	muscle LIM protein
IKr	Delayed rectifier potassium current
PNMT	Phenylethanolamine N-methyltransferase
PDE	Phosphodiesterase
DMEM	Dulbecco’s Modified Eagles Medium
DPBS	Dulbecco’s phosphate buffer saline
FBS	fetal bovine serum
[3H] DHA	Dihydroalprenolol Hydrochloride, Levo-[Ring, Propyl-3H(N)]-
Nluc	Nano Luciferase
RT-PCR	Reverse transcriptase polymerase chain reaction
STR	short tandem repeat
IBMX	3-isobutyl-1-methylxanthine
HTRF	Homogeneous Time-Resolved Fluorescence
IL-	Interleukin-
IFN	Interferon
TNFα	Tumor necrosis factor Alpha
pKi	Negative logarithm of the observed affinity (radioligand affinity)
ISO	Isoproterenol
EPI	Epinephrine
SALB	Salbutamol
INDA	Indacaterol
AgGs	Novel Gs biased agonist
NAD	Nadolol
CARV	Carvedilol
PROP	Propranolol
METO	Metoprolol
ALPR	Alprenolol

ICI	ICI 118,551
pERK	Phosphorylated ERK
tERK	Total ERK
GM-CSF	Granulocyte-macrophage colony-stimulating factor

UHGS V1:1 06201

I. Introduction

The most abundant family of proteins expressed on the plasma membrane of mammalian cells are G protein coupled receptors (GPCRs), also known as 7 transmembrane domain receptors (7TMR). GPCRs are comprised of more than 800 different types of receptors that mediate sensory (i.e., olfaction, light perception, and pheromone signaling) and non-sensory functions (i.e., neurotransmission, endocrine regulation, tissue remodeling, and immune response) (Alexander et al., 2019). Because of their relevance in (patho)physiological states in mammals, the activity of GPCRs has been pharmacologically manipulated as a therapeutic strategy to treat multiple diseases. In fact, one-third of the drugs currently available on the market target multiple GPCRs and represent about 27% of the global revenue obtained by therapeutic drugs (Hauser et al., 2017).

With the advent of genetic manipulation, together with the technological advancements in biophysics (i.e., X-ray crystallography, bioluminescence and fluorescence energy transfer, double electron-electron resonance, among others), a new revolution in the understanding of GPCRs has emerged. Mounting evidence shows GPCRs as structurally dynamic scaffolds that provide the conformational basis to recruit multiple transducers for specific cellular responses. In other words, the myriad of cellular responses elicited by the stimulation of a single GPCR is determined by the structural conformation of the receptor. This dynamic plasticity can be manipulated by several factors such as ligands (Kenakin & Strachan, 2018), receptor density (Fathy et al., 1999), mechanical stretch (Zou et al., 2004), pH (Ghanouni et al., 2000), membrane composition (Strohman et al., 2019), stoichiometry/coupling efficiency (Ostrom et al., 2001; Watson et al., 2000), among others. Thus, GPCRs behave as biological microprocessors that integrate all such inputs to induce a unique cellular response.

The versatility of GPCRs in inducing multiple and distinctive cellular responses has been explored, primarily, by using ligands that preferentially stabilize a conformational state of the receptor. This unique conformation, in turn, favors a particular downstream signaling pathway to induce a cellular response. This

phenomenon, known as biased signaling, is always compared to a reference ligand, which, by consensus, induces a 'balanced' activation of the signaling pathways pertained to the receptor. Here, the term 'balanced' is used to denote the ability of the reference ligand to strongly activate both signaling pathways regardless of the magnitude of both responses. The phenomenon of biased signaling has the potential of increasing the benefits of drug therapy by targeting the beneficial signaling pathway of a receptor while reducing the side effects elicited by an alternative pathway.

Most of the current understanding of the structure and pharmacological behavior, including the phenomenon of biased signaling, of the GPCR superfamily has come from studying the prototypical beta 2 adrenergic receptor (β_2AR), a member of the rhodopsin subfamily (Class A). This receptor is present in all mammalian cells and is stimulated by the endogenous ligand epinephrine, a hormone released by the chromaffin cells of the adrenal gland and by adrenergic neurons in the central nervous system. At least two major signaling pathways have been described after β_2AR stimulation; the canonical pathway mediated by the transducer Gs protein, and the alternative pathway mediated by the transducer β-arrestin 2 (βarr2), also known as arrestin 3 (Rosenbaum et al., 2009). Each signaling pathway has proved critical for the development of multiple diseases such as heart failure and asthma. Moreover, current pharmacological treatments targeting the β_2AR can have increased side effects by the concurrent activation of the detrimental signaling pathway. This is the case of salbutamol, a selective β_2AR agonist for asthma treatment that activates both signaling pathways. Long-term treatment with either salbutamol or salmeterol has been associated with a reduction in life quality and increased mortality in patients with asthma (Hasford & Virchow, 2006; Nelson et al., 2006). Thus, the isolation of each signaling pathway for the β_2AR can reveal the pathophysiological mechanisms involved in such diseases. Moreover, the development of biased ligands that preferentially stabilize an active conformational state of the β_2AR could be used to improve the current pharmacological treatment of multiple diseases. However, the dynamic nature of the β_2AR structure is a major impediment to stabilizing the active conformations of β_2AR and isolating both signaling pathways. To tackle this problem, we created novel fusion proteins between the β_2AR and the alpha subunit of protein Gs (Gαs) [described as β_2AR-Gαs], or the

β_2AR and βarr2 [described as β_2AR-βarr2]. These chimeric proteins were then transfected into HEK 293 cells; a widely used cell line for the pharmacological characterization of GPCRs. Key features of both chimeras are their constitutive activity for their respective signaling pathway, and they show hindrance for the recruitment of other endogenous transducers. Further pharmacological characterization of the fusion proteins β_2AR-Gαs and β_2AR-βarr2 was performed to understand the conformational selection of clinically used, and newly developed β_2AR ligands. The obtained pharmacologic parameters of affinity, efficacy, and potency were then adapted to fit the transduction coefficient quantification method for biased signaling (Kenakin et al., 2012). This new mathematical approach allowed us to determine the 'absolute' bias of the β_2AR ligands tested without the need for a reference ligand, which potentially represents another source of bias. Finally, the functionality of the chimeric proteins β_2AR-Gαs and β_2AR-βarr2 to isolate both signaling pathways was tested on the immortalized human bronchial epithelial cell line BEAS-2B. This cell line preserves the immunomodulatory function that actively regulates the inflammatory response observed in respiratory diseases (Atsuta et al., 1997). Such modulation of the inflammatory response appears to be mediated by the stimulation of the β_2AR. Therefore, each signaling pathway of the β_2AR was tested using our chimeric proteins to dissect the pro- and anti-inflammatory responses of BEAS-2B cells.

Under the scope of this work, a comprehensive theoretical framework is first presented to the reader for a better understanding of the methodology used, as well as the analysis and discussion of the results. Overall, the data gathered from experiments on the β_2AR-Gαs and β_2AR-βarr2 chimeras show a solid groundwork for their utility as tools to isolate the main signaling pathways of the β_2AR.

II. Structure of the β_2AR

The β_2AR was the first hormone receptor to be cloned (Dixon et al., 1986). The high amino acid homology between the previously sequenced bovine photoreceptor rhodopsin (Hargrave et al., 1983) and the β_2AR suggested that both structures belonged to the same superfamily of receptors (Dixon et al., 1987). Since then, multiple crystal structures of GPCRs have been solved, including rhodopsin (Palczewski et al., 2000) and the β_2AR (Cherezov et al., 2007; Rasmussen et al., 2007), showing beyond doubt the close structural resemblance among all GPCRs.

The β_2AR is composed of 413 amino acids coded by the *ADRB2* gene. Due to the lack of introns on the DNA sequence of the *ADRB2*, the β_2AR does not have any isoforms. The secondary structure of the β_2AR begins with an extracellular amino-terminal (N-terminal) domain followed by 7 transmembrane α-helixes comprised of 20-30 amino acids each. The α-helixes are connected in a continuous amino acid chain by 3 intracellular (ICL) and 3 extracellular loops (ECL). The receptor ends on the intracellular side forming an amphipathic helix (helix 8) followed by a long intracellular carboxy-terminal (C-terminal) tail. The tertiary structure of the receptor folds to form a bundle between all 7 transmembrane domains (TMDs) and create a hydrophobic pocket. This pocket is where the endogenous ligand adrenaline binds and, thus, represents the orthosteric binding site of the receptor (Ring et al., 2013). Other regions distinct from the binding pocket of the receptor, known as allosteric binding sites, have also been described for the binding of allosteric molecules at the extracellular region of the TMDs 3 and 5 (Liu et al., 2020), the N-terminal (Virion et al., 2019), the TMDs 1, 2, 3 and 4 (Hanson et al., 2008), and at a cytoplasmic pocket formed by the intracellular region of the TMDs 1, 2, 6 and 7 in combination with the ICL 1 and helix 8 (Liu et al., 2017). Moreover, bitopic ligands, known to bind simultaneously to the orthosteric and an allosteric site, have also been identified for the β_2AR as it is the case of the partial agonist salmeterol (Masureel et al., 2018). In all cases, the receptor-ligand interaction results in the formation of intermolecular (non-covalent) or intramolecular (covalent) forces that induce subtle local conformational changes. These small changes, in turn,

lead to larger structural rearrangements that ultimately affect the biological activity of the receptor.

Insights on the Role of Motifs in Receptor Conformation.

Across the TMDs of class A GPCRs, multiple highly conserved amino acid sequences, also known as motifs, directly impact the activation and signaling of the receptor, and thus, their relevance will be addressed for the β_2AR. The NPxxY motif (N322$^{7.49}$, P323$^{7.50}$, and Y326$^{7.53}$ [residues are labeled according to the Ballesteros-Weinstein numbers]) present at the TMD 7 forms hydrogen bonds between Y326$^{7.53}$ and the conserved Y219$^{5.58}$ in TMD 5 through water molecules under orthosteric ligand-receptor interaction (Venkatakrishnan et al., 2016). This chemical interaction has been regarded as the 'activation or tyrosine toggle switch' since mutations of such amino acids decrease the affinity and potency of agonists while maintaining the affinity of antagonists (Gabilondo et al., 1996; Ragnarsson et al., 2019). Moreover, mutations on N322$^{7.49}$ abolish receptor coupling, phosphorylation, and the internalization process whereas P323$^{7.50}$ mutations showed mild deficits in these processes (Barak et al., 1995).

Another highly conserved motif involved in the activation of the β_2AR is DRY (D130$^{3.49}$, R131$^{3.50}$, and Y132$^{3.51}$) at the TMD 3. The network interactions given by R131$^{3.50}$ with D130$^{3.49}$ and E268$^{6.30}$ form an intra- and interhelical salt bridge, respectively, holding together the cytoplasmic ends of the TMDs 3 and 6 and preventing receptor activation (Valentin-Hansen et al., 2012). The interactions of the DRY motif are broken in the agonist-bound receptor (Rasmussen, DeVree, et al., 2011) whereas mutations on the DRY residues produce a constitutively active receptor (Ballesteros et al., 2001; Rasmussen et al., 1999). Therefore, this motif is also referred to as the 'ionic lock switch' since the interactive amino acids 'lock' the receptor in an inactive conformation preventing the receptor from adopting an active conformational state. A deeper analysis on the relevance of the DRY motif in the coupling of the β_2AR with the Gs protein, and the consequent activation of this transducer to start signaling, has been proposed by Rovati and colleagues (Rovati et al., 2017). Following the cubic ternary complex model (see next section), Rovati and colleagues interpreted that the β_2AR can

exist in 2 active states: HRG and HR*G. HRG represents the allosteric coupling between the hormone, the conformationally active receptor, and the transducer; whereas R* refers to the active state of the receptor that induces signaling through G protein activation. This was illustrated by data where the D130N (Ballesteros et al., 2001; Rasmussen et al., 1999) and R131A (Valentin-Hansen et al., 2012) mutations independently showed increased affinity and G protein coupling to the receptor. However, only D130N had enhanced constitutive activity and agonist-induced signaling (Malik et al., 2013), suggesting that the β_2AR can couple to Gs without activating downstream signaling.

An important motif also involved in the conformational changes associated with activation of the β_2AR is the CWxP (C285$^{6.47}$, W286$^{6.48}$, x, P288$^{6.50}$) in the TMD 6. Here, W286$^{6.48}$ interacts with F290$^{6.52}$ to modulate the angle of the TMD 6 at the highly conserved proline kink (P288$^{6.50}$) by bending and outwardly displacing the cytoplasmic end of the TMD 6 upon activation by catecholamines (Shi et al., 2002). This rotamer toggle switch mechanism, however, is not observed when the β_2AR is activated by the partial agonist salbutamol. These findings suggest that the activation mechanism between partial and full agonists induces alternative active conformational states of the β_2AR (Bhattacharya et al., 2008; Swaminath et al., 2005). In molecular dynamics simulations using an F290S β_2AR mutant model, the receptor remains in an active conformation due to a rotameric flip of the W286$^{6.48}$ further suggesting this residue as the key component on the toggle switch (Tandale et al., 2016). This was further corroborated by experimental studies showing changes in the conformational behavior of the W286$^{6.48}$ when either agonists or antagonists/inverse agonists were bound to the receptor. On one hand, agonists induced a conformer of W286$^{6.48}$ that allowed increased polarity and, thus, increased regional solvation. On the other hand, an alternative conformer of W286$^{6.48}$ was observed when antagonists/inverse agonists were bound to the receptor decreasing the polarity of the region (Plazinska et al., 2017). Thus, the changes in the W286$^{6.48}$ conformation can form a cleft upon receptor activation allowing access to water molecules and, therefore, increasing the regional solvation that contributes to the activation mechanism of the receptor.

Finally, the highly conserved residues P211$^{5.50}$, I121$^{3.40}$, and F282$^{6.44}$ (PIF/connector motif) together with Asn318$^{7.45}$ form stable interactions keeping the TMDs 3, 5, 6, and 7 together as in the inactive conformational state of the receptor. Conversely, the interaction of agonists with the S203$^{5.42}$ and S207$^{5.46}$ at the binding pocket favors an active conformation showing an inward displacement of the TMD 5 at P211$^{5.50}$. In turn, the interaction of P211$^{5.50}$ with I121$^{3.40}$ and F282$^{6.44}$ is broken. Consequently, the repositioning of these residues leads to an outward movement of the cytoplasmic end of TMD 6 away from TMD 3 (Dror et al., 2011; Rasmussen, Choi, et al., 2011). Molecular dynamic simulations are consistent with such observations as the I121$^{3.40}$ and F282$^{6.44}$ residues connecting the ligand binding and the G-protein binding sites adopt discrete conformations related to the active and inactive states of the receptor (Dror et al., 2011). Specifically, the interactions of agonists with S203$^{5.42}$ and S207$^{5.46}$ at the binding pocket elicits a reconfiguration of the PIF motif that ends on the inward and outward movements of the TMD 5 and 6, respectively (Rasmussen, Choi, et al., 2011). Therefore, the connector motif links the activation of the signal transduction with the coupling of agonists to the binding pocket. Direct interaction of an allosteric ligand with the PIF motif stabilizes the inactive conformation of the β_2AR, decreasing and increasing the response of agonists and inverse agonists, respectively (Liu et al., 2020).

Of note, other non-conserved residues relevant to the interaction with multiple motifs have also been identified. For example, recent evidence has also shown the residue L124$^{3.43}$ as a linker between the behavior of the PIF and NPxxY motifs that couple ligand binding with signal transduction (Schonegge et al., 2017). A strengthening mutation of this residue with methionine (L124M) had a modest increase on the constitutive activity of the Gs pathway while allowing the weak partial agonists' salbutamol and salmeterol to recruit βarr more efficiently. A weakening mutation with glycine or serine (L124G/S), on the contrary, maximally increased the constitutive activity of the Gs pathway while abrogating the βarr recruitment induced by the full agonist Isoproterenol (Picard et al., 2019). Thus, variations in the network of the L124$^{3.43}$ residue with the PIF and NPxxY motifs are potentially responsible for the signaling bias of receptor-bound agonists.

III. Molecular Dynamics of β_2AR

The ever-changing shape of GPCRs, including the β_2AR, has posed the biggest challenge to understanding the relationship between the structure and function of the receptor. Current technology of molecular dynamic simulations and other biophysical approaches mimicking the physical behavior of the receptor has granted an opportunity for a deeper understanding of the dynamics of the β_2AR. So far, crystallographic studies have shown two well-defined conformational states of the β_2AR: active and inactive (Cherezov et al., 2007; Rasmussen et al., 2007; Rasmussen, DeVree, et al., 2011). Another "partially active" conformation, alternative from the previously resolved active structure, has also been recently resolved (Masureel et al., 2018). These static conformations, however, were possible due to specific ligands and/or antibodies or changes in the flexible structures of the receptor to stabilize the receptor (Cherezov et al., 2007; Eddy et al., 2016; Rosenbaum et al., 2007). Thus, other complementary studies have been necessary to understand the true dynamic nature of the receptor revealing the localized movements between domains in the order of femtoseconds to milliseconds. For example, long-time-scale molecular dynamics simulations have shown intermediate states present in the transition between the inactive and active conformational states of the β_2AR (Dror et al., 2011). Here, a soft coupling mechanism is described between the ligand binding, the G protein binding site, and the connector between them where each region takes multiple conformations. NMR spectroscopy studies are consistent with the flexibility of the link between the ligand binding and G protein binding sites (Nygaard et al., 2013). This study also shows that full agonists rather destabilize the inactive conformational state, instead of locking a unique active conformation. In fact, the active state of the β_2AR that recruits protein Gs is a relatively unstable high energy state that is not completely stabilized by agonists alone (Whorton et al., 2007). Therefore, is more likely that the ligands bind to the β_2AR when bound to Gs as the complex becomes more stable. This is supported by others showing that agonists cannot shift the conformation of the receptor to a single active state (Ghanouni et al., 2001; Yao et al., 2009). Furthermore, the β_2AR, when crystalized, remains in an active conformation even with a covalent (irreversible) agonist (Rosenbaum et al.,

2011). Therefore, the β_2AR shows heterogeneous populations of structurally different active and inactive conformations some of which can thermodynamically favor G protein recruitment as lower energy is required for such coupling (Nygaard et al., 2013). Even in the absence of a ligand, a small population of the receptor has been detected in the active conformation at equilibrium with a major inactive population (Lerch et al., 2020). Inverse agonism suppressed the active population compatible with a conformational selection model of a ligand for the receptor (Lerch et al., 2020).

To relate the structural plasticity with the functional versatility of the β_2AR, an energy landscape has been proposed to visualize and interpret protein activation (Deupi & Kobilka, 2010). Low energy interactions among domains would form more stable conformations of the receptor and predominate in a basal state. Conversely, other conformations thermodynamically less stable (i.e., higher energy conformations) would be less populated at basal states. The equilibrium between these states would be associated with the conformational entropy (i.e., probability of occupancy) of the β_2AR. Thus, the representation will show multiple 'wells' of energy where each minimum reflects a (meta)stable state of the receptor. The wells are connected by high energy states representing a particular conformational change between stable states. Studies analyzing the ligand-induced changes in conformation and stability show unique energy landscapes with multiple inactive and active states suggesting that each ligand populates the multiple conformations of the β_2AR to a different degree (Isin et al., 2012; Manglik et al., 2015; West et al., 2011). This is further corroborated by nuclear magnetic resonance (NMR) studies showing various ligands selectively shifting the equilibrium to multiple conformational states (Eddy et al., 2016; Liu et al., 2012; Manglik et al., 2015).

Finally, as a summary of the activation mechanism through time, β_2AR agonists interact with the S203$^{5.42}$, S207$^{5.46}$, and N293$^{6.55}$ at the binding pocket generating important polar interactions for the activation process. In contrast, there is only a polar interaction between S203$^{5.42}$ and inverse agonists. The broad polar interaction of agonists results in a 2Å inward movement of TM5 modifying the molecular interactions of the previously mentioned motifs and thus destabilizing the inactive conformation. Destabilization results in a rotation of the TMD 6 inducing a 11Å outward movement of

the cytoplasmic end of TMD 6 and an inward movement of TM3 and TM7 (Kobilka, 2011; Rasmussen, DeVree, et al., 2011). These conformational changes allow the engagement of G proteins with the cytoplasmic core of the receptor. However, the absence of Gs decreases the agonist binding affinity to the β_2AR by 100-fold (Whorton et al., 2007). Thus, the fully active state requires the formation of a ternary complex between the ligand, the receptor, and the G protein.

IV. Receptor theory to understand the behavior of the β_2AR

Over a century ago the idea that a specialized structure within a tissue, called then a 'receptive substance', was responsible for transducing the signal was first conceived by John Langley (Langley, 1905). Together with the seminal observations of Paul Ehrlich in the immunology field whereby a toxin had to bind to a chemoreceptor to work (paraphrasing the Latin phrase: Corpora non agunt nisi fixata), the conceptual framework for the receptor theory was born (Strebhardt & Ullrich, 2008). Since then, the notion of modern pharmacology where a ligand binds to a receptor and changes its activity, displayed as changes in the cellular response, has been thoroughly researched. In pharmacology, the intrinsic properties of a ligand that determine the binding to a receptor and the consequential cellular response have been termed affinity and efficacy, respectively. These two properties are the pillars from which pharmacologists can study the ligand-receptor interactions and define the behavior of GPCRs. Therefore, a description of how these properties have conceptually evolved across time is important to understand the current analytical tools employed in our study of the β_2AR.

Affinity.

In broad and simple terms, affinity refers to the ability of a ligand to bind to a receptor at any moment in time. Chemically, this interaction is fundamentally ruled by the law of mass action. Applied in a pharmacological context, the law states that, at equilibrium, the concentration of free ligand and receptor in a solution is equal to the concentration bound to a receptor. Equilibrium in this case refers to the time point at which the intrinsic motion of a defined concentration of particles (i.e., ligands) no longer alters their free or bound location in probabilistic terms. In other words, the association and dissociation rates of a ligand with respect to a receptor are the same. This was mathematically developed first by the chemist Irving Langmuir in his isotherm equation to quantify the adsorption of chemicals into metal surfaces while working at General Electric (Langmuir, 1918). His mathematical view was consistent with the previously established mathematical model developed by Archibald Hill to quantify the occupancy of hemoglobin by oxygen, also based on the law of mass action (Hill, 1913). Later

applied by A.J. Clark in his occupancy theory, the terms of drug and receptor were included to fit in his pharmacological analysis (Clark, 1926). Taken together, the now known Hill-Langmuir equation for equilibrium binding was the basis for the pharmacological adaptation of the mass action equation. Here, the rate of association (K_1) between a determined concentration of a ligand [A] and a receptor [R] ($K_1[A][R]$) is equal to the rate of dissociation (K_2) between the ligand bound to the receptor [AR] ($K_2[AR]$). Derivation of this equation ($K_1[A][R] = K_2[AR]$) reveals that the ratio between both rates (expressed as $s^{-1}M^{-1}$) results in a factor that defines the ligand's concentration needed to bind to 50% of the available receptors. This factor is named the equilibrium association constant ($K_2/K_1 = K_A$) and is directly proportional to affinity values. The inverse relationship, the equilibrium dissociation constant ($K_D=1/K_A$), is preferred in pharmacology since the numerical notation is more convenient. Thus, the higher the affinity of a ligand for a receptor the lower the K_D value will be. The reduction of these mathematical terms for their adaptation to the mass action equation in pharmacology gives:

$$[AR] = [A][R_T] / [A] + [K_A] \quad (1)$$

where $[R_T]$ refers to the total receptor number as the maximal capacity of a system. Equation 1 defines a rectangular hyperbola on a linear scale. The transformation to a logarithmic scale yields the classic sigmoidal curves observed in dose/concentration-response curves. In fact, this quantitative method was first used by Clark and Gaddum to measure the pharmacological response of multiple drugs in tissues. The conclusions Clark established from such experiments were that the hyperbolic curve observed in his drug-response studies represented the equilibrium between the excess of a ligand reacting with a finite number of receptors (Clark, 1926). Furthermore, he proposed that the occupation of the receptor based on a 1:1 stoichiometry was directly proportional to the observed response. Therefore, if 50% of the receptor was occupied then half of the maximal response would be observed. This proposition was later proven incorrect and was redefined by the experimental work of Ariens, and Stephenson as discussed in the efficacy section.

It is important to note that this model was envisioned for its applicability in chemical reactions and several assumptions were defined to fit such experimental settings. Thus, for this method to be valid in pharmacological settings the following assumptions must be true:

- Accessibility of receptors should be equal to all ligands;
- Binding is reversible;
- Receptor and ligand exist in only two states: free or bound;
- Binding does not affect the conformation of the ligand or receptor.

These stringent assumptions become invalidated when analyzing the complex behavior of GPCRs in multiple physiological systems. Thus, other parameters including efficacy had to be introduced to develop more accurate pharmacological models for the ligand-receptor interaction.

Schild regression analysis.

The previous method used by Clark for affinity measurements was the first tool in quantitative pharmacology for the use of agonists (Clark, 1927). However, this did not apply to antagonists since these ligands don't show any functional response per se (zero efficacy). An alternative approach was therefore used by Gaddum and later applied by Clark, where the proportion of the rightward shift of the dose-response curves of agonists was indicative of the activity of antagonists such that the EC_{50} in the presence of the antagonist / the EC_{50} in the absence of antagonist was labeled dose/concentration ratios; where EC50 is the concentration of agonist producing 50% of its maximal response (discussed below) (Clark & Raventos, 1937; Gaddum, 1937). This concept of competitive antagonism needed the agonist curves to be displaced in parallel (same slope) and had a determined proportion of the shift (e.g., 10-fold) to be independent of the activity of the agonist in a determined system (Gaddum, 1943). This concept was the theoretical framework used later by Heinz Schild to determine a statistical constant for the apparent affinity (pA_2) of antagonists for a receptor (Arunlakshana & Schild, 1959; Schild, 1949). Here, the parameters of dose ratio (dr=[A']/[A]) and the concentration of antagonist [B] are known and, thus, calculation of

the equilibrium dissociation constant of the antagonist (K_B) is possible based on the following equation:

$$dr = 1+[B]/K_B \quad (2)$$

Adapted to Gaddum equation for logarithmic transformation as the mathematical expression of dose-response curves:

$$Log(dr-1) = n \log[B] + \log[K_B] \quad (3)$$

where n represents the slope of the linear regression. Based on this equation a plot of log(dr-1) against pA_X values (Schild plot) with a slope of 1 (n=1) shows an estimate of the apparent affinity, the pA_2 value. Here, pA_x represents the negative logarithm of the antagonist concentration that shifts the agonist concentration curve by an 'x' proportion i.e., pA_2= 2-fold shift. When n=1 and dr=0 (the log of 1), then $pA_2 = \log[B] = \log[K_B]$. Therefore, we can conclude that the antagonist concentration that produces a rightward displacement of the agonistic curve by 2-fold (pA_2) is equal to the concentration of antagonist needed to occupy 50% of the receptors. This method has the following assumptions (Colquhoun, 2007; Neubig et al., 2003):

- The action of the agonist is based on the stimulation of a single receptor type.
- The agonist and antagonist binding to the receptor is competitive (mutually exclusive) and reversible in nature, and produces parallel rightward shifts in the agonist response
- The response is measured at equilibrium (law of mass action can be applied).
- The observed response is associated with the occupancy of the receptor by the agonist.
- The antagonist does not elicit other relevant actions upon interaction with the receptor (conformational changes).

The violation of any of these assumptions makes the interpretation of the antagonist studied invalid. Specifically, a competitive antagonist induces a parallel shift of the agonist concentration-response curve without affecting its maximal response thereby showing independence from the activity of the agonist. Multiple factors can influence the shape of the dose-response curve. For example, some competitive antagonists might

show nonparallel shifts under ‘hemi-equilibrium’ conditions, that is, the timeframe of an antagonist associated with the receptor is long, thus, affecting the steady-state between the agonist, antagonist, and receptor. In practical terms, the antagonist binding becomes irreversible and is observed as a flattening of the dose-response curve (Rang, 1966). Uptake or degradation of the agonist can also affect the shape of dose-response curves by increasing or decreasing the availability of the agonist. Additionally, significant deviations from the value of unity ($n \neq 1$) in the linear regression of the Schild plot also reveal an alternative nature of the antagonist or experimental conditions. For example, slope values smaller than 1 observed as a decrease in potency at increasing concentrations of antagonist might be observed if the receptor is not competitive, additional molecules are part of the drug receptor interaction (allosterism) or equilibrium conditions are not present. Slope values greater than 1 can be indicative of activation of alternative receptors by the agonist, the metabolism or sites of loss for the antagonist, or the antagonist that elicit physiological antagonism. More specific considerations for the validity of the Schild plot for detecting competitive antagonism have been thoroughly reviewed by others (Colquhoun, 2007; Kenakin, 1982).

In summary, the mathematical concept of apparent affinity for competitive antagonism developed by Schild has proved useful up to this day and led to the discovery of numerous therapeutic ligands. His contributions became the basis for drug classification according to their targeted receptor before the development of the radioligand binding technique (Paton & Rang, 1965). Under experimental settings carefully determined to fit the assumptions of the Schild equation, pA_2 values have been consistent with current measurements of radioligand binding assays. Ultimately, the ability to detect the binding of a radioligand to the receptor has become the gold standard for affinity measurements and allowed for the measurement of agonist affinities. This straightforward and simple technique gave researchers equivalent interpretations in the affinity constant values. Additionally, this method is also based on the mass action law and will be thoroughly explained in the methods section.

Efficacy.

The property of a ligand for changing the behavior of the receptor to induce an observable effect is known as efficacy. This property was already implicit in the previously discussed observations of Clark. However, a more direct description was first delineated by Ariens (Ariens, 1954). He described the biological effect of a ligand when bound to a receptor as *intrinsic activity* and defined a scale from 0 to 1 based on such effect; *zero* was assigned to no detectable agonism (antagonists) whereas *one* was assigned to full agonism (the maximal response [Emax] of a system). The ligands showing a response between 0 and 1 were classified as partial agonists. The main limitation of this definition was that the response was subjected to the ability of the tissue to induce a functional response. Therefore, this concept was system-dependent (variable among different tissues) and did not describe the effect as an intrinsic property of the ligand. A couple of years later, Stephenson (Stephenson, 1956) proposed that the affinity of a ligand was not directly proportional to the tissue response as previously assumed by Clark. Instead, the effect observed in tissues was due to another property different from receptor occupancy that he named efficacy. This observation was done by testing multiple agonists with similar potencies but different maximal responses which, to the eyes of Stephenson, represented that the proportion of occupation to induce a response varies per ligand. Importantly, he defined for the first time that the maximum effect could be observed by the occupation of a small portion of the receptors, giving birth to the concept of receptor reserve (spare receptors). Therefore, the response was not linearly related with receptor occupation as first stated by Clark. This concept was revolutionary at the time as it definitively separated the properties of affinity and efficacy of a ligand. However, this proposition remained system-dependent and was later refined by Furchgott (Furchgott, 1966) who introduced the term *intrinsic efficacy* to define a scale reflective of the stimulus degree per receptor. This is represented by the following mathematical expression:

$$\varepsilon = E/R_T \qquad (4)$$

where the E refers to the efficacy defined previously by Stephenson as the stimulus elicited after drug-receptor interaction, and R_T refers to the total receptor number. This

subtle distinction established the concept that Stephenson's efficacy was a response dependent on the number of receptors that couple to signaling components of a system ($E=\varepsilon R_T$). Conversely, intrinsic efficacy represented a parameter related to the ligand-receptor complex alone whereby the effect observed is independent of the sensitivity of the system (the number of receptors needed to induce a cellular response). Furchgott further explored his theory by calculating the relative effects of a tested ligand in comparison to a reference ligand (relative efficacies) under the same system and conditions (Furchgott & Bursztyn, 1967). This approach is known as agonist potency ratios and ultimately makes the dimensionless measurement of efficacy truly independent from the system. This method became a useful tool for the classification of receptors and agonists back then (alternative to the drug classification based on competitive antagonists proposed by Schild). Importantly, the agonist potency ratios are system independent if only one cellular outcome is measured (commonly referred to as a monotonic response).

The concept of efficacy was later extended by the findings of Costa and Hertz (Costa & Herz, 1989) who demonstrated that the activity of the delta opioid receptor could be artificially increased in ligand-free conditions. Additionally, this constitutive activity could be reduced by using some antagonists previously thought to have zero efficacy. Therefore, efficacy became a vectorial parameter as it had shown both a magnitude of response and a direction allowing for values of intrinsic activity below zero. Ligands that show negative efficacy and completely abolish the constitutive activity can be assigned an intrinsic activity of -1 and are known as full inverse agonists, whereas ligands in between -1 and 0 would be partial inverse agonists.

As technology advanced, other assays were able to measure alternative signaling responses that would later reveal a reversal in the rank order of agonist potency ratios when compared to the canonical response (Berg et al., 1998). This suggested that ligands targeting the same receptor have multiple efficacies. Therefore, the ligand-dependent parameter of efficacy went from describing the effect of only one signaling response to becoming a pluridimensional parameter describing the pleiotropic nature of GPCRs (Clarke & Bond, 1998; Galandrin & Bouvier, 2006). Moreover, the

magnitude of the response elicited by the same ligand-receptor interaction could favor one signaling pathway over another. This phenomenon is known as biased signaling (discussed in another section) and has been previously identified under other names including ‘agonist-directed trafficking of receptor stimulus’ (Kenakin, 1995), ‘stimulus trafficking’ (Berg et al., 1998), ‘differential engagement’ (Manning, 2002), ‘signaling bias’ (Gregory et al., 2010), ‘functional dissociation’ (Whistler et al., 1999), ‘discrete activation of transduction’ (Gurwitz et al., 1994) or ‘functional selectivity’ (Urban et al., 2007). These observations of pluridimensional efficacy and biased signaling have become universal for GPCRs and have been clearly shown for ligands targeting the β_2AR (Azzi et al., 2003; van der Westhuizen et al., 2014; Wisler et al., 2007).

In summary, the abstract concept of efficacy as an intrinsic property of ligands has become more complex as we better understand the ability of GPCRs to interact with multiple intracellular transducers. Taking the concepts of affinity and efficacy together, several pharmacological models have been proposed across time to methodically study the ligand-receptor relationship and the resulting cellular response. These evolving concepts have been translated into mathematical expressions to fit the contemporary evidence and elaborate pharmacological models of receptor function. Such models have been useful to predict other features of GPCRs in physiological systems that have not been described experimentally yet. Thus, a brief overview on the evolution of such models will be addressed as heuristic concepts describing the receptor function with a minimum emphasis on the underlying mathematical expressions (an extended mathematical description can be found in (Kenakin, 2017b; Kenakin et al., 2012)).

Pharmacological models of receptor function.

The mass action equation forms the basic building block of the ligand-receptor interaction and is visually represented as (semi)logarithmic concentration-response curves. This response is dependent on the sensitivity of the system measured and is characterized by the potency of a ligand to induce a response; that is, the amount of ligand necessary to induce a given response. The most useful value of potency in mathematical models to describe the activity of a receptor upon ligand binding is the

concentration needed to induce 50% of the maximal response (EC_{50}). Within the concept of potency, the properties of affinity and efficacy of a ligand, as well as the activity of the receptor, represented as conformational shifts, and the efficiency of the system to induce a response, are tightly ingrained. Thus, the simplest representation of the classical model was the first observations of ligand-receptor interaction in the form of potency that was represented as:

$$L + R_i \leftrightharpoons LR_a \quad (5)$$

where the ligand L binds to the inactive receptor R_i reversibly. The onset (lower arrow) and offset (upper arrow) rates would determine the binding of a ligand to a receptor. Under equilibrium conditions, this was expressed as the dissociation constant (K_D). This classical model shows that after ligand binding (LR), the receptor becomes active (R_a) and causes a response. However, this representation assumes the active receptor as a whole tissue and thus becomes system-dependent. Additionally, the ligand only shows the binding property indistinguishable from the activity of the system. Therefore, the model was merely descriptive of the first observations about ligand-receptor interaction.

Two-state model.

Once affinity and efficacy were conceived as separate entities, the mass action equation was set as a series of reactions that described the binding of the ligand to the receptor and a subsequent activation step. This idea was independently introduced by del Castillo and Katz (Del Castillo & Katz, 1957) using a model with an intermediate step regulating the conformational change of a receptor to become activated after ligand binding. Thus, the rate at which the effect was produced was not directly dependent on the affinity of a ligand for the receptor (K_A) but also by the rate at which the inactive receptor changes its conformation to an active state. This was represented as:

$$L + R_i \leftrightharpoons LR_i \leftrightharpoons LR_a \quad (6)$$

This mechanism shows that another equilibrium constant, namely efficacy, determined the receptor activation (simple two-state model). This was consistent with the concept of intrinsic activity where antagonists would shift the equilibrium towards the

LR_i state whereas agonists would shift the equilibrium towards LR_A state. This model was further developed by suggesting that the ligand could independently interact with both states of the receptor (Katz & Thesleff, 1957). This full two-state model can be expressed as:

$$\begin{array}{ccc} L + R_i & \leftrightharpoons & LR_i \\ \updownarrow & & \updownarrow \\ L + R_a & \leftrightharpoons & LR_a \end{array} \qquad (7)$$

Here, the equilibrium between free and ligand-bound receptors depends on the K_A which is multiplied by a factor α, in the case of the active state, which describes a differential affinity between the active and inactive states of the receptor. Thus, if there is a difference in affinity of a ligand for both states of the receptor α must be different from 1 ($\alpha \neq 1$). In such circumstances, the ability of a ligand to preferentially bind to one of the states of the receptor depends on the conformation of the receptor in a process called conformational selection. This implies that, under equilibrium conditions, ligands will shift the equilibrium between the inactive and active states of the receptor based on their affinity preference. Thus, one conformational state of the receptor will be enriched over another based on the le Châtelier's principle. This principle states that alterations of dynamic equilibrium by external conditions will be compensated by counteractive changes to reset the equilibrium. For example, if the ligand prefers the active conformation of the receptor, the occupied active receptors will no longer be part of the equilibrium and other receptors will shift towards the active conformation to compensate for this loss ($\alpha > 1$). If $\alpha < 1$, then there is a preference of the ligand for the inactive state and this conformation will be enriched to reach a new equilibrium.

Ternary Complex Model.

Since this model was proposed based on experiments testing ion channels, the active state referred to the open state whereas the inactive state was the closed state of the channel. Years later, with the discovery of G proteins and their function as interacting molecules with activated receptors for signal transduction, the simple ternary

complex model was proposed (De Lean et al., 1980). This was translated to the simple two-state model for GPCRs as:

$$L + R \leftrightharpoons LR + E \leftrightharpoons LRE \quad (8)$$

where the binding of the effector E to the receptor is responsible for the activation step in this model and is determined by the equilibrium association constant (K_E) between LR and LRE. This constant is the ratio between coupling and uncoupling of the receptor with the effector and manifest ligand efficacy. Considering the full two sate model and the evidence on affinity changes for the same agonist in the presence or absence of guanine nucleotides (Stadel et al., 1980), the full two-state model for GPCR is represented as:

$$\begin{array}{ccc} & E & E \\ & + & + \\ L + R & \leftrightharpoons & LR \\ & \downuparrows & \downuparrows \\ L + RE & \leftrightharpoons & LRE \end{array} \quad (9)$$

This model was soon expanded to accommodate for the constitutive activity observed in GPCRs (Costa & Herz, 1989) shown as:

$$\begin{array}{ccccc} AR & \leftrightharpoons & AR^* & \leftrightharpoons & AR^*E \\ \downuparrows & & \downuparrows & & \downuparrows \\ R & \leftrightharpoons & R^* & \leftrightharpoons & R^*E \end{array} \quad (10)$$

This is known as the extended ternary complex model (Samama et al., 1993). Here, the receptor can exist in an active conformational state (R*) even if the agonist is not bound to the receptor. Therefore, a spontaneous association of the active receptor with the effector will induce a modest response observed as the basal activity in a system. This model accommodates the concept of inverse agonists that preferentially bind to the inactive state shifting the equilibrium towards the inactive conformation of the receptor (R). This way, the reduction of the constitutive activity by a ligand can be explained.

Cubic ternary complex model and beyond.

The previous model did not allow the inactive receptor to interact with an effector and, therefore, was thermodynamically incomplete. In other words, the existence of a ligand, inactive receptor, and effector allows for their collective interaction at a given point even if the interaction implies a high energy requirement. Thus, the cubic ternary model proposed that the inactive receptor can interact with the effector, shown as:

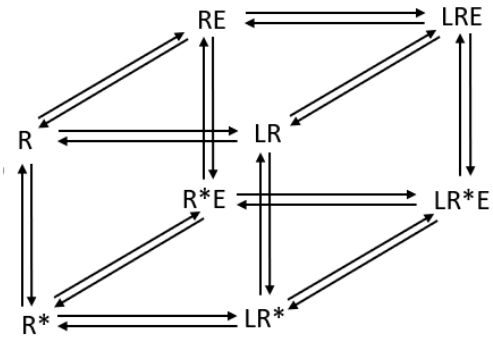

(11)

As a result, eight different receptor species, 4 active and 4 inactive could coexist in a system in statistical terms, although the probability for certain species to exist will be minimal. The interaction between an inactive state with the effector would also allow for inverse agonists to sequester the function of the effector by forming inactive ternary complexes (Weiss et al., 1996). In fact, this has been observed in cannabinoid receptors where the CB1 receptor, upon binding with an inverse agonist, recruits the Gi protein and restricts its downstream signaling (Bouaboula et al., 1997). Because the constants that determine the equilibrium between the multiple receptor species cannot be experimentally quantified, this model is only used to explain mechanistic events in practice. If we also consider the pluridimensional nature of efficacy, then the concept of this model can be expanded proportionately to the number of efficacies detected for each receptor. Thus, for the simplest multi-cubic ternary complex model, the receptor will show 2 active states, R* and R**, that could be represented by connecting or stacking the cubic model of R* with the cubic model of R** using one edge of the cube as the common denominator (perhaps at the inactive state R).

Black and Leff operational model.

The previous models were established under a mathematical foundation to describe the underlying mechanisms of receptor behavior. However, the equations behind these models did not fulfill the description of the allosteric nature of GPCRs in physiological systems. Allostery refers to the ability of a macromolecule (receptor) to interact with ligands (small molecules or proteins) in topographically distinct sites mediated by a conformational change (Christopoulos et al., 2014). Therefore, these models were impractical to predict the response of a ligand in different physiological systems that is fundamental for the development of pharmacological therapies to treat diseases. Additionally, the elusive nature of efficacy does not yield any objective values to determine the power of a ligand towards a physiological function. To address these issues, Black and Leff (Black & Leff, 1983) proposed an operational model considering the ligand-receptor complex as a substrate, the functional response as the product, and the whole-cell as the allosteric machinery responsible for this change. This was conceived under the basis that the law of mass action also applied to the occupancy-effect relationship observed as hyperbolic curves of agonist-concentration effect, E/[A]. The operational model was mathematically expressed as:

$$\text{Response}=[A]\,\tau\,E_{max} / ([A]\,(1+\tau)+KA) \qquad (12)$$

where a factor called 'transducer ratio' (τ) is introduced to represent the efficacy of an agonist in a system. This factor is defined as $[R_T]/K_E$, where K_E is the equilibrium dissociation constant between the concentration of agonist-receptor complexes and the response elements of the cell. In more simplistic terms it can be seen as the equilibrium constant between the substrate and the product. Therefore, τ represents the intrinsic potential of a ligand to induce a response as well as the efficiency of the system to convert the ligand-receptor binding into a cellular response. Since the model represents the intrinsic properties of the ligand to generate an effect, it has been used as a predictor of agonist response in other tissues based on functional measurements of a single tissue. This is because the term τ is independent of the system by incorporating ligand efficacy, receptor density, and system efficiency into a single value. Thus, using τ

ratios between two tissues can predict agonist response based on the ternary complex only while eliminating the influence of receptor concentration and efficiency of the system. The accurate predictability of the operational model has become a powerful tool to characterize agonist responses through GPCRs. Additionally, the model became the basis for quantifying receptor selectivity and signaling bias when measuring two distinct signaling pathways (Kenakin, 2016).

V. Biased Signaling at the β_2AR

Over the past 30 years, data has shown that GPCRs can couple to multiple signaling proteins that in turn activate distinct signaling pathways, thereby allowing for a myriad of cellular responses (Wootten et al., 2018). The use of synthetic small molecules targeting GPCRs has also shown that a given signaling pathway could be preferentially stimulated over other pathways relative to the endogenous hormone or reference ligand, a phenomenon known as biased signaling (Kenakin, 2019). The β_2AR, part of the GPCR superfamily, is no exception showing at least two well-described signaling pathways, protein Gs and β arrestin 2, that can be preferentially activated by synthetic ligands. To understand the signaling mechanisms and develop the concept of biased signaling quantification for the β_2AR, the signaling mechanisms of both pathways will be addressed.

β_2AR signaling.

Upon activation of the β_2AR, the structural changes of the receptor promote the association of the receptor with at least 2 different intracellular transducers: the stimulatory heterotrimeric guanine nucleotide-binding protein (Gs) or β-arrestin 2. The former induces canonical cell responses mediated by the intracellular increase of the second messenger cyclic adenosine monophosphate (cAMP). The latter works as a scaffold protein that determines the fate of the receptor either by internalization and later degradation by proteasomes or lysosomes, or reinsertion into the membrane. During internalization, an alternative signaling function through the activation of other multiple downstream proteins eliciting different cellular responses has also been well characterized (Luttrell et al., 1999; Shenoy et al., 2006). To better understand the molecular mechanisms of activation and signaling a brief description of both transducers is given below.

Gs protein.

The Gs protein, like the other 15 G protein family members, is a heterotrimeric transducer composed of a Gα subunit and a Gβγ subunit dimer. The Gα and γ subunits are tethered to the membrane using lipid anchors formed by the palmitoylation and

prenylation, respectively, of amino acids at their N-terminal domain. This anchorage allows the Gs protein to be near GPCRs at the cell membrane (Higgins & Casey, 1994; Wedegaertner et al., 1993). The Gα subunit has two regions: the Ras-like GTPase domain which interacts with the Gβ subunit and the α-helical domain (Sprang, 1997). The interface of both domains forms a nucleotide-binding pocket allowing stabilization of the Gα subunit under the presence of a nucleotide (Chung et al., 2011; Liu et al., 2019). The GTPase domain hydrolyzes the nucleotide guanosine triphosphate (GTP) into guanosine diphosphate (GDP) while the helical domain buries the GTP at the core of the Gα subunit. At rest (inactive state), the Gs protein remains in its heterotrimeric Gαβγ conformation while bound to a GDP molecule. The stabilization of the β_2AR active conformational state by an agonist triggers the recruitment and coupling of the Gs protein to the receptor. After the β_2AR-Gs complex is formed, GDP is released and the highly concentrated GTP (200-300μM) quickly occupies the nucleotide-binding pocket (McKee et al., 1999). This leads to a conformational change in the Gs protein that dissociates the Gα from the Gβγ subunit and starts the modulation of the activity of multiple cellular effectors by each subunit. The catalytic activity of the GTPase domain at the Gα subunit then hydrolyzes the bound GTP into GDP allowing for reassociation of Gα-GDP and Gβγ subunits terminating the signaling cascade. This process appears to be mediated by the interaction of the receptor with the GTPase domain of the Gαs subunit only (Du et al., 2019; Rasmussen, DeVree, et al., 2011).

The downstream signaling of the Gαs subunit, on one hand, starts with the activation of adenylate cyclase to catalyze the conversion of adenosine triphosphate (ATP) into cAMP. Increasing concentrations of the second messenger cAMP, in turn, classically activate the protein kinase A (PKA) that phosphorylates multiple proteins, including the β_2AR (Benovic et al., 1985), to induce a cellular response. Other proteins such as exchange proteins directly activated by cAMP (Epac) and the popeye domain containing (POPDC) proteins have also been identified as effectors of cAMP and can be explored in detail elsewhere (Robichaux & Cheng, 2018). On the other hand, the dissociated Gβγ subunit activates G protein coupled receptor kinases (GRKs) known to phosphorylate the C-terminal of the GPCRs (Benovic et al., 1986). The C-terminal phosphorylation pattern then triggers the recruitment and coupling of β-arrestins to the

β_2AR while decoupling the Gαs subunit from the receptor (Nobles et al., 2011; Violin et al., 2006).

β-arrestin 2.

First isolated from rat brains (Attramadal et al., 1992), β-arrestin 2 (βarr2), also known as arrestin 3, is one of the two non-visual arrestins. The conserved structure of β-arrestins is constituted by two antiparallel β sheets forming two baskets connected by a hinge domain and a short α-helix at the amino-terminal domain (Sutton et al., 2005; Vishnivetskiy et al., 2002). Other conserved elements critical in the interaction with GPCRs include the uppermost (finger) loop on the hinge domain (Granzin et al., 1998; Zheng et al., 2019) and the polar core that acts as the phosphate sensor that interacts with the phosphorylated C-terminus of GPCRs (Kovoor et al., 1999; Shukla et al., 2013). The overall structure remains in a basal state as a result of the weak hydrogen bond networks at the polar core. These hydrogen bonds are quickly disrupted upon interaction with the active conformation of a GPCR changing the conformational state of β-arrestins (Gurevich & Gurevich, 2004; Kim et al., 2013). Multiple studies have shown different conformations of the βarr2 associated with a change in function indicating a structural basis for the function of this scaffolding protein (Lee et al., 2016; Shukla et al., 2008). Research on the interactions between the activated β_2AR and βarr2 has also shown that phosphorylation of the C-terminal domain of the receptor is not necessary for βarr2 coupling (Eichel et al., 2018; Violin et al., 2006).

The first discovered function of non-visual arrestins was to reduce the G protein-mediated response of GPCRs stimulated for a second time, a phenomenon known as homologous desensitization (Benovic et al., 1986). Therefore, the ad-hoc name at that moment was based on the function of “arresting” the receptor which stopped the binding to the G protein and decreased the signal transduction upon ligand binding (Attramadal et al., 1992; Benovic et al., 1987; Strasser et al., 1986). Later, other functions such as internalization via clathrin coated pits, trafficking, and signaling were observed using the prototypical GPCR, the β_2AR (Azzi et al., 2003; Goodman et al., 1996; Luttrell et al., 1999; Shenoy et al., 2009). Moreover, the strength of the interaction between β-arrestins and GPCRs revealed two major classes of receptors. The class A GPCRs

show transient binding to β-arrestins with increased affinity for βarr2 as is the case for the β_2AR. The class B GPCRs show stable binding and similar affinity for both β-arrestin subtypes (Kohout et al., 2001; Oakley et al., 2001; Oakley et al., 2000). The strength of these interactions determines, at least in part, the specific trafficking and signaling patterns of a receptor. This implies that the transient interaction of the β_2AR with βarr2 allows for rapid recycling to the membrane after desensitization and later interaction with other transducers. Importantly, the active conformation of βarr2 persists after dissociation from the active β_2AR presumably allowing for the activation of alternative signaling cascades (Nuber et al., 2016).

Among the multiple signaling cascades downstream from βarr2, the ERK1/2 signaling pathway has been involved as one of the main effectors of the alternative cellular responses elicited after β_2AR stimulation (Shenoy et al., 2006). The extracellular signal-regulated kinase 1 and 2 (ERK1/2) is one of the three main families of mitogen-activated protein kinases (MAPK). For ERK1/2 to become phosphorylated and therefore active, a sequential phosphorylation cascade needs to occur. The phosphorylation cascade starts with the activation of the MAPKKK, Raf, followed by MEK, and finally ERK1/2. On one hand, the Raf-MEK-ERK1/2 cascade can be rapidly and transiently triggered (5 to 10 mins) by Gαs activation through PKA activity. On the other hand, a slower and long-lasting (>30mins) βarr2-dependent ERK1/2 phosphorylation after β_2AR stimulation has also been observed implying alternative physiological functions (Carr et al., 2016; Shenoy et al., 2006). This is supported by the individual and collective interactions between β-arrestins and the three MAP kinases that allow for localized activation and regulation of the signaling cascade (Bourquard et al., 2015; Coffa et al., 2011; Luttrell et al., 2001; Song et al., 2009). These interactions occur once the βarr2 adopts an active conformational state after coupling with the activated receptor (Lee et al., 2016). Importantly, the phosphorylation of the C-terminal domain of the β_2AR appears to be unnecessary for βarr2 coupling and ERK1/2 signaling (Shenoy et al., 2006).

Overall, the βarr2-dependent ERK1/2 signaling is fundamental for cell survival, migration, growth, and proliferation (Pierce et al., 2001). Other specific functions of

βarr2-dependent ERK1/2 signaling, such as immune regulation and contractility, are dependent on the nature of the tissue observed (Bond et al., 2019). Finally, the regulation of the ERK1/2 signaling is modulated by the ubiquitination status of the βarr2 catalyzed by the ubiquitin E3 ligase Mdm2 (Shenoy et al., 2001). Ubiquitination of βarr2 can also be induced upon interaction with the β_2AR by the ubiquitin E3 ligase, Nedd4 (Nabhan et al., 2010). Ubiquitination then promotes downregulation of the β_2AR by proteosomal degradation (Shenoy et al., 2008). Conversely, deubiquitination of βarr2 by the deubiquitinase, ubiquitin-specific protease 33 (USP33), elicits signal termination and receptor recycling (Shenoy et al., 2009). Taken altogether, βarr2 is a fundamental protein in GPCR-mediated signaling that orchestrates the function and trafficking of the β_2AR. Based on its conformational signature and interactions with other regulatory proteins, βarr2 integrates the conformational changes of the β_2AR by an external stimulus to determine the multiple outcomes of the receptor.

VI. Biased signaling detection and quantification

Classically, the methods to quantify the properties of affinity and efficacy that are unique to the ligand for receptor binding and activation assumed the receptor had a monotonic response. That is, the receptor had only one active state and therefore could only elicit a single response after activation. In this way, the method of potency ratios was effective at measuring the relative activity of a ligand in a system to predict its activity in a different system. If there are multiple responses after receptor stimulation then the relative activity of a ligand becomes dependent on the effect measured in the system, hence, becoming system dependent.

Currently, measurements on the unique chemical properties of a ligand that can predict its biological activity across systems remain the fundamental goal in drug discovery. This is important because the chemical structures of ligands can be manipulated to induce the desired response whereas biological systems are stochastic in nature. This makes the manipulation of biological systems more unpredictable for the desired biological outcome. However, the intrinsic power of a molecule to induce a biological response has no direct measurements. In other words, there are no reliable physical or chemical methods to interrogate the biological activity of a ligand without using a biological system. Thus, we rely on the observable phenomenon of efficacy and affinity to determine the intrinsic properties of ligands to produce a determined biological response. It is now understood that efficacy has a 'polytonic' response and a magnitude that can be measured and exploited to our advantage. The pleiotropic nature of GPCRs (the ability to couple to multiple signaling pathways) has caused pharmacologists to reconsider new quantification methods to detect ligands that preferentially activate the desired signaling pathway (Kenakin, 2011, 2017a; Kenakin & Christopoulos, 2013b). For this to be possible we have used a drug discovery system that relies on *in vitro* and *in vivo* experiments that can potentially be translated into clinical settings. However, the translation of the biological activity of a ligand in *in vitro* and *in vivo* studies into beneficial outcomes in human trials has often proven unsatisfactory (Hauser et al., 2017). This is in part due to the constraints of variability in the experimental conditions as well as in the very complex and dynamic molecular interactions of the human body

(Michel et al., 2014). While these variables can't be manipulated, these factors help the development of mathematical considerations for ligand bias quantification. Therefore, these biases will be first identified to separate such phenomena from the more useful variable of ligand bias that can be effectively manipulated for drug discovery.

Observational bias.

The measurements of the classical semilogarithmic concentration-response curves depend on the bioassay employed to detect the response. The sensitivity to detect the signal is variable among assays and can give the false impression of changing the potency of a ligand. Therefore, the response observed for the same ligand using two different assays to measure alternative signaling pathways would be different. For example, the potency of the full agonist isoproterenol for cAMP is increased by approximately 500-fold when compared to ERK phosphorylation (Galandrin & Bouvier, 2006). This difference does not represent the intrinsic power of isoproterenol to activate a signaling pathway. Instead, this difference reflects the distinct experimental conditions, such as buffers, temperature, pH, the kinetics of the ligand, among others, that are used to observe such response. Thus, the observational bias is not a useful parameter to manipulate the intrinsic properties of ligands to achieve the desired response.

System bias.

The biological component that determines the efficiency of response observed once a ligand activates the receptor varies within and among different systems (i.e., tissues). These differences can be enclosed into two main factors, protein availability and coupling efficiency. Each tissue serves multiple functional purposes to maintain the homeostasis of the whole organism and, in doing so, expresses a specific set of proteins that enable the necessary physiological function. Furthermore, the activity of such proteins is conditional on the interaction with other molecules (i.e., second messengers, proteins, RNA, etc) that are instrumental for the genesis of the biological response. Therefore, pharmacological measurements of a specific biological activity after ligand stimulation will include the protein availability and coupling efficiency for the

activated pathway. Differences in these parameters will translate into changes in potency. Perhaps an extreme example is the manipulation of the components necessary for the generation of cAMP after β_2AR stimulation (Cerione et al., 1983). Here, the progressive addition of, adenylate cyclase, the Gs protein, and the β_2AR induce the observable activity of isoproterenol. This observation can be extended to physiological settings where the cAMP levels to induce contraction (inotropy) in rat atria are higher compared to cardiac relaxation (lusitropy) (Kenakin & Boselli, 1991). Thus, the ligand is again dependent on external variables pertaining to the system and does not reflect the potential of the ligand's molecular structure to induce a response.

There has been a great expansion in new genetic manipulation techniques including in the field of pharmacology. Mutations or differential splicing of receptors have also been used to understand how ligand stimulation and transducer recruitment are affected. This has been termed receptor bias as the change in specific amino acids of the receptor can alter or shift the response to an alternative pathway in this artificial system (Smith et al., 2018). This is of great benefit in understanding the structural mechanisms that make signal transduction possible. However, this remains part of the system bias as it falls into the efficiency of coupling to induce a response and thus is not currently useful for drug development.

Dynamic bias.

Another source of bias related to the forces of the system that constantly change its properties across time upon interaction with external factors is known as dynamic bias (Michel et al., 2014). Compared to the system bias that refers to the efficiency of the system to produce a response in a rather static environment, dynamic bias refers to the essential variable of time that rules the constant changes in the system. This bias can be readily observed in pathologic states or chronic drug treatments where the efficacy of a ligand changes depending on the stage of the disease or the length of the treatment, respectively. Indeed, one of the most common examples of dynamic bias in disease is heart failure. Acute treatment of heart failure with the beta-blocker carvedilol worsens cardiac function (Bozkurt et al., 2012; Hall et al., 1995) whereas the long-term effects of carvedilol have beneficial effects on heart function and survival (Packer et al.,

1996; Waagstein, 1993). This paradoxical response is also observed in a rodent model of asthma when treated with the beta-blocker nadolol (Callaerts-Vegh et al., 2004). Extrapolation of these findings to humans shows a similar improvement in airway compliance in asthma patients after long-term treatment with nadolol (Hanania et al., 2008).

The example of heart failure can also be used to illustrate the dynamic bias of the endogenous ligand epinephrine in heart failure. The molecular mechanisms involved in the development of this disease include sympathetic system overactivation, β_2AR desensitization, and β_1AR downregulation, and other genetic adaptations affecting the downstream signaling of adrenergic receptors (Bristow et al., 1986; Brodde, 2007). These molecular changes take place over a long period and modify the otherwise compensatory response of contractility and heart rate under epinephrine exposure. Accordingly, in acute pathologic conditions such as angina, epinephrine increases the contractility and heart rate by activating the Gs signaling pathway to maintain cardiac performance as a compensatory mechanism (Bristow et al., 1989; Swedberg et al., 1984). However, this compensatory mechanism becomes maladaptive in heart failure as the βARs are desensitized and the expression of other signaling molecules, like the GPCR kinase GRK2, favor cardiotoxicity and cell death (de Lucia et al., 2018; Ferrara et al., 2014; Mann & Young, 1994). Thus, the once cardiotonic and beneficial β_2AR ligand epinephrine becomes cardiotoxic and detrimental for heart function by the dynamic evolution of the disease.

Taken together, the dynamic bias is also independent of the ligand's intrinsic properties. However, exploration of these effects might prove useful in the development of drugs as it directly targets the health problem at hand. This can only be accounted for if new methodologies are developed in the pipeline of drug discovery. That is, establishing disease animal models that resemble the human pathologic states through time to develop parameters relating the ligand bias with the dynamic bias. This approach might show superiority and complement drug discovery using the current, often minimalistic, high throughput screening, and *in vitro* testing for extrapolation into the treatment of human disease states.

Ligand bias.

The power of manipulating the activity of the receptor to elicit a predominant biological response by a ligand is held within its chemical structure. This is based on our current understanding of the existence of multiple receptor conformations, each with specific activation energy (Isin et al., 2012; Manglik et al., 2015; West et al., 2011). Based on their chemical structure, ligands can preferentially bind to an array of receptor conformational subpopulations inducing the cognate response associated with the receptor conformation. Thus, even among ligands of the same class, slight changes in the binding arrays for the receptor subpopulations will confer unique degrees of efficacy and magnitude of such effects to each ligand. For example, beta-blockers are classically known to bind to the β_2AR and impede the binding of the endogenous ligand epinephrine, therefore, inhibiting the canonical response of cAMP accumulation through Gs activation. Exploration of alternative signaling pathways has shown that among this class of ligands, carvedilol shows a preference for the activation of the βarr2 signaling pathway increasing the phosphorylation of ERK1/2 (Wisler et al., 2007). This has also been observed for the beta-blockers nevibolol and propranolol which preferentially activate the βarr2 signaling pathway (Azzi et al., 2003; Erickson et al., 2013). Furthermore, a reclassification of β_2AR ligands based on the multiple efficacies for alternative pathways has been proposed (van der Westhuizen et al., 2014). Therefore, the structural composition of these ligands can confer the selectivity for a unique signaling pathway. This is known as ligand bias.

For the accurate measurement of ligand bias, it is necessary to correct for the observational and system bias by using a reference ligand that shows a robust response for the pathways measured. This response becomes the definition of full agonism for both pathways, and therefore is referred to as “balanced” or “unbiased’ signaling. The current standard in pharmacology arbitrarily defines the endogenous ligand with such characteristics. Nevertheless, it is important to note that the endogenous ligand is not truly unbiased *per se* because the dynamic bias is constantly affecting its biological response. Yet, endogenous ligands serve the function of

comparison with other ligands to give a relative activity ratio and correct for the observational and system bias. Then, the relative activity ratio can be used across assays detecting different signaling pathways to reveal the true ligand bias between signaling pathways. Therefore, when expressing ligand bias the reference ligand must be mentioned (e.g., ligand *x* is biased towards the Gs pathway when compared to ligand *z*). With this concept in mind, at least 4 main bias quantification methods have been developed. Ideally, the best practice to measure the response in any of these methods is to establish a scale that is independent of the activation elicited by the ligand-receptor interaction. In this way, the quantification of the maximal response will be independent of the maximal response elicited by the reference ligand. Each method will be briefly addressed to understand the reason for the adaptation of the mathematical approach proposed in this work.

Relative potency ratios (ΔΔ pEC_{50}).

This method quantifies the differences in the negative logarithm of the ligand concentration that elicits a half-maximal response (Δ pEC_{50}). This method of quantification can only be used if the ligands analyzed are full agonists for both signaling pathways. The difference between relative potency ratios among signaling pathways (ΔΔ pEC_{50}) can then reveal the ligand bias for two signaling pathways. While the strength of this method lies in its simplicity of use from concentration-response curves, its main limitation is that ligands that do not produce a maximal response (i.e., partial agonists) cannot be compared. This is because the maximal response of partial agonists is dependent on the receptor expression, therefore, affecting the sensitivity of the system. For example, reductions in receptor density will reduce the maximal response of partial agonists without affecting the pEC_{50} values. Conversely, the pEC_{50} of full agonists will shift to the right (higher EC_{50}) without changing their maximal response. Therefore, full versus partial agonists comparison is incompatible using this method as it becomes system biased.

Relative activity ratios (ΔΔ log(RA)).

This method of quantification proposed by Ehlert (Ehlert, 2005) considers the concept that an allosteric element (i.e., signaling molecule) influences the maximal

response (Emax) of an agonist. Therefore, the maximal response is taken into consideration for the calculation of an individual value for each ligand to establish a single index of agonism. This is mathematically expressed as RA = log(Emax/ pEC_{50}), where the relative activity (RA) normalizes the agonist activity in systems with multiple sensitivities. Once more, a reference ligand is needed to cancel the observational and system bias (Δ log(Emax/ pEC_{50}) and create a scale of agonism for a given system. This allows for comparison between different signaling pathways if the same reference ligand is used to measure the relative activity of test ligands. This comparison across systems (ΔΔ log(Emax/pEC_{50}) yields values that are independent of cross-system effects (e.g. assay sensitivity). Therefore, the numerical value unique to each ligand represents the power to elicit a response compared to another. This is a simple yet powerful method to characterize biased agonism and can be expanded to other applications such as receptor selectivity, cell-based agonist selectivity. For this method to be valid two main requirements should be met; (1) the slope of the concentration-response curves should not be statistically different from unity, and (2) agonists should have a maximal response greater than 35% of the total response (>35%). If these criteria are not met the indices of agonism given by RA ratios become misleading on detecting biased agonism (Kenakin, 2017a).

Relative transducer coefficient ratios (ΔΔ log(τ/K_A)).

The theoretical framework that gave birth to this method comes from the Black and Leff operational model (Black & Leff, 1983) to assess agonism. As described in the operational model section, this model integrates the agonist efficacy, receptor density, and the coupling of the ligand-receptor complex with the responsive elements of the system in a single coefficient, τ. This coefficient can be obtained from functional curves using Eq. 12 which mathematically describes the operational model. By incorporating the functional affinity of a ligand for the multiple conformations of the receptor into the equation, the values of agonism can be represented as transducer coefficients (log(τ/K_A)). The functional affinity (K_A) in this method describes the binding of a ligand to a receptor pre-coupled with a transducer (i.e., conditional affinity). The receptor-transducer coupling implies that the conformation of the receptor has changed from the

inactive conformation and therefore affects the binding properties of the ligand. Since different active receptor conformations represent an α value different from one (i.e., the factor that numerically represents the differences in affinity between active conformational states) then the possible active conformations adopted by the receptor become infinite. In the case of bias signaling analysis for two pathways, the α values are constrained to the two active conformations of the receptors that are under analysis. This yields two distinct K_A values, one for each signaling pathway. Therefore, radioligand experiments directly measuring the affinity of ligands are not useful in this analysis since they represent an average of the multiple conformations of the receptor that exist in a system. Only if the receptor was held in the active conformation that binds to the signaling molecule involved in the studied pathway could the affinity be measured using the radioligand technique. This way, the numerical representation of the transducer coefficient will enclose the infinite possibilities of affinity and efficacy values of an agonist into a single value (Jakubik et al., 2019).

Experimental studies have shown that transducer coefficients remain constant across a wide range of receptor densities (Kenakin et al., 2012) underlining the system-independent feature of this method. Like the previous methods, using a reference ligand to determine activity ratios cancels the observational bias. The transducer coefficient ratios for each signaling pathway ($\Delta \log(\tau/K_A)$) can then be subtracted ($\Delta\Delta \log(\tau/K_A)$) to determine a unique value representing the agonist bias. Finally, to express the bias factor (i.e., the numerical value of selectivity for a signaling pathway compared to another) the $\Delta\Delta \log(\tau/K_A)$ is converted to a linear scale by using an antilogarithmic function ($10^{\Delta\Delta \log(\tau/KA)}$). Of note, an adapted version of the operational model (Black et al., 1985) can also be used to calculate ligand bias from functional curves that do not have a slope of unity. Thus, this method has proven as the most robust for bias quantification and has been used for the study of multiple GPCRs (Gomes et al., 2020; Reyes-Alcaraz et al., 2018; van der Westhuizen et al., 2014).

VII. Clinical relevance in detecting biased signaling for the β_2AR

After the discovery of alternative signaling pathways mediated by GPCRs (Attramadal et al., 1992; Shenoy et al., 2006), our understanding of them has gone from on/off switches to signaling hubs that orchestrate multiple functional responses in tissues. Each signaling pathway contributes to the homeostasis of the system by activating a specific cellular response. Under pathologic states (i.e., when the homeostasis is broken) one signaling pathway might predominate over another and cause the pernicious effects that favor the progression of the disease. Therefore, identifying and targeting specific signaling pathways that predominate in disease can help in the development of pharmacologic treatments that improve the therapeutic outcome of patients. The main challenge lies in the identification and characterization of biased ligands that are ultimately useful for the treatment of pathologic conditions.

For the β_2AR, the main signaling pathways, protein Gs and βarr2 can have either beneficial or detrimental effects based on the disease studied. For example, the activation of the βarr2 signaling pathway in heart failure and asthma show beneficial and adverse effects, respectively. Furthermore, pharmacologic manipulation of the β_2AR with different beta-blockers for the treatment of such illnesses is not consistent with a single mechanism of action (Casella et al., 2011; Thanawala et al., 2014; Wisler et al., 2007). The best explanation for this apparent discrepancy is the biased signaling profile each member of this class of drugs has that modifies the disease in distinct ways. Therefore, the next sections will review the existing evidence on how the biased signaling and biased ligands affect the outcome of both pathologies reciprocally. In this regard, the importance of exploring both signaling pathways is highlighted as each one can become beneficial or detrimental based on the pathology. Characterization of each signaling pathway in multiple diseases can then be the basis for the development and detection of ligands biased towards enhancing or blocking the beneficial and detrimental pathways, respectively.

β_2AR biased signaling in heart failure.

Heart failure (HF) is characterized by a decrease in contractility that leads to the inadequate perfusion of tissues. Insults to the heart such as coronary artery disease, myocardial infarction, and valvulopathies, among others, activate compensatory mechanisms largely mediated by the sympathetic system. The sympathetic overactivation is mediated by the release of the catecholamines epinephrine and norepinephrine that activate β-adrenoceptors to increase cardiac contractility and heart rate thereby increasing blood ejection fraction (Swedberg et al., 1984). However, in the long-term, this compensatory mechanism becomes maladaptive as it increases cardiac remodeling leading to impaired β-adrenoceptor signaling and left ventricle (LV) dysfunction as the pathognomonic event of HF (Bristow, 2000). Indeed, plasma catecholamine content is directly correlated with mortality in HF (Cohn et al., 1984).

At a cellular level, cardiomyocytes undergo selective downregulation of the β_1AR while keeping the β_2AR expression constant because of the chronic exposure to high concentrations of catecholamines in HF (Bristow et al., 1986; Bristow et al., 1989). Changes in the stoichiometry of these receptors appear to favor the β_2AR signaling in this pathologic state. Cardiac-specific overexpression of the β_2AR in a mouse model of heart failure shows increased left ventricular hypertrophy which was translated into cardiac dysfunction (Du et al., 2000). This detrimental outcome has been associated with the quantity of β_2AR expression as well as the temporal length of signaling; mice with high overexpression show cardiac dysfunction earlier than mice with moderate overexpression of the β_2AR whereas low overexpression is associated with LV function improvement (Liggett et al., 2000). Since cardiac contractility is the most affected function in HF, other mouse models with genetic cardiomyopathy affecting the sarcomeric muscle LIM protein (MLP) have also been used as models of HF. Here, overexpression of the β_2AR does not change the cardiac phenotype of the genetically modified mice (Rockman et al., 1998) whereas β_2AR deletion recovers the contractile function in these mice (Fajardo et al., 2013). Moreover, GRK overexpression, known to phosphorylate the receptor, therefore, favoring β arrestin recruitment, also rescues the

cardiac function on these mice (Rockman et al., 1998). Altogether, this data implies that the β_2AR is a regulator of cardiac contractility in the pathologic state of heart failure.

At a molecular level, the canonical Gs-adenylate cyclase-cAMP-PKA signaling cascade of the β_2AR has been associated with the cardiotoxic effects that perpetuate the disease. For example, the β_2AR-mediated response of the agonist isoproterenol induces cell death in human induced pluripotent stem cell-derived cardiomyocytes (hiPSC-CMs) (Jung et al., 2016). This cytotoxic response induced by adrenergic overstimulation is linked to the activation of the Calcium calmodulin-dependent kinase II (CaMKII) by direct or indirect PKA-dependent mechanisms (El-Armouche et al., 2008; Ferrero et al., 2007; Grimm & Brown, 2010). Moreover, the coordination of cardiac contractility at the LV by electrical stimulation is also impaired in HF and this impairment is associated with the activation of the Gs signaling pathway of the β_2AR. This has been evidenced by treating cardiomyocytes from guinea pigs with HF with the β_2AR selective agonists' salbutamol or fenoterol. Here, these agonists induced a reduction of the delayed rectifier potassium current (IKr), known to repolarize cardiomyocytes for the next contractile cycle. This was prevented by the blockade of the β_2AR or cAMP, or by using PKA inhibitors indicating that the β_2AR-Gs pathway is also involved in the arrhythmogenic events observed in HF (Wang et al., 2012; Wang et al., 2015). Accordingly, sympathetic overdrive as well as treatment with epinephrine in patients with heart diseases has historically shown an increased risk for ventricular arrhythmias (Kaye et al., 1995; Tovar & Jones, 1997). Finally, manipulation of the expression or activity of other members of the Gs pathway is also consistent with molecular events that induce cardiac dysfunction (Antos et al., 2001; Iwase et al., 1997; Mougenot et al., 2019). Altogether, this data suggests that the β_2AR negatively impacts cardiac function in HF when the canonical Gs signaling pathway is constantly activated.

In contrast, the βarr2 pathway of the β_2AR appears to be beneficial for cardiac function. Perhaps the first inadvertent evidence of these beneficial effects is the use of the beta-blocker carvedilol which has become the gold standard for treatment of HF as it improves heart function and increases overall survival (Bristow, 2011; Packer et al., 1996; Poole-Wilson et al., 2003). This ligand was later proven to increase ERK1/2

phosphorylation through the βarr2 pathway while decreasing cAMP accumulation through inhibition of the Gs pathway (Wisler et al., 2007). Therefore, this is the first known β_2AR biased agonist that is available in the market for the treatment of common pathology. Of note, other beta-blockers have not been as effective as carvedilol to treat HF most likely because they don't have the same biased signaling profile as carvedilol (Bristow, 2011; Poole-Wilson et al., 2003; van der Westhuizen et al., 2014; Wisler et al., 2007). Accordingly, an allosteric agonist biased towards βarr2, ICL1-9, can also induce contractility *in vitro* and improve cardiac function and decrease cardiomyocyte death after an ischemic insult *in vivo* (Carr et al., 2016; Grisanti et al., 2018). These effects are inhibited by βarr2 or β_2AR deletion corroborating that the observed cardioprotective responses are mediated by the β_2AR-βarr2 signaling pathway (Carr et al., 2016; Grisanti et al., 2018). Consistent with these findings, the deletion of the βarr2 in senescent mice shows decreased contractility and cardiac dysfunction (Capote et al., 2021). Taken the previous data together, the β_2AR-βarr2 signaling pathway becomes beneficial during aging and in heart disease, and therefore targeting this pathway using biased ligands can prove therapeutic.

β_2AR biased signaling in asthma.

A convenient example of the antithetical behavior in the biological outcomes produced by the β_2AR signaling pathways when compared to heart failure is the respiratory disease of asthma. This heterogeneous condition is characterized by chronic airway inflammation, remodeling, and bronchial hyperreactivity (Lambrecht & Hammad, 2015; Pascual & Peters, 2005). Although the triggering factors are still not well understood, the immune response is central to the pathophysiology of asthma and, therefore, much of the efforts to understand and treat the disease have focused on this field (Barnes, 2008; Murphy & O'Byrne, 2010). Based on this, the current standard of treatment in asthma is glucocorticoids to reduce airway inflammation. Additionally, β_2AR agonists have been widely used historically as an acute and chronic treatment of asthma because of their bronchodilation properties to increase airway compliance (Giembycz & Newton, 2006; Tattersfield, 2006). However, long-term treatment with β_2AR agonists increases exacerbation events and mortality in asthmatic patients

(Nelson et al., 2006; Salpeter et al., 2006). Therefore, the current paradigm of asthma treatment has been challenged (as was the case for HF in the past) to use some beta-blockers as the chronic treatment for asthma patients (Bond, 2001). This paradigm shift also lies at the core of the β_2AR activity and its distinct signaling pathways.

So far, the most striking evidence on the relationship between asthma development and β_2AR activity is that the deletion of this receptor completely suppresses the asthma phenotype in a rodent model of asthma (Nguyen et al., 2017; Nguyen et al., 2009). As a reciprocal approach, mice devoid from the endogenous β_2AR agonist epinephrine by deletion of the phenylethanolamine N-methyltransferase (PNMT$^{-/-}$) enzyme do not develop asthma either (Forkuo et al., 2016; Thanawala et al., 2013). This enzyme converts norepinephrine into epinephrine and is predominantly expressed in the adrenal glands, the main supplier of epinephrine to the peripheral circulatory system (de Diego et al., 2008). Chronic treatment with the selective β_2AR inverse agonists nadolol or ICI 118,551 attenuated the asthma phenotype in a mice model of asthma whereas the β_2AR agonists' formoterol, salmeterol, and epinephrine restored the asthma phenotype in PNMT$^{-/-}$ mice (Callaerts-Vegh et al., 2004; Forkuo et al., 2016; Nguyen et al., 2008; Thanawala et al., 2013). Accordingly, a pilot study in humans with mild asthma shows symptomatic improvement and increased airway compliance after chronic treatment with nadolol (Hanania et al., 2010; Hanania et al., 2008). Therefore, activation of the β_2AR is essential for the development of asthma phenotype.

The use of other beta-blockers has yielded no clinical benefit or even opposite results in *in vivo* studies suggesting that distinct β_2AR signaling pathways might mediate opposite effects in asthma. For example, another small pilot study showed no benefit and even a small worsening of the physiological respiratory parameters in mild asthma patients under chronic treatment of propranolol, a ligand that activates βarr signaling (Azzi et al., 2003; Short et al., 2013). Additionally, treatment with the neutral antagonist alprenolol did not attenuate the asthma phenotype in a mice model of asthma while carvedilol restored the asthma phenotype in PNMT$^{-/-}$ mice (Callaerts-Vegh et al., 2004; Nguyen et al., 2009; Thanawala et al., 2015). The discrepancy about the opposite responses among the class of beta-blockers has been explained by the signaling profile

of each ligand. Propranolol and carvedilol are inverse agonists for the activation of the canonical Gs pathway but partial agonists for ERK1/2 activation (Azzi et al., 2003; Wisler et al., 2007). Moreover, the ERK1/2 activation elicited by carvedilol is mediated by βarr2 signaling. Comparatively, nadolol and ICI 118,551 are inverse agonists for both signaling pathways (Wisler et al., 2007). Therefore, the β_2AR signaling that favors activation of ERK1/2 through βarr2 is detrimental in asthma therapy. Accordingly, βarr2 knockout mice show an attenuated asthma phenotype (Nguyen et al., 2017; Walker et al., 2003) which is also consistent with the alleviation of the pathologic features of asthma in conditional βarr2 knockout mice (Chen et al., 2015). Taking all together, these data show that the β_2AR-βarr2 signaling pathway is involved in the pathogenesis and perpetuation of the disease and its activation by β_2AR ligands is detrimental for the treatment of asthma. Reductions in the constitutive activity of this pathway further become beneficial for the treatment of asthma.

On the other hand, the experimental evidence on the activation of the β_2AR-Gs-cAMP pathway is scarce as currently there are no Gs biased β_2AR ligands available in the market. The only developed β_2AR ligand that has promoted Gs mediated signaling without recruiting βarr2 is the pepducin ICL 3-9 and has not been tested yet in asthma models (Carr et al., 2014; Ippolito & Benovic, 2021). Nevertheless, indirect evidence on the stimulation of the Gs pathway has shown beneficial effects in the treatment of asthma by using phosphodiesterase (PDE) inhibitors. As their name indicates, these drugs inhibit the enzyme responsible for degrading cAMP thereby inducing accumulation of this second messenger. Using $PMNT^{-/-}$ mice, Forkuo and colleagues (Forkuo et al., 2016) showed that the asthma phenotype rescued by β_2AR agonists was attenuated by cotreatment with the PDE-4 inhibitors, roflumilast or rolipram. A recent systematic review and meta-analysis of 14 studies spanning from 1946 to 2016 concluded that oral PDE4 inhibitors are an alternative treatment to regular bronchodilators in mild asthmatic patients (Luo et al., 2018). However, none is currently approved by the FDA due to their heterogeneous side effects (Matera et al., 2021). Finally, *in vitro* evidence also showed Gαs and β_2AR upregulation under chronic nadolol treatment suggesting that nadolol can functionally favors the Gs pathway in the long

term (Peng et al., 2011). Altogether, these data support the β_2AR-Gs-cAMP pathway as beneficial for the treatment of asthma.

In summary, the β_2AR-dependent signaling of either Gs or βarr2 is not fixed to a unique clinical outcome among tissues. Instead, the clinical consequence of activating a single β_2AR signaling pathway, either beneficial or detrimental, varies depending on the tissue. Therefore, exploring both signaling pathways of the β_2AR is important to identify the molecular mechanisms underlying the pathophysiology of a given disease in each organ. Furthermore, the development of biased ligands targeting the beneficial pathway might show superiority at improving the clinical outcomes of multiple diseases when compared to unbiased ligands, or at least, at reducing side effects from the activation of the detrimental signaling pathway.

VIII. Rationale

The β_2AR is a seven-transmembrane domain receptor that induces a cellular response by activating a unique signaling pathway dependent on the conformational state of the receptor. At least two signaling pathways have been characterized for the β_2AR: the canonical Gs pathway and the βarr2 pathway. So far, the determination of the signaling preference of multiple β_2AR ligands (biased signaling) is compared to the reference β_2AR endogenous ligand, epinephrine (EPI), which by convention is defined as unbiased. However, the absolute biased signaling of β_2AR ligands on the basis for the distinct active conformational states of the β_2AR is unknown. Thus, we used novel fusion proteins made of the β_2AR receptor fused to Gαs or to βarr2 to stabilize the β_2AR conformation, isolate each signaling pathway, and characterize the pharmacological properties (affinity, efficacy, and potency) of the β_2AR ligands. Our fusion proteins were designed using short linkers between the β_2AR and the signaling molecules Gαs, or βarr2. This approach increases the proximity between the β_2AR and the fused signaling molecule to favor their interaction while excluding the interaction of other endogenous signaling molecules with the fused receptor.

IX. Hypothesis

Fusion proteins exist in a single conformational state of the receptor that will dissect each signaling pathway and its absolute preference for each β2AR ligands to classify them according to their preferred signaling pathway.

X. Specific Aims

- **AIM 1**: Elucidate the pharmacological properties of β_2AR ligands in HEK293 cells that express β_2AR fused with either Gs or β-arr2.
- **AIM 2**: Establish the inflammatory profile elicited by the immunomodulatory BEAS-2B cell line transfected with the fusion protein β2AR-Gs or β2AR-βarr2.

XI. Materials and Methods

Materials.

All β2AR ligands were purchased from Sigma-Aldrich (St. Louis, MO). Dulbecco's Modified Eagles Medium (DMEM), Trypsin/EDTA 0.25%, Dulbecco's phosphate buffer saline (DPBS), Penicillin, G-streptomycin-amphotericin B, and fetal bovine serum (FBS) were purchased from GenDepot (Katy, TX. USA). Dihydroalprenolol Hydrochloride, Levo-[Ring, Propyl-3H(N)]- ([3H] DHA) and FlashPlate® were purchased from PerkinElmer (Waltham, MA. USA). 384-well small volume white plates were purchased from Greiner Bio-one (Monroe, NC. USA).

Constructs.

The β_2AR, Gαs, and βarr2 constructs were obtained from human cDNA. The β_2AR construct was ligated in-frame to the Gαs coding region by substitution of the stop codon at the β_2AR 3' end using an XhoI site followed by the 5' starting codon methionine of Gαs coding region. For the β_2AR-βarr2 fusion construct, the stop codon for the β_2AR was replaced by the sequence: 5' CTCGAGGGGGGGCCCGGTACCGAGCTCGGATCCACC 3' (The underlined nucleotides represent a BamHI site for in-frame ligation to the βarr2 construct) and immediately followed by the 5' starting codon encoding for methionine of the βarr2 coding region. The β_2AR, β_2AR-Gαs, and β_2AR-βarr2 constructs were subcloned into the expression vector pcDNA3.1(+) (Invitrogen) for cell transfection. All procedures were done by Norclone Biotech labs, Inc (London, Ontario, Canada).

Cell Culture and Transfection.

Human Embryonic Kidney 293 (HEK 293) cells, a gift from Dr. Kehe Ruan, were tested for cell line authentication using a short tandem repeat (STR) profile analysis offered by ATCC (ATCC® 135XV™). This profile showed a 93% similarity to the HEK 293 cell line offered by ATCC (ATCC® CRL1573™). HEK 293 cells were plated in 60mm or 100mm cell culture plates, depending on the number of cells needed in each experiment, and maintained in DMEM supplemented with 10% FBS and 1% penicillin-

streptomycin-Amphotericin B. BEAS-2B cells were purchased from ATCC (ATCC® CRL-9601) plated in 100mm cell culture plates and maintained with BEGMTM bronchial epithelial growth medium bulletkitTM (Lonza Inc). Both cell lines were kept at 37oC with 5% CO2. Cells were stably transfected using a pCDNA3.1 vector encoding for the β_2AR alone or fused to the protein Gαs or βarr2. Lipofectamine 3000 transfection reagent (ThermoFisher Scientific) was used for transfection (where t = transfected) following the manufacturer's instructions. 48 hours after transfection, cells stably expressing the receptor (t β_2AR) or the fusion proteins (t β_2AR-Gαs or t β_2AR- βarr2) were selected using Geneticin (G-418) 1mg/ml for 12-14 days, and the resultant cell colony was later maintained using 800ug/ml. Non-transfected and transfected groups were subcultured as necessary using trypsin/EDTA 0.25% solution for detachment of cells from the culture plate.

RNA Extraction and Reverse Transcriptase-Polymerase Chain Reaction.

Total RNA was extracted from all groups using the PureLink™ RNA mini kit (Invitrogen) following the manufacturer's instructions. In brief, cells were detached with Trypsin/EDTA 0.25% and centrifuged at 300 g for 5 mins at 4^{o}C. The supernatant was removed, and the pellet was resuspended in ice-cold lysis buffer containing 1% 2-mercaptoethanol. Mechanical lysis was performed by pipetting up and down until the solution was clear. The homogenized solution was then centrifuged at 10 000 g for 3 mins. The supernatant was transferred to a new tube and a similar volume of 70% ethanol was added and mixed thoroughly. The mix was transferred to a column containing a membrane with a high affinity for RNA and a collection tube and centrifuged at 16 000 g for 1 min at 4^{o}C. After discarding the flow-through, the spin cartridge was washed twice with washing buffers and dried by centrifugation. Finally, RNAase-Free water was added to the cartridge and centrifuged at max speed for 1 min to detach the RNA from the membrane and collect the elution. The total RNA was quantified using NanoDrop spectrophotometer (Thermo Fisher Scientific, Waltham, MA, USA). One-step RT-PCR was then performed using the SuperScript III One-Step RT-PCR System with Platinum Taq DNA Polymerase (Life Technologies) and 200–400 ng RNA template according to the manufacturer's instructions. PCR products were

analyzed via agarose gel electrophoresis. PCR samples were resolved on a 1% agarose gel containing ethidium bromide and visualized under u.v. light using the ChemiDoc MP Imaging System (Bio-Rad, USA). Primer sequences are listed in Figure 1C.

Detection of βarr2 and Gαs Recruitment.

Using a structural complementation reporter system (NanoBiT®; Promega, Madison, WI) to monitor protein interaction across time, the recruitment of the protein Gαs or βarr2 to the β_2AR alone or fused to the protein Gαs or βarr2 was measured according to manufacturer instructions. In brief, HEK293 cells were seeded in white 96-well plates at a density of 2.5×10^4 cells per well. The next day the cells were transfected using a mixture containing 50ng of βarr2 or Gαs construct containing the LgBit or SmBit and 50ng of the β_2AR or fused with either βarr2 or Gαs containing with one of the two domains of Nano Luciferase (Nluc), and 0.2µl Lipofectamine 3000 (Invitrogen) was prepared and added to each well. We tested four Receptor/fusion-βarr2/Gαs plasmid combinations to find the highest fold increase in luminescence after ligand stimulation. The plasmid combination that showed the highest luminescent signal (Receptor/fusion protein-LgBiT:SmBiT-βarr2/Gαs) was chosen for further experiments. The medium was aspirated 24 h after transfection and replaced with 100µl Opti-MEM at room temperature. After a 10 mins incubation, 25µl substrate (furimazine) was added and the luminescence was monitored for 10 min in the absence of ligand to obtain the baseline values. After ligand addition, luminescence was immediately recorded. In the case of Gαs recruitment luminescent signal was measured every 20 seconds for 45 mins, whereas for βarr2 recruitment the signal was monitored every 30 seconds for 1h. The luminescence values were recorded using a Synergy 2 Multi-Mode Microplate Reader (BioTek).

Membrane Preparation for Radioligand Binding Experiments.

Non-transfected and transfected cells were grown in a 100mm culture plate until total confluency before harvesting cells. After medium aspiration, 3ml of cold DPBS per plate was added and cells were detached from the plate surface using a cell scraper,

placed in 15ml tubes, and centrifuged at 300 g for 5 mins at 4^{o}C. The supernatant was discarded, and the pellet was resuspended and homogenized on cold lysis buffer (Tris-HCl 50mM; pH 7.4). The homogenate was then centrifuged at 22 000 g for 30mins at 4^{o}C to obtain a pellet of the membrane fraction. The pellet was resuspended in lysis buffer, homogenized, and stored at -80^{o}C until needed. Before the saturating or competitive binding experiments, protein quantification from the thawed homogenates was performed using the bicinchoninic acid (BCA) protein assay following the manufacturer's instructions.

Saturation Binding Assays.

Cell membranes obtained in the previous step were diluted in Binding buffer (Tris-HCl 50mM, EDTA 2mM, MgCl 12.5mM; pH 7.4), placed on ice, and further homogenized using a polytron homogenizer for 2 periods of 30 seconds at maximum speed. The resultant homogenate was added to 96 well FlashPlate® in a volume of 200µl per well and centrifuged for 10 mins at 1000 g for 10mins at 4^{o}C. Optimal concentrations of cell membrane per well were previously determined for the transfected groups (t β_2A-Gαs=30µg/well; t β_2AR- βarr2=20µg/well; t β_2AR=3µg/well) to detect the final saturation curve. After centrifugation, the supernatant was discarded and 100µl of Binding Buffer was added to each well. Increasing concentrations of [^{3}H] DHA (from 0.125nM to 8nM) were then added to separate wells of the FlashPlate® in a volume of 100µl to detect total binding (TB) at a constant volume of 200µl per well. The wells of FlashPlate® are coated with scintillation fluid and, thus, no filtration or washing steps were needed. The FlashPlate® were incubated for 2 hours at room temperature to reach equilibrium and radioactivity was measured using a MicroBeta^{2}® microplate counter (PerkinElmer Life and analytical sciences). The non-specific binding (NSB) was determined by adding 30µM propranolol in 100µl of binding buffer before adding the radioligand. The final curves are reported as specific binding (SB) where SB = TB - NSB. The dissociation constant (Kd) and the receptor density (Bmax) were determined using one site-specific binding regression curve (Graphpad Prism 9; San Diego, CA). The values of Kd and Bmax were converted from counts per minute to fmoles/mg of protein. This set of experiments was done in triplicate using membranes extracted at 3

different cell passages per group to account for variability in protein expression through time.

Competition Binding Assays.

Like the saturation binding assays, cell membranes were homogenized in binding buffer, added to a 96 well FlashPlate®, centrifuged, and the supernatant discarded. Increasing log unit concentrations of multiple ligands were first tested to identify the binding curve for each β_2AR ligand. Once identified, indicated concentrations of all β_2AR ligands were added to separate wells in a volume of 100µl. Based on the Kd values of the transfected groups, 1nM of [^{3}H] DHA in 100µl per well (final volume = 200µl) was used in all groups to detect the affinity of β_2AR ligands for the receptor alone or the fusion proteins. The affinity was expressed as Ki. This set of experiments was run in duplicate with an n≥3.

Cyclic Adenosine 3',5'-Monophosphate (cAMP) Measurements.

To measure the cAMP accumulation as a direct response of the Gs pathway of the β_2AR, the cAMP-Gs dynamic kit (Cisbio) was used according to the manufacturer's instructions with a few modifications. In brief, cells from all groups were detached using trypsin/EDTA 0.25%, counted by the automatic Countess II Automated Cell Counter (Invitrogen) to obtain the proper cell density per well, centrifuged at 300 g for 5 mins, and resuspended in DMEM. A 45 min preincubation period with 100nM of the selective β_1AR antagonist, CGP 20712A, in a 37ºC chamber with 5%CO_2 was done in all experiments to isolate the β_2AR response. When indicated, the selective β_2AR antagonist/inverse agonist, ICI 118,551, was preincubated together with CGP 20712A. Before cells were dispensed in a volume of 5µl/well to 384-well small volume white plates, the phosphodiesterase inhibitor, 3-isobutyl-1-methylxanthine (IBMX), was added to the cell suspension for a final concentration of 10µM/well. The indicated concentrations of the β_2AR ligands were freshly prepared from 10mM stock solutions in DMEM (pH 5.1) and added to individual wells to obtain the concentration-response curves. The change of the DMEM pH was necessary to stabilize the pH ~7.4 at the well and observe a response since the pH of DMEM at room temperature (~8.1) induces

oxidation of ISO and completely blunts the response of all β_2AR ligands. The stimulation buffer included in the kit was not used as it did not give any detectable signal under the previously mentioned settings (data not shown). The β_2AR agonists or antagonists were incubated for 10 mins or 20 mins, respectively, at room temperature. These time frames showed the biggest response window to detect agonism and inverse agonism, respectively. Immediately after incubation, 5µl of the cAMP-tagged d2 fluorophore followed by 5µl of the Anti-cAMP-Cryptate antibodies were added to each well. The plate was incubated for 1 hour at room temperature and the fluorescent signal was read using Synergy H1 (BioTek). Since the response measured was inversely proportional to the Homogeneous Time-Resolved Fluorescence (HTRF) signal-ratio, all generated data was transformed so the lowest values of the HTRF ratio for each group, equivalent to the highest levels of cAMP in that system, become 100% of the response, and the lowest HTRF ratio for each group, equivalent to the lowest levels of cAMP in the system, become the basal line (0%). The in-between values were fitted in this scale. All experiments were performed in triplicate on at least 3 separate occasions (n≥3).

Total ERK1/2 and PhosphoERK1/2 Measurements.

This set of experiments was performed to test the alternative pathway, βarr2, of the β_2AR. The total-ERK1/2 and the advanced phosphoERK1/2 (THR202/TYR204) kits (Cisbio) were used to measure total and phosphorylated ERK1/2, respectively, following the manufacturer's instructions with some modifications. In brief, 1.5 x 10^5 or 2.2 x 10^5 cells per well -for agonism and inverse agonism experiments, respectively- were seeded in a 96 well cell culture plate and incubated with supplemented DMEM at 37^{o}C and 5% CO_2 for 22-24hours. Then, supplemented DMEM was removed, and cells were starved in DMEM supplemented with 1% FBS (starvation media) for 20-22 hours. The media was aspirated and 100nM of the selective β_1AR antagonist, CGP 20712A, was added in 40µl of starvation media for a 45 min preincubation period in a 37^{o}C chamber with 5% CO_2. ICI 118,551 was preincubated together with CGP 20712A when indicated. Ascending half log unit concentrations of β_2AR ligands were freshly prepared in DMEM and added into separate wells for a final volume of 80µl/well. For β_2AR agonists, ERK1/2 phosphorylation was detected at a 5-minute incubation whereas, for β_2AR

antagonists, 90 mins were necessary to achieve equilibrium with antagonists/inverse agonists. After the incubation period with β_2AR ligands, the media was carefully removed and 60µl of the supplemented lysis buffer was added to each well. The 96 well plates were thoroughly shaken at 1000rpm for 35 mins. Then, 16µl of the lysed solution was added to 384-well small volume white plates followed by 4µl of the premixed antibody solution (Phospho-ERK1/2 -d2 and -cryptate antibodies). The plate was sealed and incubated for 4 hours at room temperature before the HTRF signal was detected with Synergy H1 (BioTek). Total ERK was measured by adding a 4µl premixed solution of antibodies (Total-ERK1/2 -d2 and -cryptate antibodies) to the 16µl of lysed solution. The data were expressed as relative ERK1/2 = phosphoERK/Total ERK. All phosphoERK1/2 measurements were performed in duplicate whereas one total ERK measurement per concentration was done as a control. The average value of 8 to 9 total ERK measurements per curve was used to express relative ERK1/2 values. All experiments were done on at least 3 separate occasions (n≥3).

Cytokine Profile Measurements.

Non-transfected and transfected BEAS-2B cells were cultured in 12-well plates and grown to ~80% confluency. Then, cells were starved using BEBM™ Bronchial Epithelial Cell Growth Basal Medium (Lonza Inc.) and the medium was collected 24 hours later. Samples were centrifuged at 800 g for 5 mins at 4°C and stored at -80°C until needed. The concentration of human TNFα, IL-1β, IL-4, IL-5, IL-6, IL-8, IL-10, IL-13, CCL2, GM-CSF, and IFNγ were measured using a commercially available human multiplex cytokine assay (Eve Technologies; Calgary, AB, Canada).

Immunofluorescence.

Cells were cultured in 35mm ibidi dishes. Once 70% confluency was reached, the media was extracted and 200µl of ice-cold 4% paraformaldehyde (PFA) was incubated for 10 mins. Cells were washed 3 times with cold PBST and blocked using 1% BSA for 30 mins. Primary antibodies directed against β2AR (Abcam; ab182136), Gαs (Novus; NBP1-49874), or βarr2 (Mybiosource; MB52522670) at a dilution of 1:300 for one hour at room temperature. Cells were washed 3 times with PBST and incubated

with the secondary antibodies anti-rabbit Alexa 488 (Abcam; ab150077), anti-goat Alexa 568 (Abcam; ab175474) at a concentration of 1:1000, or with anti-rabbit Alexa 594 (Jackson Immunoresearch; 111-585-003) at a 1:200 dilution. Because two secondary antibodies had reactivity to the same species, the primary and secondary antibody incubation for each targeted protein was done separately with an extra blocking step in between to avoid cross-reactivity of the secondary antibodies. The secondary antibodies were incubated for one hour at room temperature in a humidified chamber and washed 3 times with PBST. Finally, cells were mounted using fluoro-gel II with DAPI (electron microscopy services) and imaged using a DMi8 confocal laser scanning microscope (Leica).

Development of the model for absolute bias quantification.

Based on the concept of the operational model that calculates the affinity and efficacy of an agonist when measuring only its functional response in a specific system, we calculated these parameters directly from our experimental data. The affinity measurements used were the ligand's equilibrium dissociation constant (Kd) from the competition binding curves using the one site-Fit Ki algorithm of GraphPad 9 (San Diego, CA) (takes the Cheng and Prusoff equation into account to calculate Ka represented by them as Ki). Accordingly, the values of the Kd for each transfected group (HotKdNM) and the concentration of radioligand (RadioligandNM = 1nM) used for all experiments were constrained to fit the following model: $\log EC_{50}=\log(10^{\log Ki*(1+RadioligandNM/HotKdNM)})$. The assessment of ligand selectivity as a first step to observe the functional affinity of ligands for the β_2AR-Gαs group was done using a simple ratio = $Ki_{\beta2AR\text{-}G\alpha s}/Ki_{\beta2AR\text{-}\beta arr2}$. Note that the inverse of this ratio ($Ki_{\beta2AR\text{-}\beta arr2}/Ki_{\beta2AR\text{-}G\alpha s}$) also shows the selectivity of ligands for the β_2AR-βarr2 group.

Under normal experimental conditions (i.e., when the affinity of a ligand is for the receptor only) the Ka values are invalid for the operational model as they do not reflect the selective nature of a ligand for an active conformational state of the receptor (when the receptor is bound to a signaling molecule). However, our experimental settings favor the receptor to be in two different active conformational states, when the β_2AR is fused to Gαs and when it is fused to βarr2. Thus, we obtained two different Ka values per

ligand that reflect the selective nature of ligands for the active conformations of the receptor. For efficacy measurements, two important parameters define this property. One is the effective/inhibitory concentration 50 (EC/IC_{50}) of a ligand when tested in a functional system. The other parameter, dependent on the previous one, is the concentration of ligand-receptor complexes that causes the EC/IC_{50} in a functional system. This parameter is also known as Ke and is composed of the variable effect of the functional system and the stable effect of the structural component of the ligand that reflects its intrinsic efficacy. For bias quantification, the intrinsic efficacy is the most valuable parameter of a ligand since it is independent of the variability given by receptor expression in multiple functional systems (different tissues). Thus, the Ke needs to be "normalized" with the total receptor density [R_t] to obtain a value that represents the intrinsic efficacy of the ligand, namely tau (τ), which creates a constant scale of agonism/inverse agonism. The mathematical expression used to obtain tau is as follows:

$$\tau=[R_t]/Ke \qquad (13)$$

Here, [R_t] was directly calculated for all transfected groups with saturation binding assays whereas Ke was calculated with a new approach. First, the $logEC/IC_{50}$ values of multiple ligands were calculated separately using a non-linear regression curve that fitted the experimental data with a transducer slope equal to unity. The transducer slope value of unity is a required assumption for the operational model as the functional response observed must be at equilibrium and will keep the coupling efficiency constant among systems. For each pathway, two $logEC/IC_{50}$ values per ligand were obtained, one with the system expressing the β_2AR-Gαs fusion protein and another with the system expressing the β_2AR-βarr2 fusion protein. Therefore, four values of $logEC/IC_{50}$ were obtained (two for the Gαs pathway by means of cAMP accumulation and two for the βarr2 pathway by means of ERK phosphorylation) per ligand. These values where later used as a guide to finding a specific point in the affinity curves. To isolate a unique Ke for each pathway, the $logEC/IC_{50}$ values obtained from cAMP measurements were extrapolated only to the affinity curves obtained when the receptor was fused to Gαs. The opposite is also true, $logEC/IC_{50}$ values obtained from ERK phosphorylation were

extrapolated only to the affinity curves of the receptor when fused to βarr2. To perform the extrapolation of the logEC/IC_{50} values to the affinity curves, the affinity data were fit to the model of GraphPad for finding EC anything in the concentration-response curve with a variable slope as shown below:

$$\log EC_{50} = \log ECF - (1/HillSlope) * \log(F/(100 - F)) \quad (14)$$

where F represents the inverse value of the percentage of receptors occupied by a ligand for a given response, and ECF represents the ligand concentration at which a selected percentage of the response is observed in functional studies. In all calculations, the Hill slope was not significantly different from unity as assessed by a 95% confidence interval. The value of F was then manipulated to match the values of logEC/IC_{50}. The GraphPad program would then show the value of logECF which would be the same as the logEC/IC_{50} from the functional experiments. Once the F values that matched the logEC/IC_{50} were found, a simple calculation of the receptor occupancy was performed:

$$\%\text{Receptor occupancy} = 100\% - F \quad (15)$$

where 100% represents total receptor expression, and the value of F represents the rest of receptors not bound to the ligand since the competition curves are inverted (in the binding experiments 100% represents the radioligand attached to all receptors whereas 0% represents the tested ligand attached to all receptors). When the functional response was >98% or <2% of receptor occupancy (i.e., at the asymptotes of the curve) the receptor occupancy was taken as 99.9 or 0.1% respectively. Similarly, when ligands behaved as neutral antagonists for a pathway (i.e., no detectable EC/IC50) the receptor occupancy was taken as 99.9%. The percentage of receptor occupancy was then converted to concentration to match the measurement units of $[R_t]$ (fmol/mg) to calculate τ. By the end of this process, we obtained two Ke values for each ligand per pathway. Therefore, two τ values were also calculated per pathway:

$$\tau 1_{ligand} = [R_t]_{\beta 2AR\text{-}Gs} / Ke_{cAMP/Gs} \quad \text{and,} \quad \tau 2_{ligand} = [R_t]_{\beta 2AR\text{-}Gs} / Ke_{cAMP/\beta arr2} \quad (16)$$

where cAMP/Gs stands for the measurements of cAMP under the system expressing the β_2AR-Gs fusion protein and cAMP/βarr2 stands for the measurements of cAMP under the system expressing the β_2AR-βarr2 fusion protein using the same ligand and,

$$\tau 3_{ligand}=[R_t]_{\beta 2AR\text{-}\beta arr2}/Ke_{pERK/Gs} \quad \text{and,} \quad \tau 4_{ligand}=[R_t]_{\beta 2AR\text{-}\beta arr2}/Ke_{pERK/\beta arr2} \qquad (17)$$

where pERK/Gs stands for the measurements of phosphoERK under the system expressing the β_2AR-Gs fusion protein, and pERK/βarr2 stands for the measurements of phosphoERK under the system expressing the β_2AR-βarr2 fusion protein using the same ligand.

Since the τ values represent the ligand's intrinsic efficacy for the Gαs and βarr2 pathways when the receptor is coupled to Gαs or βarr2 and the Ka (expressed as Ki) in our system is also based on the affinity a ligand has for the receptor when coupled to a signaling molecule, we obtained 2 values from the transduction coefficient (expressed as log[τ/Ka]) for each ligand per signaling pathway: $Log[\tau 1/Ka_{\beta 2AR\text{-}Gs}]$, and $Log[\tau 2/Ka_{\beta 2AR\text{-}Gs}]$ for the Gs signaling pathway, and $Log[\tau 3/Ka_{\beta 2AR\text{-}\beta arr2}]$, and $Log[\tau 4/Ka_{\beta 2AR\text{-}\beta arr2}]$ for the βarr2 pathway.

The Ka values of the β_2AR alone were also used as controls since, theoretically, these values represent the affinity of a ligand for the receptor when the receptor displays all its conformational states. The subtraction of the transduction coefficients (Δ log[τ/Ka]) of a single pathway and for the same ligand reveals the true efficiency to stimulate such pathway calculated as follows:

$$\Delta \log[\tau/ka]_{ligand/Gs} = Log[\tau 1/ka_{\beta 2AR\text{-}Gs}] - Log[\tau 2/ka_{\beta 2AR\text{-}Gs}] \text{ and,} \qquad (18)$$

$$\Delta \log[\tau/ka]_{ligand/\beta arr2} = Log[\tau 4/ka_{\beta 2AR\text{-}\beta arr2}] - Log[\tau 3/ka_{\beta 2AR\text{-}\beta arr2}] \qquad (19)$$

where $_{ligand/Gs}$ refers to the Gs pathway using the same ligand as its own reference and $_{ligand/\beta arr2}$ refers to the βarr2 pathway using the same ligand as its own reference.

Finally, to calculate the absolute bias (without the need of a reference ligand that can itself introduce another source of bias in the analysis of biased signaling) we subtracted the Δ log[τ/ka] of the Gs pathway from the Δ log[τ/ka] of the βarr2 pathway for the same ligand:

$$\Delta\Delta \log[\tau/ka]_{Gs} = \Delta \log[\tau/ka]_{ligand/Gs} - \Delta \log[\tau/ka]_{ligand/\beta arr2} \text{ or,} \quad (20)$$

$$\Delta\Delta \log[\tau/ka]_{\beta arr2} = \Delta \log[\tau/ka]_{ligand/\beta arr2} - \Delta \log[\tau/ka]_{ligand/Gs} \quad (21)$$

Both values are reciprocal and reflect the selectivity a ligand can have for the Gs or the βarr2 pathway. To reveal this selectivity numerically we used the following:

$$\text{Gs selectivity} = 10^{\Delta\Delta \log[\tau/ka]Gs} \text{ or,} \quad (22)$$

$$\beta arr2 \text{ selectivity} = 10^{\Delta\Delta \log[\tau/ka]\beta arr2} \quad (23)$$

This approach was also followed to determine the selectivity between the receptor alone versus the fusion proteins. The resultant numerical expression served as quantification of the absolute bias for all β_2AR ligands tested.

Statistical Analysis.

Except for ERK experiments, which were done in duplicate, all experiments were performed in triplicate on at least 3 separate occasions (n≥3). Measurements were analyzed using one- or two-way ANOVA according to the nature of the experiment. For pEC/IC_{50} comparisons, extra sum-of-squares F test analysis was used. Receptor selectivity analysis was done with 95% confidence intervals. Tukey test was used as the post hoc analysis for multiple comparisons. For cytokine experiments, the concentrations were transformed to log2 values and analyzed as mentioned previously. P values lower than 0.05 (*p≤0.05) were taken as statistically significant.

XII. Results

Fusion Protein Design, Expression, and Quantification.

To independently explore the two of the most studied signaling pathways of the β_2AR, separate DNA constructs containing either the β_2AR fused with Gαs protein (β_2AR-Gαs) or β_2AR fused with βarr2 (β_2AR-βarr2), were designed by Dr. Ruan (collaborator) and manufactured by Norclone laboratories. Both constructs were designed to ideally allow structural flexibility between the receptor and the fused protein while also restricting other signaling proteins to be recruited to the receptor (Fig. 1A). For the β_2AR-Gαs fusion protein, a two amino acid linker (Leu-Glu) between the C-terminal tail of the β_2AR and the N-terminal of the Gαs protein was added. A 12 amino acid linker (Leu-Glu-Gly-Gly-Pro-Gly-Thr-Glu-Leu-Gly-Ser-Thr) was added between the C-terminal tail of the β_2AR and the N-terminal of the βarr2 (Fig. 1B). After stable transfection of either: the β_2AR alone (t β_2AR), the β_2AR-Gαs, or the β_2AR-βarr2 fusion proteins in HEK 293 cells, RT-PCR was employed to detect the mRNA expression of our constructs. A forward primer targeting the β_2AR and a reverse primer targeting either the β_2AR, Gαs, or βarr2 was used to detect the receptor alone and the fusion proteins (Fig. 1C). As expected, the nucleotide base pairs of the non-transfected (HEK 293) group and the group transfected with the t β_2AR alone were 1.23kb, whereas the molecular weights were 2.5Kb and 2.4Kb for the groups transfected (t) with either the β_2AR-Gαs (t β_2AR-Gαs) or β_2AR-βarr2 (t β_2AR-βarr2) fusion proteins, respectively (Fig. 1D). To further quantify the protein expression of all transfected groups we performed saturation binding assays using [^{3}H] DHA. The expression of the t β_2AR group was at least 10 times higher (1.238 ± 0.106 pM/mg) than the fusion protein groups (t β_2AR-Gαs = 22.08 ± 1.3 fmol/mg; t β_2AR-βarr2 = 121.3 ± 6 fmol/mg) (Fig. 1E). Although the functional response of the β_2AR in the wild-type (WT) HEK 293 group was quantifiable (see Fig. 4A, B), there was no adequate signal in radioligand binding assays (low signal-to-noise ratio) to allow quantification of the receptor expression.

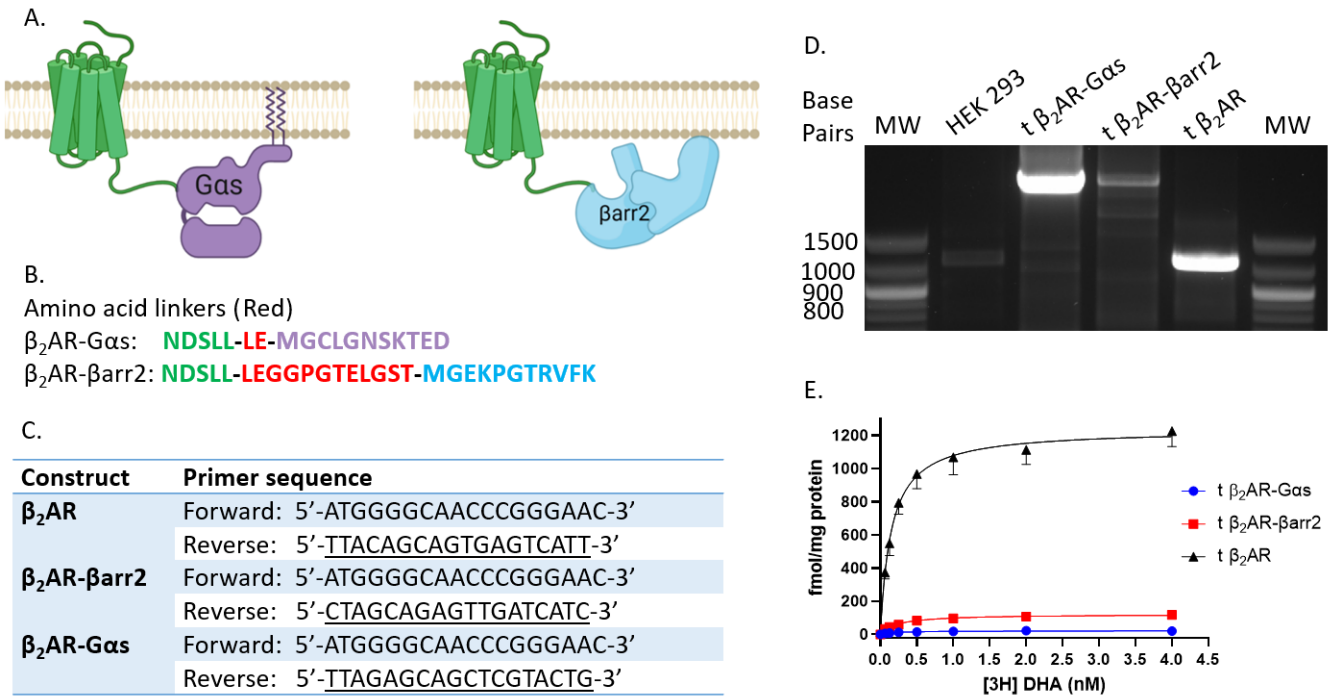

Figure 1. Design and expression of the fusion proteins β2AR-Gαs and β2AR-βarr2 in HEK 293 cells.

(A) Schematic representation of the β2AR (green) at the membrane tethered by its C-terminal to the N-terminal of the signaling proteins Gαs (purple) or βarr2 (blue). (B) Amino acids (red) are used for protein linkage between the C-terminal of the β2AR and the N-terminal of the signaling molecules Gαs and βarr2. (C) Forward and reverse primers were used to detect the genetic expression of β2AR alone or when fused to either Gαs or βarr2. (D) Reverse transcriptase-PCR shows the gene expression of either β2AR alone (t β2AR) and when fused to Gαs (t β2AR-Gαs) or βarr2 (t β2AR-βarr2). The first and last columns show the molecular weight ladder for base-pair quantification. (E) Saturation binding assays using increasing concentrations of [3H] dihydroalprenolol (DHA) in all transfected groups. The transfected group with the β2AR alone (black) showed a Kd=147.6 ± 28nM. The β2AR-Gαs (blue) and β2AR-βarr2 (red) showed a Kd=213± 49nM and 232.7 ± 22nM, respectively. Data shown are the means ± S.E.M. from 3 independent experiments. Molecular weight; MW.

Some β_2AR ligands show a differential affinity for the β_2AR when fused to either Gαs or βarr2.

Competitive binding assays were used to determine if the fusion of the β_2AR with either Gαs or βarr2 modified the affinity of selected β_2AR ligands for the receptor moiety. All data was fit into a one-site (monophasic) model to obtain the binding affinities (Ki) for comparison between groups. As seen in table 1, the pKi values of the tested β_2AR ligands on the t β_2AR control group are similar to previously reported values (Baker, 2005; Hoffmann et al., 2004; Louis et al., 1999). All the β_2AR agonists had higher affinity for the t β_2AR-Gαs group compared to the t β_2AR-βarr2 group as shown by higher pKi values on the t β_2AR-Gαs group whereas isoproterenol and epinephrine were the only agonists to show an increased affinity for the t β_2AR-Gαs group compared to the t β_2AR group (Table 1). Additionally, AgGs showed an increased affinity for the t β_2AR group compared to the t β_2AR-βarr2 group. Regarding the β_2AR ligands known as beta-blockers, propranolol was the only beta-blocker with a higher affinity for the t β_2AR-βarr2 group compared to the t β_2AR-Gαs group. Nadolol showed a higher affinity for the t β_2AR group versus both fusion proteins. Carvedilol and propranolol had higher affinity for the receptor alone when compared to the t β_2AR-Gαs group. Comparatively, alprenolol had increased affinity only for the t β_2AR group when compared to the t β_2AR-βarr2 group. ICI 118,551 and metoprolol did not significantly change their affinity for the receptor alone or when fused to the signaling molecules. All competition binding curves are shown in Fig. 2. Further analysis on the selectivity of ligands for the t β_2AR-Gαs group showed that the preference of all β_2AR agonists, apart from SALB, is at least doubled. On the other hand, propranolol is twice more selective for the t β_2AR-βarr2 group. This data suggests that the fusion proteins can detect small changes in affinity between the two main active conformational states of the receptor which facilitates the identification of affinity bias for currently used and new β_2AR ligands.

Table 1. Functional Affinity

Radioligand binding experiments to calculate the differential affinity of multiple β_2AR ligands in HEK293 cells transfected with β_2AR-Gαs, β_2AR-βarr2, or WT β_2AR. Measurements are expressed as -pKi values. Data are the mean ± S.E.M. of 3 independent experiments with repeats in duplicate.

Ligands	t β_2AR-Gαs	t β_2AR-βarr2	t β_2AR	β_2AR-Gαs selectivity (ratio)
Isoproterenol	7.09±0.09*@	6.44±0.07	6.67±0.04	4.47
Epinephrine	6.54±0.11*@	5.93±0.08	6.16±0.05	4.07
Indacaterol	7.58±0.10*	7.17±0.06	7.41±0.04	2.57
Salbutamol	5.98±0.09*	5.73±0.09	5.84±0.06	1.78
AgGs	5.88±0.09*	5.42±0.09	5.77±0.07*	2.88
Nadolol	8.30±0.07	8.09±0.08	8.55±0.05*&	1.62
Carvedilol	9.31±0.09	9.52±0.08	9.56±0.08&	0.62
ICI 118,551	8.89±0.09	8.94±0.06	8.94±0.07	0.89
Propranolol	8.72±0.08	9.00±0.04&	9.14±0.05&	0.52
Metoprolol	5.90±0.08	5.97±0.10	6.12±0.06	0.85
Alprenolol	8.96±0.05	8.86±0.08	9.16±0.08*	1.26

**P<0.05 vs t β_2AR-βarr2, @P<0.05 vs t β_2AR and &P<0.05 vs t β_2AR-Gαs. Two-way AVNOVA. Tukey post-hoc test.*

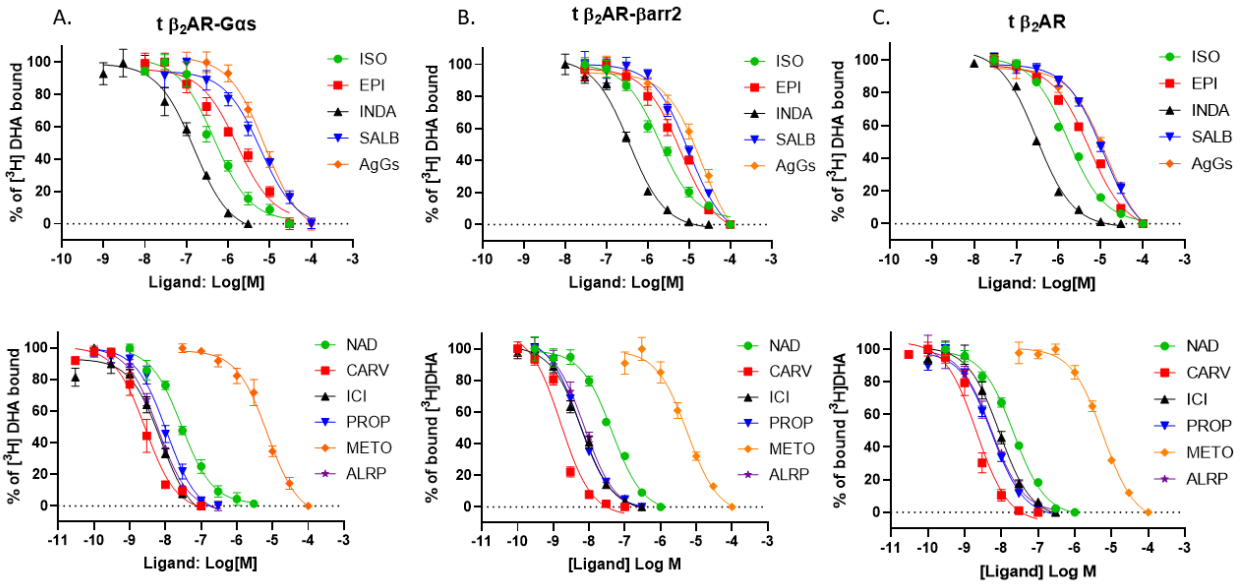

Figure 2. Competition binding curves of multiple β2AR ligands in all transfected groups.

Increasing concentrations of β_2AR ligands were added to HEK 293 membrane preparations after 2-hour incubation with 1nM of radioligand Dihydroalprenolol Hydrochloride, Levo-[Ring, Propyl-3H(N)]- ([3H] DHA). This concentration was previously determined by saturation binding studies. Full receptor occupancy by [3H] DHA was observed as 100% whereas complete displacement of [3H] DHA from the receptor was measured as 0%. The agonists' isoproterenol (ISO; green), epinephrine (EPI; red), indacaterol (INDA; black), salbutamol (SALB; blue), and a novel biased agonist for Gs (AgGs; orange) are shown in the upper graphs. The antagonists/inverse agonists' nadolol (NAD; green), carvedilol (CARV; red), ICI 118,551 (ICI; black), propranolol (PROP; blue), metoprolol (METO; orange), and alprenolol (ALPR; purple) are shown in the lower graphs. (A) HEK 293 cells transfected with the β_2AR-Gαs fusion protein. All agonists show a leftward displacement of the binding curves compared to the t β_2AR-βarr2 group. (B) HEK 293 cells transfected with the β_2AR-βarr2 fusion protein. PROP was the only curve significantly shifting to the left when compared to the t β_2AR-Gαs group. (C) HEK 293 cells transfected with the wild type β_2AR. NAD, CARV, and PROP curves showed a leftward shift compared to the t β_2AR-Gαs group whereas NAD and ALPR curves were displaced to the left when compared to the t β_2AR-βarr2

group. All data points are shown as the mean ± S.E.M. The competitive curves were performed in duplicate on 3 separate occasions (n=3).

The fusion proteins show constitutive activity for a single pathway and sterically hinder the reciprocal protein from coupling to the receptor.

Since the fusion of a signaling protein with the receptor forces both proteins to be in close proximity, we tested the constitutive activity of the fusion proteins in the absence of ligand on the Gαs signaling pathway, through cAMP accumulation, and on the βarr2 signaling pathway, through ERK1/2 phosphorylation. For the Gαs pathway, all transfected groups showed increased constitutive activity compared to the HEK 293 group (Fig. 3A). By adding 10μM ICI 118,551 (a selective β_2AR antagonist/inverse agonist) the constitutive activity of the t β_2AR-βarr2 was completely inhibited, whereas the t β_2AR-Gαs activity remained highly increased and the t β_2AR was reduced by half (Fig. 3A). For ERK phosphorylation, the only group with a significant increase in constitutive activity compared to the HEK 293 control group was the t β_2AR-βarr2 (Fig. 3B). Because recent studies showed the formation of a GPCR–G-protein–βarrestin super-complex with sustained activation and signaling of Gαs proteins (Nguyen & Lefkowitz, 2021; Thomsen et al., 2016), we assessed for the potential protein-protein interactions of the β_2AR-Gαs or β_2AR-βarr2 fusion proteins with the reciprocal signaling proteins, βarr2 and Gαs, using a nano luciferase structural complementation reporter system (NanoBiT; described in the *Methods Section*). The control group (t β_2AR) showed the well-established transient interaction between the receptor and the two signaling proteins, Gαs and βarr2, after stimulation with 10μM isoproterenol (ISO), eliciting a 20-fold and 10-fold change in the luminescence intensity for Gαs and βarr2 recruitment, respectively (Fig. 4A, B). The recruitment of Gαs and βarr2 after ISO stimulation was blunted when the receptor was fused to the alternative/reciprocal Gαs or βarr2 proving that the fusion proteins exhibit steric hindrance to Gαs or βarr2 when stimulated by a ligand (Fig. 4A, B). Thus, our fusion proteins can be used to isolate a single signaling pathway by producing a gain-of-function allowing for the exploration of the physiological role of each pathway in different cell systems.

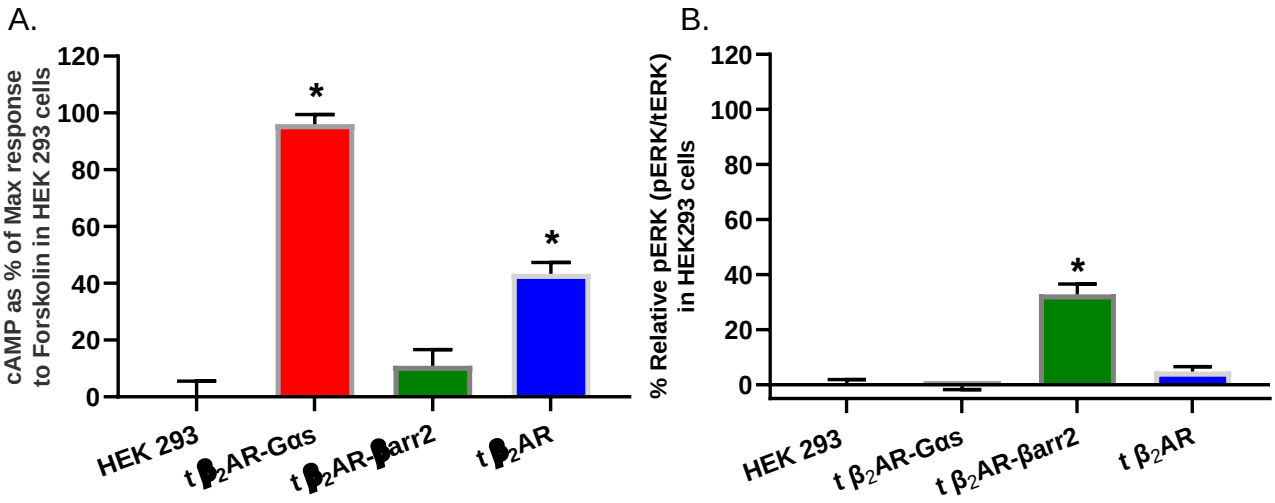

Figure 3. Constitutive activity for Gαs and βarr2 signaling pathways in HEK 293 cells transfected with the fusion proteins.

(A) cAMP measurements represent the Gαs pathway using a scale based on the adenylate cyclase activator, Forskolin (10μM). Forskolin was used to define 100% of the response whereas the basal response of the untransfected HEK 293 cells was used to define 0% of the response in all groups. Under 10μM of ICI 118,551, the t β_2AR-Gαs group (red) proved to be the most constitutively active regardless of the low protein expression levels. The highly expressed t β_2AR group (blue) also shows increased constitutive activity when compared to the basal activity of untransfected HEK 293 cells. Conversely, the t β_2AR-βarr2 group (green) had a similar basal activity when compared with the untransfected HEK 293 cells. (B) ERK1/2 phosphorylation (pERK) is relative to total ERK1/2 (tERK) representing the βarr2 pathway. Here, only the t β_2AR-βarr2 group (green) showed a significant increase in constitutive activity compared to the control untransfected HEK 293 cell group. Data are the means ± S.E.M. from at least 3 independent experiments. *P<0.0001 was considered significant by one-way ANOVA and Tukey was used as the post hoc test.

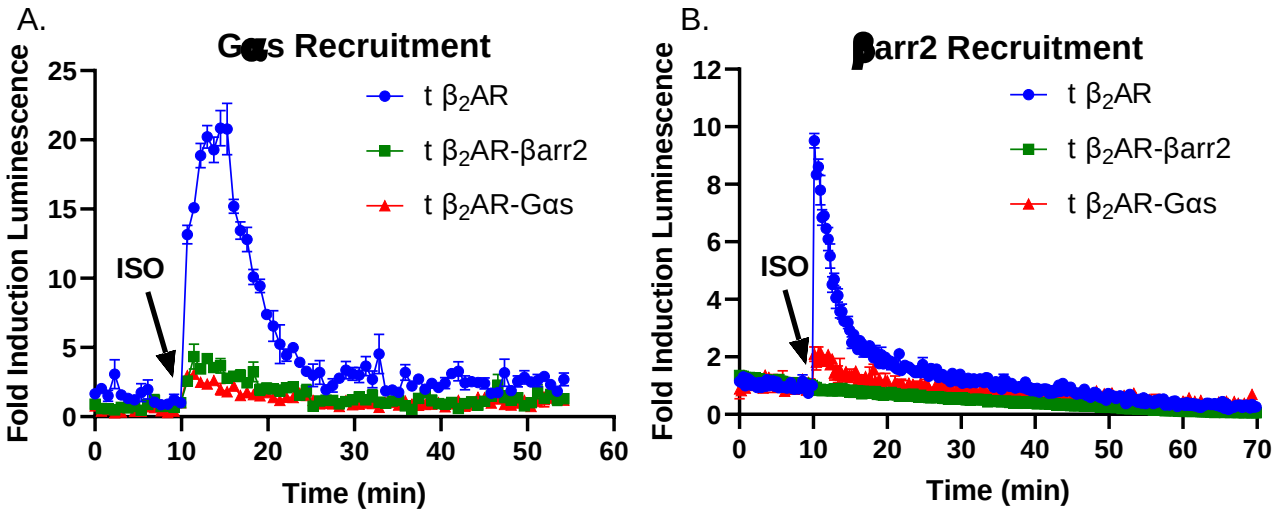

Figure 4. Recruitment of the signaling molecules Gαs and βarr2 is hindered by the fusion moiety tethered to the β_2AR.

Fusion proteins and signaling molecules were labeled with LgBiT and the complementary SmBiT, respectively, using NanoBiT technology to detect protein-protein interactions by changes in luminescence. (A) The overexpressed β_2AR (blue) recruits Gαs after 10μM Isoproterenol (ISO) stimulation. This recruitment is drastically blunted when the receptor is fused to either Gαs (red) or βarr2 (green). (B) Similarly, the recruitment of βarr2 is triggered by stimulation with 10μM ISO, and such recruitment is diminished when the receptor is fused to either Gαs or βarr2. All experiments are expressed as the mean ± S.E.M from 3 independent experiments (n=3).

The fusion proteins remain functionally responsive to ligand stimuli.

To test if the fusion between the β_2AR with either Gαs or βarr2 affected the capacity of the receptor to elicit a functional response after ligand delivery, we performed concentration-response curves for both signaling pathways using the β_2AR agonist ISO followed by competitive antagonist displacement curves using ICI 118,551. For measurement of cAMP accumulation, we first established the response window for each group by using 10μM Forskolin, an adenylate cyclase activator, to elicit the maximal response on cAMP (labeled as 100%) independent from the stimulation of any β_2AR ligand (Fig 5). To define the basal cAMP levels (labeled as 0%) of each group separately, 300nM ICI was used to inhibit the constitutive activity of the non- and transfected groups. This set of experiments revealed a unique window for each group for cAMP accumulation that was used to quantify the response of all β_2AR ligands and determine their biased signaling, if any, in a scale independent from a reference ligand. Alternatively, a scale independent from ligand stimulation was established by using measurements on ERK1/2 phosphorylation (pERK) relative to the value of total ERK1/2 (tERK) in each group to evaluate the βarr2 signaling response.

For the cAMP measurements representing the Gαs pathway, all groups showed classic sigmoidal curves under increasing concentrations of ISO and, as anticipated, increasing concentrations of ICI 118,551 proportionately displaced the ISO concentration-response curve to the right (Fig. 6). The maximal response (Emax) of ISO was decreased ~25% and ~21% in the HEK 293 and the t β_2AR-βarr2 groups, respectively, even at the lowest concentration used of ICI 118,551 (10nM). Alternatively, the Emax of ISO under any ICI 118,551 concentration remained the same for the t β_2AR-Gαs and t β_2AR groups. Importantly, the potency of ISO was increased by more than one logarithmic unit (10-fold increase) in the t β_2AR-Gαs and t β_2AR groups compared to the HEK and t β_2AR-βarr2 groups (Table 2). Further analysis on the rightward shift of the ISO concentration response curves by ICI 118,551 suggested a higher apparent affinity (pA_2) of ICI 118,551 for the fusion proteins β_2AR-Gαs and β_2AR-βarr2 (pA_2=10.16 and 10.38, respectively) compared to both control groups (HEK 293 pA_2=9.21; t β_2AR pA_2=9.42) (Table 3). However, the Schild plot slope is greater than

unity for the control groups which might invalidate this analysis (Kenakin 1997). Therefore, we reanalyzed the data excluding the lowest concentration of ICI and under a linear slope with a value of one using the log (concentration ratio - 1). This analysis showed decreased pA_2 values that did not differ amongst groups (Table 3) and was closer to the values obtained from binding affinity experiments.

Regarding the βarr2 signaling, the same pattern of sigmoidal curves under increasing concentrations of ISO and a rightward shift by ICI 118,551 was observed in all groups when relative ERK1/2 (pERK/tERK) was measured. The right-shift displacement of the ISO curve in the t β_2AR was only apparent when 30nM of ICI 118,551 was used (Fig. 7). The intrinsic activity of ISO was unaffected in the t β_2AR-βarr2 and t β_2AR groups and significantly reduced by ~40% for the HEK 293 and t β_2AR-Gαs groups under pretreatment with ICI 118,551. ISO displayed similar potency among all groups (Table 2). The pA_2 values of ICI 118,551 were also similar among all groups (Table 3). Together with the cAMP measurements, this data shows that the fusion proteins are functionally responsive to ligand stimuli and that the maximal response of ISO for each pathway is affected by ICI 118,551 when the alternative signaling molecule is fused to the receptor.

Table 2. Competitive antagonism

The potency of ISO and rightward displacement by the competitive agonists ICI 118,551.
Measurements are expressed as -pEC$_{50}$ values obtained from semilogarithmic concentration-response curves of the control HEK 293 and t β_2AR groups, and the fusion protein groups t β_2AR-Gαs and t β_2AR-βarr2. The displacement curves were generated using increasing concentrations of ICI 118,551 (10nM to 300nM). The two main signaling pathways of the β_2AR, Gαs, and βarr2, are explored by measurements of cAMP accumulation and ERK phosphorylation (pERK), respectively. Data are the mean ± S.E.M. of at least 3 independent experiments with repeats in triplicate for cAMP and duplicate for ERK.

	cAMP					pERK		
ICI	**No ICI**	**10nM**	**30nM**	**100nM**	**300nM**	**No ICI**	**10nM**	**30nM**
HEK 293	8.43±0.09	7.15±0.16	6.73±0.16	6.26±0.19	5.72±0.23	6.93±0.21	6.61±0.3	6.39±0.44
t β_2AR-Gαs	10.12±0.3	9.02±0.07	8.55±0.07	8.07±0.05	7.57±0.06	7.01±0.16	6.98±0.17	6.66±0.17
t β_2AR-βarr2	8.99±0.12	7.58±0.1	7.12±0.08	6.74±0.09	6.21±0.1	7.37±0.17	6.98±0.22	6.42±0.22
t β_2AR	10.28±0.65	9.84±0.28	9.04±0.09	8.43±0.07	7.91±0.05	6.97±0.19	6.95±0.29	6.79±0.23

Table 3. Schild regression analysis

Schild regression analysis for the competitive antagonism of ICI 118,551.
The apparent affinity (pA$_2$) of the competitive antagonist ICI 118,551 was calculated in non-transfected HEK 293 cells and transfected with the wild type β_2AR, or the fusion proteins β_2AR-Gs or β_2AR-βarr2 using the Schild analysis. The adapted analysis for pA$_2$ calculation was necessary as the slopes were different from unity. Data are the mean ± S.E.M. of at least 3 independent experiments

	cAMP			**pERK**	
	pA$_2$	**Schild-plot Slope**	**pA$_2$ (adapted analysis)**	**pA$_2$**	**Schild-plot Slope**
HEK 293	9.43±0.16	1.191±0.08	9.19	8.96±0.58	0.95±0.44
t β_2AR-Gαs	10.16±0.11*	1.049±0.03	9.05	8.75±0.30	1.11±0.31
t β_2AR-βarr2	10.38±0.16*	1.031±0.05	9.3	8.4±0.17	1.08±0.23
t β_2AR	9.21±0.25	2.015±0.06	8.8	8.04±0.41	0.77±0.58

**P<0.05. Two-way AVNOVA. Tukey post-hoc test.*

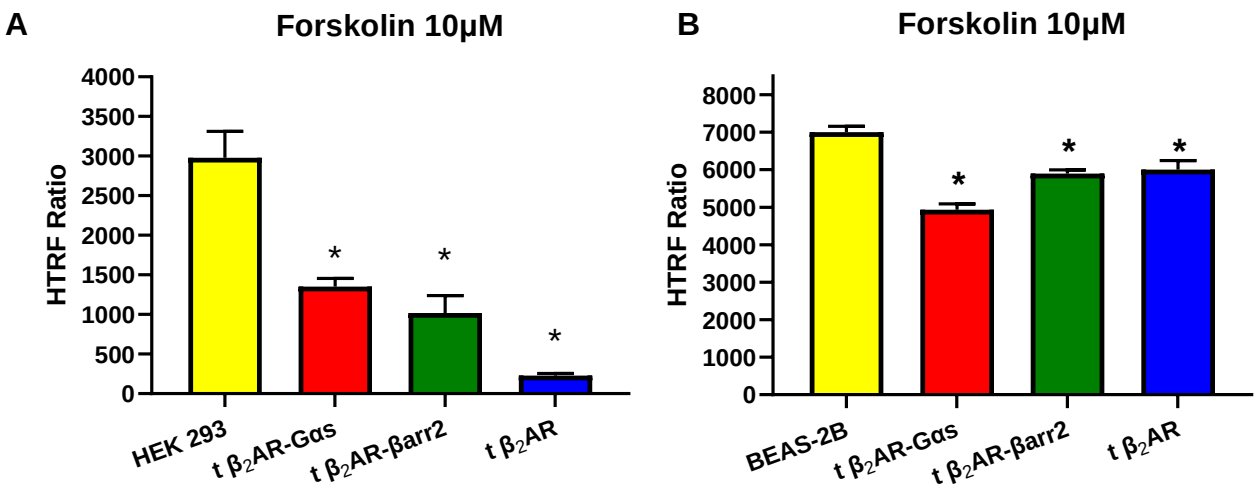

Figure 5. Homogeneous Time-Resolving Fluorescence (HTRF) technology to measure cAMP levels.

To define the maximal response for cAMP measurements in all groups, a saturating concentration of the adenylate cyclase stimulator, Forskolin (10μM), was used. The HTRF ratio represents the signal between the cAMP-tagged d2 fluorophore and the anti-cAMP-Cryptate antibodies. The signal recorded as the HTRF ratio is inversely proportional to the cAMP levels in the system. (A) The t β_2AR (blue) shows the highest cAMP levels whereas the HEK 293 group (yellow) shows the lowest cAMP levels after Forskolin stimulation. (B) The BEAS-2B group (yellow) and the t β_2AR-Gαs group (red) have the lowest and highest cAMP levels, respectively. All experiments were performed in triplicate on three separate occasions (n=3).

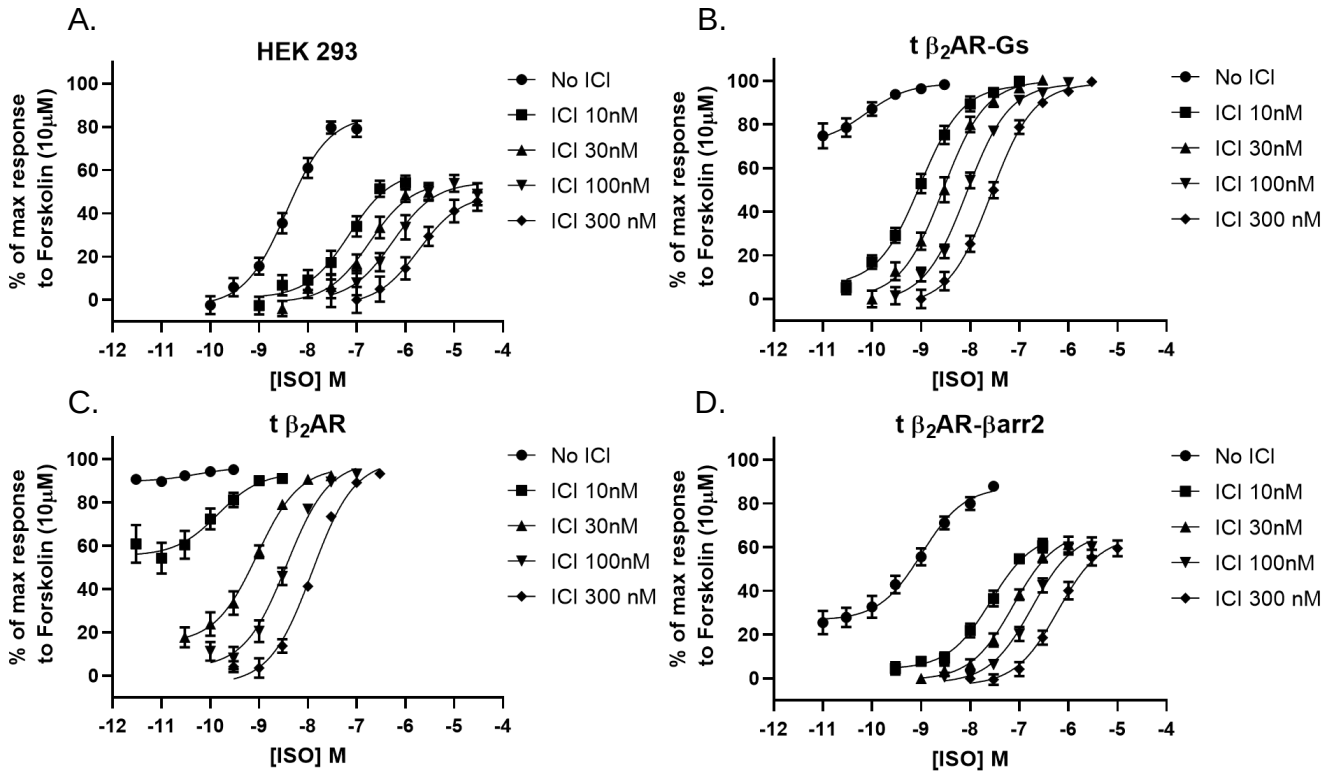

Figure 6. Schild regression analysis for the Gαs signaling pathway using the competitive antagonist ICI 118, 551.

Semi logarithmic concentration-response curves of increasing concentrations of isoproterenol (ISO) at the Gαs pathway of the β_2AR. Accumulation of cAMP levels represents the Gαs pathway using a scale based on the adenylate cyclase activator, Forskolin (10µM). Forskolin was used to define 100% of the response whereas the basal response was determined under 300nM of ICI 118,551 (ICI) to define 0% in each group. Thus, the response window was unique to each group. Pre incubation with increasing semilogarithmic concentrations of ICI (10nM to 300nM) elicited the progressive rightward shift of ISO curves. The pEC_{50} values were used to calculate the pA_2 of ICI in all groups. Circles = No ICI; squares = ICI 10nM; triangles = ICI 30Nm; inverted triangles = ICI 100nM; diamonds = ICI 300nM (A) Non-transfected HEK 293 cells. Preincubation with ICI decreases the maximal response of ISO. (B) HEK 293 cells transfected with the β_2AR-Gαs fusion protein (t β_2AR- Gαs). (C) HEK 293 cells transfected with the wild type β_2AR (t β_2AR). (D) HEK 293 cells transfected with the β_2AR-βarr2 fusion protein (t β_2AR-βarr2). Like the non-transfected HEK 293 cells,

preincubation with ICI decreases the maximal response of ISO in this group. All data points are shown as the mean ± S.E.M. The competitive curves were performed in triplicate on at least 3 separate occasions (n≥3).

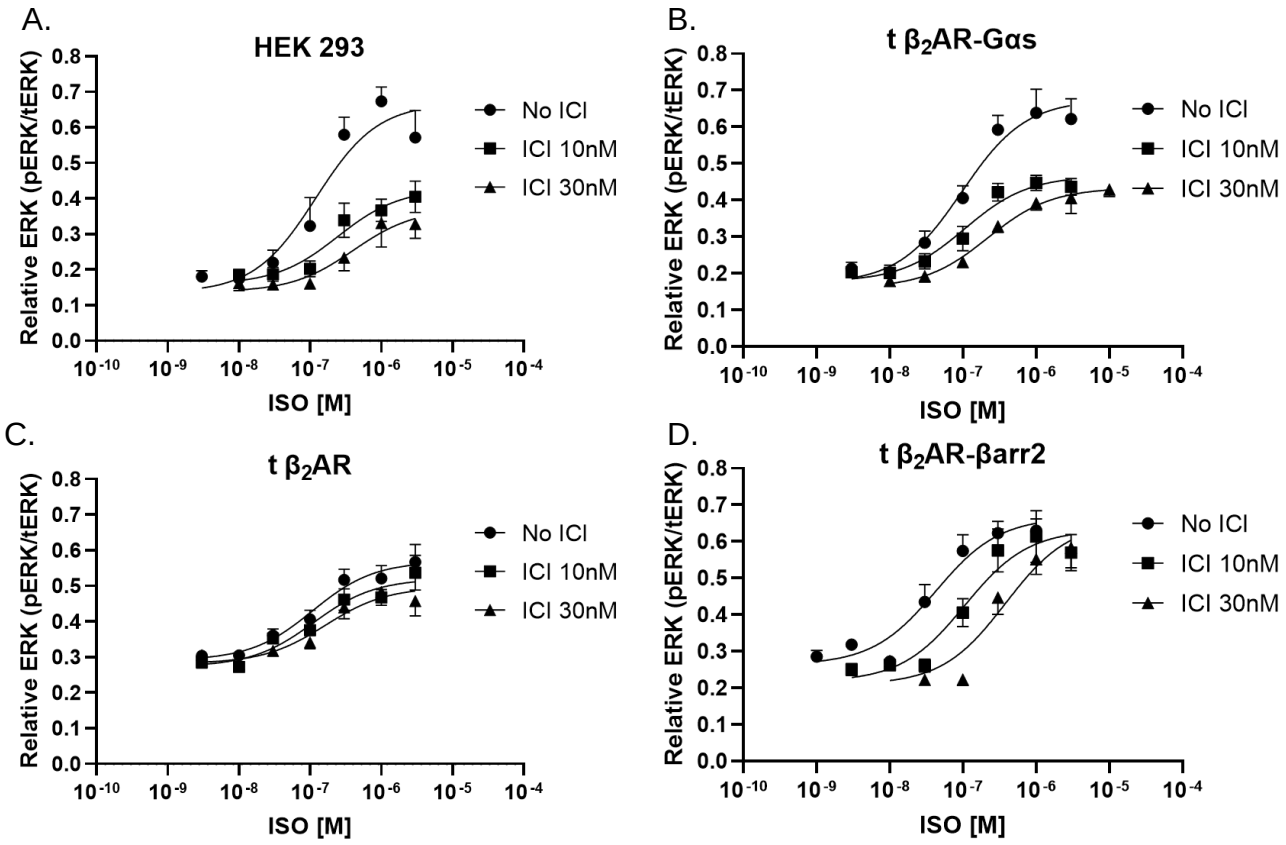

Figure 7. Schild regression analysis for the βarr2 signaling pathway using the competitive antagonist ICI 118, 551.

Semi logarithmic concentration-response curves of increasing concentrations of isoproterenol (ISO) at the βarr2 pathway of the β_2AR. ERK1/2 phosphorylation (pERK) is relative to total ERK1/2 (tERK) representing the βarr2 pathway in all groups. Preincubation with increasing semilogarithmic concentrations of ICI (10nM to 30nM) elicited the progressive rightward shift of ISO curves. The pEC_{50} values were used to calculate the pA_2 of ICI in all groups. Circles = No ICI; Squares = ICI 10nM; triangles = ICI 30nM. (A) Non-transfected HEK 293 cells. Preincubation with ICI decreases the maximal response of ISO. (B) HEK 293 cells transfected with the β_2AR-Gαs fusion protein (t β_2AR- Gαs). Like the non-transfected HEK 293 cells, preincubation with ICI decreases the maximal response of ISO in this group. (C) HEK 293 cells transfected with the wild type β_2AR (t β_2AR). (D) HEK 293 cells transfected with the β_2AR-βarr2 fusion protein (t β_2AR-βarr2). All data points are shown as the mean ± S.E.M. The competitive curves were performed in duplicate on at least 3 separate occasions (n≥3).

The fusion proteins serve as tools to discriminate ligand bias.

Because of the nature of the fusion proteins (spontaneous receptor-signaling protein interaction) and restricting the active conformational state of the receptor to a single pathway, we hypothesized that the fusion proteins could discriminate the β_2AR ligands that preferentially bind to one conformational state of the receptor and modify their potency. To maximize the signaling window of each assay, for agonism experiments on the Gαs pathway, the constitutive activity of all transfected groups was decreased by ICI 118,551 to obtain the largest response window (as observed in Fig. 3). For measurement of antagonism/inverse agonism, no ICI 118,551 was used but cell number was decreased to 2,000 cells/well to increase the responsive window of the receptor to β_2AR ligands in all groups when possible (i.e., the HEK 293 control group was not responsive under these settings). On the measurements of the βarr2 pathway, agonism was tested as previously described, whereas an increase in cell number (i.e., 220,000 cells/well) was necessary to raise the constitutive activity of our test system and maximize inverse agonism after receptor stimulation.

The potency of β_2AR agonists on cAMP accumulation is enhanced when the β_2AR is overexpressed or fused with protein Gαs.

Besides the previously tested isoproterenol (ISO), we also tested the β_2AR endogenous ligand Epinephrine (EPI) and the commonly used β_2AR ligands for respiratory diseases indacaterol (INDA) and salbutamol (SALB). Additionally, we also included a novel β_2AR ligand that has shown biased agonism for the Gαs pathway (AgGs) and could potentially be used for the treatment of respiratory diseases. All agonists had a decreased intrinsic activity in the HEK 293 group of more than 30% compared to the t β_2AR group (Table 4). Additionally, the concentration response curves for all ligands showed a leftward shift in the t β_2AR group compared to the HEK 293 group (Fig 8A and C). Because there is a difference of at least 3 orders of magnitude in the receptor density between these groups (Fig. 1E), this data consistently shows that the potency of β_2AR agonists on the Gαs pathway is directly proportional to the receptor density. When the fusion proteins were tested, the t β_2AR-Gαs group behaved similarly to the t β_2AR in displacing the concentration-response curves of all

ligands to the left (Fig. 8B and C). However, all ligands, except for ISO, decreased their intrinsic activity to a similar extent as in the HEK 293 group (Table 4). The concentration-response curves of the β_2AR agonists in the t β_2AR-βarr2 group were to the right compared to the t β_2AR-Gαs and t β_2AR group (Fig 8B and D). Additionally, all agonists in the t β_2AR-βarr2 group showed the lowest intrinsic activity of all groups, consistent with the inability of the β_2AR-βarr2 fusion protein to recruit Gαs and signal through this pathway (Table 4). Finally, the order of potency was the same between fusion protein groups (ISO≈EPI>INDA>SALB≈AgGs) whereas the order of potency for the HEK 293 and t β_2AR group was ISO>INDA≈EPI>SALB>AgGs and ISO>EPI>INDA>SALB>AgGs, respectively (Table 4).

Table 4. Potency quantification of β_2AR agonists for the Gs pathway

Quantification of the potency and maximal response of β_2AR agonists for the Gαs signaling pathway.
The cAMP accumulation was measured as a surrogate of the Gαs signaling pathway to obtain the potency and maximal response of β_2AR agonists. Potency is expressed as the -pEC$_{50}$ whereas the maximal response (Emax) is expressed as the percentage of response relative to Forskolin. Data are the mean ± S.E.M. of at least 3 independent experiments with repeats in triplicate

Ligands	HEK 293		t β_2AR-Gαs		t β_2AR-βarr2		t β_2AR	
	-pEC$_{50}$	Emax (%)	-pEC$_{50}$	Emax (%)	-pEC$_{50}$	Emax (%)	-pEC$_{50}$	Emax (%)
ISO	6.73±0.16	56.52±4.26	8.55±0.07*	100.3±2.43	7.12±0.09	67.39±3.08	9.04±0.09	95.77±3.69
EPI	6.12±0.28	40.33±4.34	8.32±0.18*	35.40±3.07	7.16±0.52	18.87±4.75	8.19±0.11	80.71±2.90
INDA	6.33±0.33	52.85±7.32	7.07±0.38	58.02±11.84	6.81±0.78	33.99±17.75	7.85±0.06	95.07±2.13
SALB	5.77±0.14	41.05±2.69	6.39±0.16	45.52±3.32	5.75±0.65	23.01±9.75	7.34±0.15	78.34±4.45
AgGs	5.46±0.38	29.62±6.58	6.31±0.5	39.46±9.65	5.71±0.61	24.34±10.51	6.61±0.12	88.96±4.46

**P<0.05 vs t β_2AR-βarr2. least square fit*

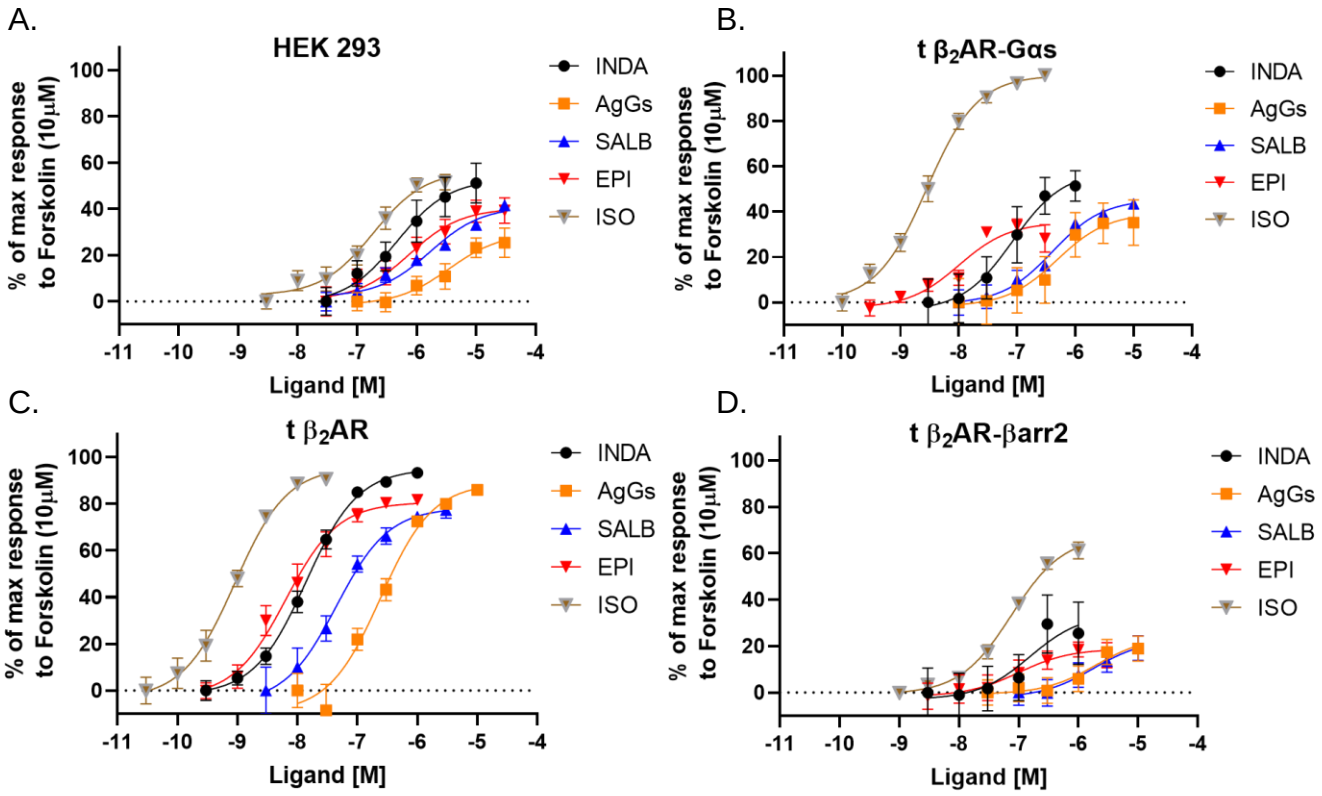

Figure 8. Concentration response curves of multiple β2AR agonists for the Gαs signaling pathway.

Semi logarithmic concentration-response curves of increasing concentrations of indacaterol (INDA; black), a novel biased agonist towards the Gs signaling pathway (AgGs; orange), salbutamol (SALB; blue), epinephrine (EPI; red), and isoproterenol (ISO; grey) at the Gαs signaling pathway. Accumulation of cAMP levels represents the Gαs pathway using a scale based on the adenylate cyclase activator, Forskolin (10µM). Forskolin was used to define 100% of the response whereas the basal response was determined under 30nM of ICI 118,551 (ICI) to define 0% in each group. Thus, the response window was unique to each group. All experiments were preincubated with ICI 118,551 30nM to maximize the response window. The pEC_{50} values obtained from these curves were used as part of the mathematical approach to calculate signaling bias. (A) Non-transfected HEK 293 cells. (B) HEK 293 cells transfected with the β2AR-Gαs fusion protein (t β2AR- Gαs). (C) HEK 293 cells transfected with the wild type β2AR (t β2AR). The β2AR ligands tested become full agonists when the β2AR is overexpressed. (D) HEK 293 cells transfected with the β2AR-βarr2 fusion protein (t

β_2AR-βarr2). All data points are shown as the mean ± S.E.M. The concentration-response curves were performed in triplicate on at least 3 separate occasions (n≥3).

Inverse agonism on cAMP production can be readily detected when the β_2AR is overexpressed or fused to βarr2.

The clinically relevant β_2AR blockers nadolol (NAD), carvedilol (CARV), propranolol (PROP), alprenolol (ALPR), and metoprolol (METO), as well as the selective β_2AR antagonist/inverse agonist, ICI 118,551 (ICI), were tested for distinctive responses elicited by the receptor alone and, by the fusion proteins. The set of experiments testing for antagonism/inverse agonism on the control group HEK 293 did not change the basal level of cAMP production (Table 5). Moreover, the increasing concentrations of all β_2AR blockers did not elicit any detectable response in this group (Fig. 9A). Thus, the herein tested β_2AR blockers behave as neutral antagonists in a cellular system with scarce receptors, showing low constitutive cAMP production which cannot be further decreased pharmacologically. Conversely, the elevated constitutive activity of the t β_2AR group, given by the receptor overexpression, allowed for the detection of inverse agonism elicited by all β_2AR blockers (Fig. 9C). Similarly, the increased constitutive cAMP levels observed in the t β_2AR-βarr2 group were reduced after increasing concentrations of any β_2AR blocker (Fig. 9D). All β_2AR blockers showed a similar IC_{50} between the t β_2AR-βarr2 and the t β_2AR group. Thus, apart from increasing the expression of the receptor, the detection of inverse agonism can also occur when the β_2AR is fused to βarr2. This suggests that these β_2AR blockers preferentially bind to the inactive conformation and/or the conformation of the receptor that favors βarr2 coupling. Accordingly, all β_2AR blockers except for NAD, which showed inverse agonism at high concentrations (pIC_{50}= 5.85 ± 0.4), behaved as neutral antagonists in the t β_2AR-Gαs group even though the constitutive cAMP levels of this group were similar to the t β_2AR-βarr2 group (Fig. 9B). This is also suggestive of the preference of β_2AR blockers for a receptor conformation different from the one that couples to Gαs. The potency order of t β_2AR blockers for the t β_2AR-βarr2 group was ALPR>PROP≈ICI>NAD>CARV>>METO, whereas the potency order for the t β_2AR group was ALPR>ICI≈PROP>CARV>NAD>>METO.

Table 5. Potency quantification of β2AR antagonists for the Gs pathway

Quantification of the potency and maximal response of β_2AR antagonists/inverse agonists for the Gαs signaling pathway. The cAMP accumulation was measured as a surrogate of the Gαs signaling pathway to obtain the potency and the inverse maximal response of β_2AR antagonists/ inverse agonists. Potency is expressed as the -pEC50 whereas the inverse maximal response (Emax) is expressed as the percentage of response relative to Forskolin. Data are the mean ± S.E.M. of at least 3 independent experiments with repeats in triplicate

Ligands	HEK 293		t β_2AR-Gαs		t β_2AR-βarr2		t β_2AR	
	-pIC$_{50}$	Emax (%)	-pIC$_{50}$	Emax (%)	-pIC$_{50}$	Emax (%)	-pIC$_{50}$	Emax (%)
NAD	N.D.	N.D.	5.85±0.4	9.36±3.07	7.10±0.57*	9.14±1.57	6.59±0.67	10.79±2.02
CARV	N.D.	N.D.	N.D.	N.D.	6.74±0.31	15.17±1.76	7.16±0.57	15.85±2.5
ALPR	N.D.	N.D.	N.D.	N.D.	8.68±1.15	9.96±2.67	8.04±0.62	13.37±2.24
PROP	N.D.	N.D.	N.D.	N.D.	8.30±0.35	11.08±1.37	7.39±1.57	17.09±3.82
METO	N.D.	N.D.	N.D.	N.D.	5.28±0.3	15.52±2.15	5.48±0.26	13.15±4.71
ICI	N.D.	N.D.	N.D.	N.D.	8.22±0.74	10.46±2.91	7.51±0.37	17.32±2.17

*N.D.= non detectable. *P≤0.05 vs β_2AR-Gαs. Least square fit.*

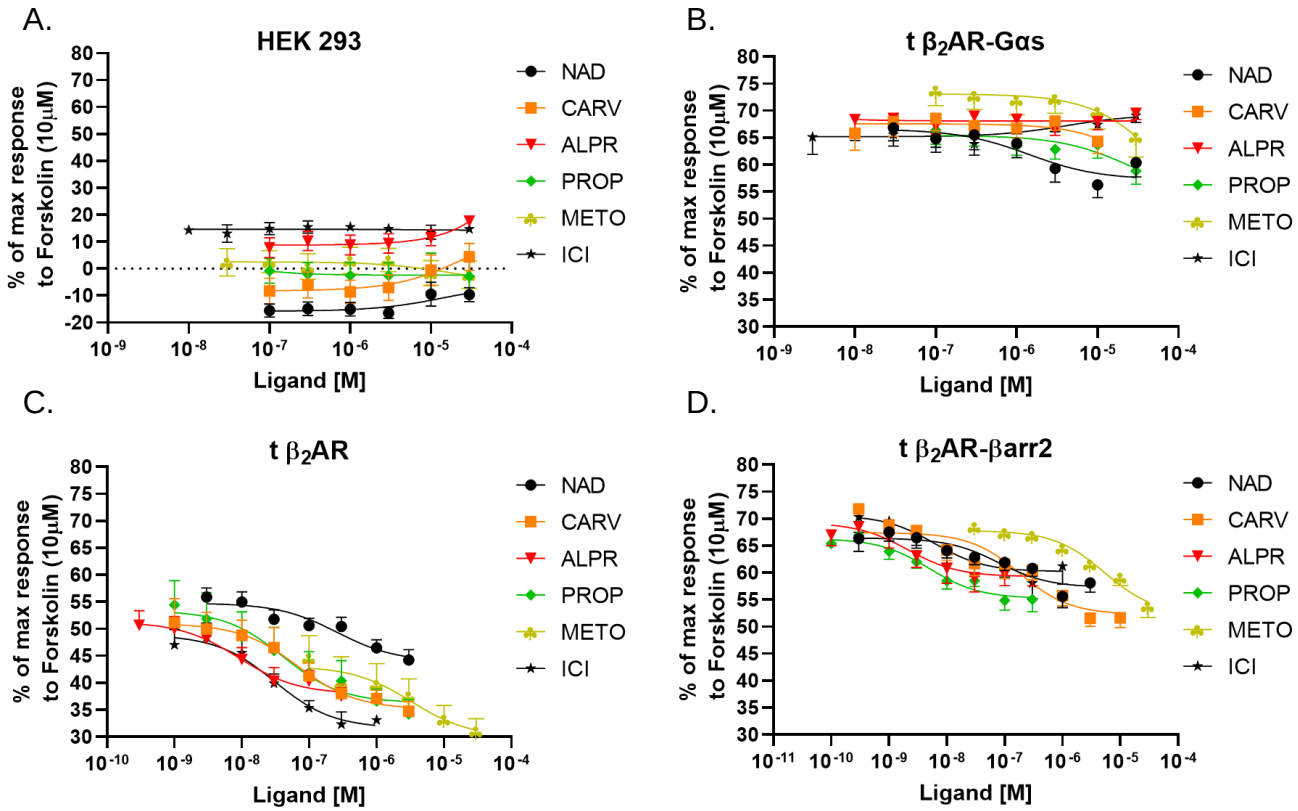

Figure 9. Concentration response curves of multiple β2AR antagonists/inverse agonists for the Gαs signaling pathway.

Semi logarithmic concentration-response curves of increasing concentrations of nadolol (NAD; circle black), carvedilol (CARV; orange), alprenolol (ALPR; red), propranolol (PROP; green), metoprolol (METO; yellow), and ICI 118,551 (ICI; star black) at the Gαs signaling pathway. Accumulation of cAMP levels represents the Gαs pathway using a scale based on the adenylate cyclase activator, Forskolin (10μM). Forskolin was used to define 100% of the response whereas the basal response was determined under 30nM of ICI 118,551 (ICI) to define 0% in each group. Thus, the response window was unique to each group. Note that all transfected groups show high constitutive activity that was not blocked with ICI when increasing concentrations of the β_2AR ligands were tested. The pIC_{50} values obtained from these curves were used as part of the mathematical approach to calculate signaling bias. (A) Non-transfected HEK 293 cells. All ligands behaved as antagonists in this group as shown by the lack of intrinsic activity. (B) HEK 293 cells transfected with the β_2AR-Gαs fusion protein (t β_2AR-Gαs). Only NAD behaved as an inverse agonist by significantly decreasing the constitutive activity of this

group at high concentrations. (C) HEK 293 cells transfected with the wild type β_2AR (t β_2AR). The β_2AR blockers became inverse agonists when the β_2AR is overexpressed. (D) HEK 293 cells transfected with the β_2AR-βarr2 fusion protein (t β_2AR-βarr2). Like the t β_2AR, all β_2AR blockers became inverse agonists when the β_2AR is fused to βarr2. All data points are shown as the mean ± S.E.M. The concentration-response curves were performed in triplicate on at least 3 separate occasions (n≥3).

The potency of β_2AR agonists on ERK1/2 phosphorylation is enhanced when the β_2AR is fused with protein βarr2.

In this set of experiments, we tested the alternative signaling pathway of the β_2AR, βarr2, by measuring ERK1/2 phosphorylation using the previously tested β_2AR agonists. The intrinsic activity of all ligands was decreased in the t β_2AR group compared to the HEK 293 group (Table 6) suggesting that the increase in receptor density does not favor the coupling efficiency between the β_2AR and βarr2. Accordingly, the subsequent group with high receptor density, t β_2AR-βarr2, also blunted the maximal response of all agonists compared to the HEK 293 group, whereas only INDA, SALB, and AgGs were affected in the overexpressed t β_2AR-Gαs group (Table 6).

Despite the decreased maximal response, the t β_2AR-βarr2 group evoked a leftward shift in concentration response curves of all ligands compared to the HEK 293 group (Fig 10D). For the t β_2AR group, only INDA, SALB, and AgGs showed a leftward displacement compared to the HEK 293 group (Fig 10A and C). EPI and AgGs curves showed a rightward and leftward displacement, respectively, by the fusion of the β_2AR with Gαs when compared to the endogenously expressed β_2AR group HEK 293, whereas ISO, INDA, and SALB were unchanged (Fig 10A and B). Further analysis of the best-fit pEC_{50} values of all agonists using an extra sum-of-squares F test, showed EPI pEC_{50} values as significantly different between groups expressing the fusion proteins and between the t β_2AR-Gαs and HEK 293 group (Table 6). The pEC_{50} values of ISO and AgGs were also statistically different between the t β_2AR-βarr2 group and the HEK 293 group. Finally, the order of potency for all groups is as follows:

- HEK 293: INDA>SALB>ISO>EPI>AgGs
- t β_2AR-Gαs: INDA>SALB>ISO≈AgGs>EPI
- t β_2AR-βarr2: INDA>SALB>ISO>AgGs≈EPI
- t β_2AR: INDA>SALB>AgGs>ISO>EPI

Altogether, this data shows that, except EPI, the potency of all β_2AR agonists is not affected by the signaling molecule fused to the receptor. An increase of potency for ISO and AgGs is only detected by the β_2AR-βarr2 fusion protein when compared to the

untransfected group and the potency of EPI is decreased when the receptor is fused to Gαs.

Table 6. Potency quantification of β_2AR agonists for the βarr2 pathway

Quantification of the potency and maximal response of β_2AR agonists for the βarr2 signaling pathway. ERK1/2 phosphorylation relative to total ERK1/2 (pERK/tERK) was measured as a surrogate of the βarr2 signaling pathway to obtain the potency and the maximal response of β_2AR agonists. Potency is expressed as the -pEC50 whereas the maximal response (Emax) is expressed as the percentage of response relative to tERK. Data are the mean ± S.E.M. of at least 3 independent experiments with repeats in duplicate.

Ligands	HEK 293		t β_2AR-Gαs		t β_2AR-βarr2		t β_2AR	
	pEC50	Emax (%)	pEC50	Emax (%)	pEC50	Emax (%)	pEC50	Emax (%)
ISO	6.92±0.2	53.33±5.57	7.01±0.16	50.22±4.16	7.37±0.17$^{\#}$	40.31±3.49	6.97±0.19	27.8±2.82$^{\#}$
EPI	6.76±0.09*	117.3±5.9	6.37±0.14	92.72±6.86	7.01±0.16*	73.81±6.54$^{\#}$	6.72±0.19	29.5±2.95$^{\#}$
INDA	8.04±0.18	66.67±6.51	8.18±0.22	31.88±3.68$^{\#}$	8.37±0.12	43.19±2.87$^{\#}$	8.93±0.40	12.85±3.03$^{\#}$
SALB	7.51±0.15	58.50±4.46	7.60±0.18	26.87±2.53$^{\#}$	7.98±0.22	34.91±3.89$^{\#}$	8.14±0.29	16.74±2.41$^{\#}$
AgGs	6.35±0.18	53.62±5.47	6.93±0.29	22.06±3.36$^{\#}$	7.07±0.2$^{\#}$	43.55±4.52	7.48±0.39	16.84±3.39$^{\#}$

**P≤0.05 vs β_2AR-Gαs. $^{\#}$P≤0.05 vs HEK 293. Least square fit.*

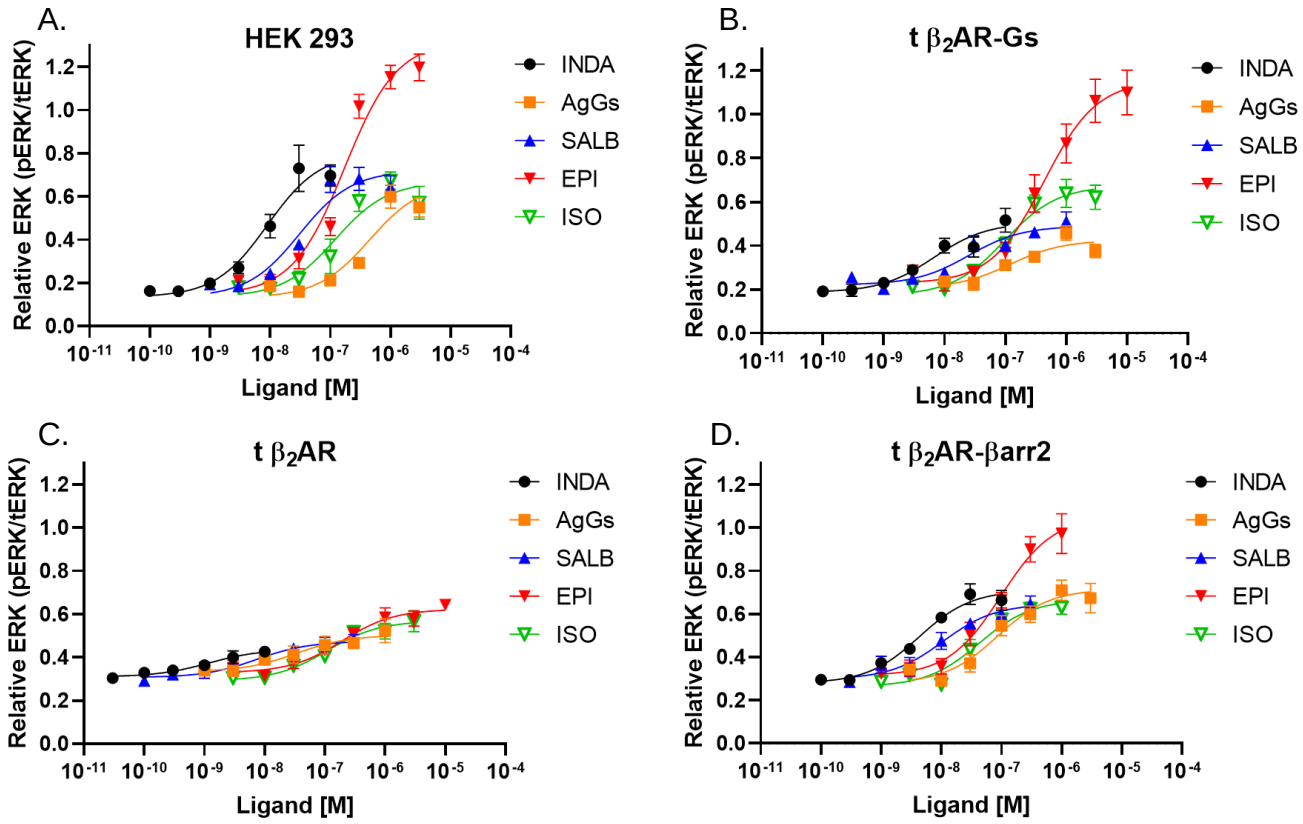

Figure 10. Concentration response curves of multiple β_2AR agonists for the βarr2 signaling pathway.

Semilogarithmic concentration-response curves of increasing concentrations of indacaterol (INDA; black), a novel biased agonist towards the Gs signaling pathway (AgGs; orange), salbutamol (SALB; blue), epinephrine (EPI; red), and isoproterenol (ISO; grey) at the βarr2 signaling pathway. ERK1/2 phosphorylation (pERK) is relative to total ERK1/2 (tERK) representing the βarr2 signaling pathway in all groups. The pEC_{50} values obtained from these curves were used as part of the mathematical approach to calculate signaling bias. (A) Non-transfected HEK 293 cells. The intrinsic activity of all agonists was the highest in this group. (B) HEK 293 cells transfected with the β_2AR-Gαs fusion protein (t β_2AR- Gαs). (C) HEK 293 cells transfected with the wild type β_2AR (t β_2AR). (D) HEK 293 cells transfected with the β_2AR-βarr2 fusion protein (t β_2AR-βarr2). The intrinsic activity of all agonists is significantly reduced in this group. All data points are shown as the mean ± S.E.M. The concentration-response curves were performed in triplicate on at least 3 separate occasions (n≥3).

Inverse agonism for ERK1/2 phosphorylation can be detected by increasing the constitutive activity which allows for direct quantification of potency.

Similar to the previous experiments on β_2AR agonists, we quantified ERK1/2 phosphorylation, this time under increased constitutive activity. All beta-blockers showed an inverse agonist response regardless of the group tested, suggesting that the influence of receptor density is secondary to the constitutive activity of the βarr2 pathway. The maximal response of CARV and ALPR was higher on the t β_2AR group compared to the HEK 293 group whereas the opposite was true for NAD (Table 7). The maximal response of PROP, METO, and ICI was similar among control groups. The maximal response of all beta-blockers did not differ between groups expressing the fusion proteins β_2AR-Gαs or β_2AR-βarr2. All concentration response curves shifted to the left in the t β_2AR-βarr2 group when compared to the t β_2AR-Gαs group except for ALPR that showed a non-significant rightward shift (Fig. 10B and D). NAD, CARV, METO, and ICI curves showed a significant rightward shift in the t β_2AR-Gαs group when compared to both control groups whereas ALPR exhibited a leftward shift compared to the control groups. PROP remained with a similar potency across all groups. Together with the β_2AR agonists, these data can be organized according to an increase in potency at the βarr2 pathway where ALPR is favored by β_2AR-Gαs fusion protein whereas NAD, CARV, METO, ICI, and EPI are favored by β_2AR-βarr2 fusion protein with the rest of ligands (i.e., PROP, ISO, INDA, SALB, and AgGs) showing no preference between fusion proteins.

Table 7. Potency quantification of β_2AR antagonists for the βarr2 pathway

*Quantification of the potency and maximal response of β_2AR antagonists/inverse agonists for the βarr2 signaling pathway. ERK1/2 phosphorylation relative to total ERK1/2 (pERK/tERK) was measured as a surrogate of the βarr2 signaling pathway to obtain the potency and **the inverse** maximal response of β_2AR agonists. Potency is expressed as the -pEC$_{50}$ whereas the maximal response (Emax) is expressed as the percentage of response relative to tERK. Data are the mean ± S.E.M. of at least 3 independent experiments with repeats in duplicate.*

Ligands	HEK 293		t β_2AR-Gαs		t β_2AR-βarr2		t β_2AR	
	-pIC$_{50}$	Emax %	-pIC$_{50}$	Emax %	-pIC$_{50}$	Emax %	-pIC$_{50}$	Emax %
NAD	8.69±0.22*	11.33±1.4	6.95±0.3	9.12±1.42	8.97±0.23*	8.4±1.03	8.88±0.53*	5.45±1.64 $^{\#}$
CARV	8.96±0.34*	6.08±1.07	7.85±0.16	11.35±0.91	9.82±0.24*	9.70±1.2	9.06±0.21*	11.67±1.36$^{\#}$
ALPR	7.69±0.26*	6.57±0.9	9.11±0.24	10.93±1.43	8.56±0.41	8.78±1.6	8.25±0.18*	13.12±1.22$^{\#}$
PROP	7.2±0.32	9.15±1.5	6.30±0.41	8.92±2.05	7.46±0.41*	7.76±1.72	6.82±0.24	9.9±1.28
METO	8.32±0.4*	6.13±1.34	6.03±0.25	9.12±1.31	9.35±0.33*$^{\#}$	10.32±1.83	6.56±0.36*	6.9±1.27
ICI	9.69±0.29*	7.34±1.08	7.42±0.35	8.58±1.59	9.1±0.31*	9.93±1.57	8.86±0.21*	9.37±1.24

**P≤0.05 vs β_2AR-Gαs. $^{\#}$P≤0.05 vs HEK 293. Least square fit.*

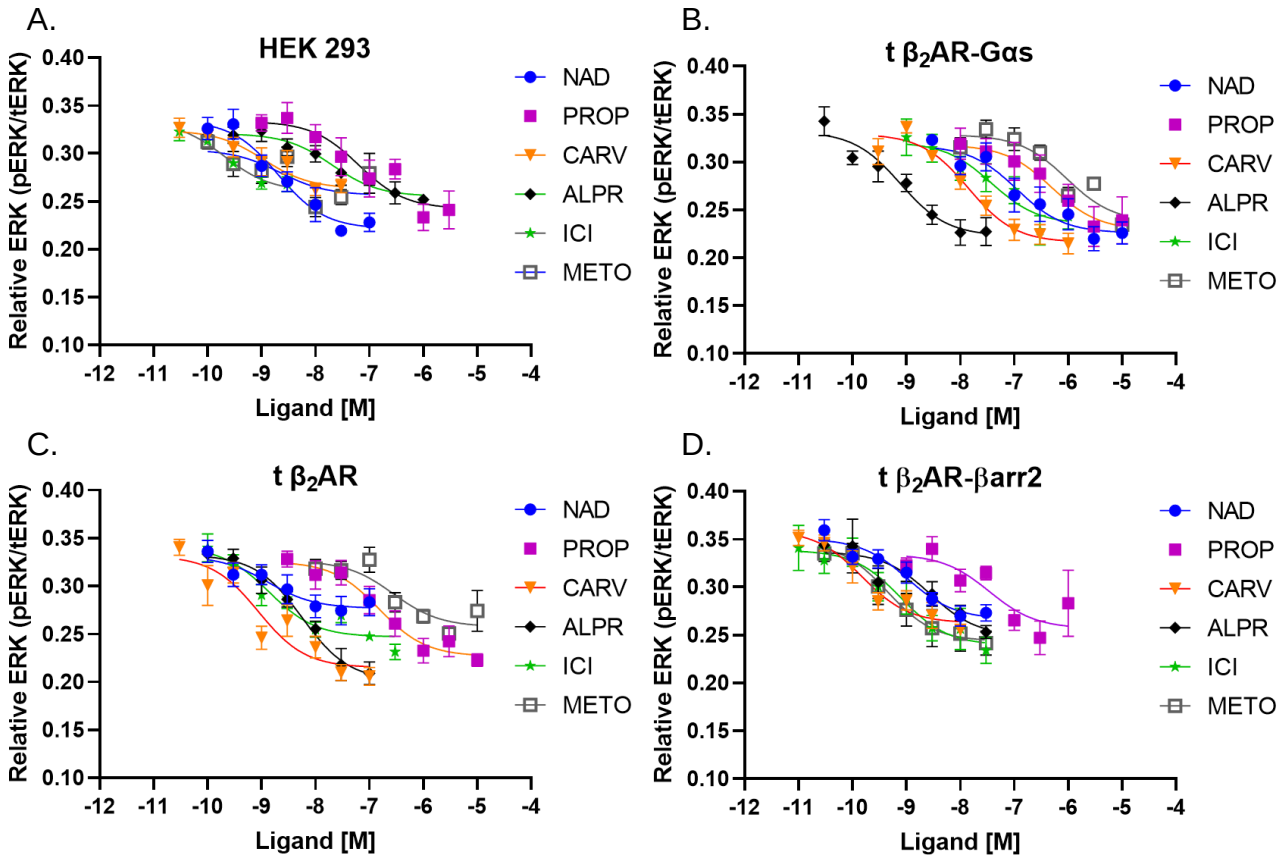

Figure 11. Concentration response curves of multiple β_2AR agonists for the βarr2 signaling pathway.

Semilogarithmic concentration-response curves of increasing concentrations of nadolol (NAD; blue), propranolol (PROP; purple), carvedilol (CARV; orange), alprenolol (ALPR; black), ICI 118,551 (ICI; green), and metoprolol (METO; empty squares) at the βarr2 signaling pathway. ERK1/2 phosphorylation (pERK) is relative to total ERK1/2 (tERK) representing the βarr2 signaling pathway in all groups. The constitutive activity was elevated in all groups to detect inverse agonism by increasing the number of cells (2.2 x 10^{-5} cells). The pIC_{50} values obtained from these curves were used as part of the mathematical approach to calculate signaling bias. (A) Non-transfected HEK 293 cells. NAD, CARV, METO, and ICI curves show sinistral displacement when compared to the t β_2AR-Gαs group. (B) HEK 293 cells transfected with the β_2AR-Gαs fusion protein (t β_2AR-Gαs). Except for ALPR showing a leftward shift, all inverse agonist curves were displaced to the right when compared to the t β_2AR-βarr2 group. (C) HEK 293 cells transfected with the wild type β_2AR (t β_2AR). (D) HEK 293 cells transfected with the

β_2AR-βarr2 fusion protein (t β_2AR-βarr2). All data points are shown as the mean ± S.E.M. The concentration-response curves were performed in triplicate on at least 3 separate occasions (n≥3).

Assessment of signaling bias reveals the absolute bias of β_2AR ligands between the Gs and βarr2 pathways.

Because the pharmacodynamic properties of affinity, potency, and efficacy for each ligand are always conditional to observational and system bias, the translation of the effect of β_2AR ligands observed in our *in vitro* studies into *in vivo* systems for therapeutic use is inappropriate. Therefore, the use of the operational model (Black & Leff, 1983) was necessary to determine the transduction coefficients as a measure of the intrinsic efficacy of a ligand which is independent of the system (i.e., coupling efficiency, receptor density). Since the pharmacological properties of the receptor were measured under the allosteric interaction of both signaling molecules separately (i.e., restricted conformational state with no competition with other signaling molecules), and the functional responses were measured on a scale-independent from the response of a reference ligand, two transduction coefficients per ligand where calculated. Importantly, the two transduction coefficients allowed for the analysis of efficiency and selectivity of ligands for either pathway independent from a reference ligand, another source of bias when analyzing functional selectivity. The difference in transduction coefficients, namely Δ log(τ/Ka), shows the independent efficiency each ligand has for the stimulation of the Gs or the βarr2 pathway. As seen in table 8, the ability of ISO and EPI to activate the Gs pathway was the highest as observed by the Δ log(τ/Ka) values 1.89 and 1.32, respectively. The partial agonists SALB and AgGs show a moderate efficiency for Gs activation with values of 0.41 and 0.27. The partial agonist INDA showed the lowest efficiency for Gs activation with a Δ log(τ/Ka) value of -0.12. Comparatively, INDA, SALB, and AgGs showed a negligible activation profile for the βarr2 pathway [Δ log(τ/Ka) values of 0.02, 0.02, and 0.04 respectively]. ISO had a moderate efficiency whereas EPI showed high efficiency for ERK phosphorylation [Δ log(τ/Ka) values of 0.34 and 0.93, respectively].

Since, for the most part, all beta blockers behaved as inverse agonists in our experimental settings, the efficacy to modify the response of a signaling pathway was uncovered and, thus, calculations for transduction coefficient values were possible. The exception was observed at cAMP accumulation for the t β_2AR-Gαs group showing neutral antagonism when CARV, PROP, ICI, METO, or ALPR was used. In these

cases, the receptor occupancy was assumed to be 99.9% (described in methods) to allow for the calculation of bias. ALPR showed the lowest efficiency (-0.70) followed by METO, PROP, ICI, and NAD [Δ log(τ/Ka) values of -0.31, -0.31, -0.30, and -0.21, respectively] for reducing the cAMP accumulation of constitutively active receptors. CARV showed a neutral efficiency of 0.01 indicating that the deactivation of the Gαs pathway is the same in either conformational state of the β_2AR. For the deactivation of the βarr2 pathway, CARV showed the highest efficiency (2.98) followed by METO, NAD, and ICI [Δlog(τ/Ka) values of 1.99,1.36 and 0.86, respectively]. PROP was neutral for both conformational states of the receptor (0.04) and ALPR had the lowest efficiency at deactivating ERK phosphorylation (-0.80) (Table 8).

Further quantification of the absolute biased signaling of all ligands, expressed as ΔΔ log(τ/Ka) (Kenakin et al., 2012), revealed the absolute bias each ligand has for either the Gs or the βarr2 pathway. Remarkably, ISO is 35 times more selective for the Gs pathway whereas NAD, CARV, ICI, and METO showed 37, 938, 14, and 199 times, respectively, more selectivity for the βarr2 pathway. EPI, INDA, SALB, AgGs, PROP, and ALPR did not show any significant bias for either pathway (Table 8).

Table 8. Biased Signaling quantification

Biased signaling quantification using transduction coefficient ratios [ΔΔ log(τ/Ka)].
HEK 293 cells transfected with the fusion proteins β_2AR-Gαs or β_2AR-βarr2 were stimulated with increasing concentrations of several β_2AR ligands and the response was measured for the two different signaling pathways Gαs and βarr2. Ke values were obtained using Eq 14 and 15 and later applied to Eq 13 to obtain τ. Δ log(τ/Ka) values indicate the ligand selectivity for a fusion protein under the same signaling pathway. ΔΔ log(τ/Ka) values indicate the absolute signaling preference (independent from a reference ligand) of β_2AR ligands for one of the two pathways measured. Note: the selective bias of β_2AR ligands was expressed as integer numbers with decimals for clarity

	cAMP			ERK1/2					
	log(τ/Ka)		Δ log(τ/Ka) Gs/βarr2	log(τ/Ka)		Δ log(τ/Ka) βarr2/Gs	ΔΔ log(τ/Ka) Gs/βarr2	Selective Bias	
Ligands	β_2AR-Gαs	β_2AR-βarr2		β_2AR-Gαs	β_2AR-βarr2			Gs	βarr2
ISO	2.15	0.26	1.89	0.09	0.43	0.34	1.55	35.37	--
EPI	2.18	0.87	1.32	-0.18	0.75	0.93	0.38	2.42	--
INDA	-0.35	-0.24	-0.12	2.12	2.14	0.02	-0.14	--	1.39
SALB	0.47	0.05	0.41	2.22	2.24	0.02	0.39	2.48	--
AgGs	0.51	0.24	0.27	2.23	2.27	0.04	0.24	1.73	--
NAD	-0.91	-0.70	-0.21	-0.82	0.55	1.36	-1.57	--	37.43
CARV	-0.97	-0.98	0.01	-0.96	2.02	2.98	-2.97	--	938.20
ICI	-0.95	-0.65	-0.30	-0.89	-0.03	0.86	-1.16	--	14.58
PROP	-0.94	-0.63	-0.31	-0.94	-0.90	0.04	-0.35	--	2.22
METO	-0.77	-0.47	-0.31	0.23	2.22	1.99	-2.30	--	199.53
ALPR	-0.95	-0.25	-0.70	0.45	-0.36	-0.80	0.10	1.27	--

BEAS-2B also shows selective constitutive activity and different patterns of protein expression when transfected with the fusion proteins.

First, using a similar approach to that used for HEK 293 cells, BEAS-2B cells were successfully transfected with the receptor alone or with the fusion proteins as observed by RT-PCR (Fig. 10A). The protein expression was observed using immunofluorescence. For colocalization of the β_2AR together with Gαs, cells transfected with β_2AR-Gαs showed protein co-expression at the cell membrane only (Fig. 12B). Conversely, the t β_2AR-βarr2 group showed abundant co-expression at the cell's cytoplasm but no fluorescence was detected at the cellular membrane (Fig. 12B). The t β_2AR group showed a mixed pattern of co-expression at the membrane as well as at the cytoplasm whereas fluorescence was not detected in the control BEAS-2B group (Fig. 10B). When colocalization of the β_2AR with βarr2 was tested, only the t β_2AR-βarr2 and t β_2AR groups had a detectable fluorescent signal (Fig. 12C). Like the previous experiments, the t β_2AR-βarr2 group showed co-expression of β_2AR with βarr2 at the cytoplasm only, predominantly at the perinuclear region whereas a mixed pattern of co-expression at the cytoplasm and the cell membrane was observed in the t β_2AR group (Fig. 12C).

Second, the measurements of cAMP levels and ERK1/2 phosphorylation in BEAS-2B cells were conducted using the same methods as with HEK 293 cells. Transfection of BEAS-2B cells with the β_2AR-Gαs fusion protein produced a significant increase in basal cAMP levels when compared to the non-transfected BEAS-2B cells (Fig. 13A). The other transfected groups, t β_2AR-βarr2, and t β_2AR had similar cAMP levels when compared to the control BEAS-2B group. Regarding the βarr2 pathway, non-transfected BEAS-2B cells showed overall increased constitutive activity observed as a high relative ERK1/2 phosphorylation that was comparable to the t β_2AR-βarr2 group (Fig. 13B). Compared to the control BEAS-2B group, the t β_2AR-Gαs, and t β_2AR groups had a significant reduction in the basal ERK1/2 phosphorylation. After treatment with the inverse agonist ICI, the ERK1/2 phosphorylation of the non-transfected BEAS-2B cells and the t β_2AR-βarr2 group was significantly reduced whereas the t β_2AR-Gαs and t β_2AR groups remained at a similar basal activity (Fig. 14). These findings suggest that the low constitutive activity observed in the t β_2AR-Gαs and t β_2AR groups is not

related to β_2AR signaling. Therefore, there is an increased constitutive activity for the respective pathway in BEAS-2B cells transfected with either the β_2AR-Gαs or β_2AR-βarr2 fusion proteins, thus corroborating the findings observed in HEK 293 cells.

A.

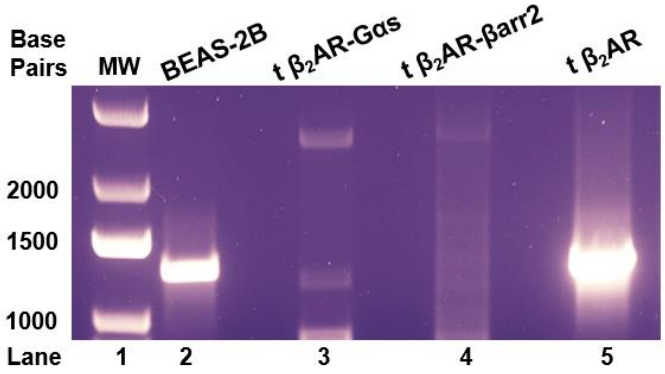
Base Pairs
MW
BEAS-2B
t β2AR-Gαs
t β2AR-βarr2
t β2AR
2000
1500
1000
Lane
1
2
3
4
5

B.

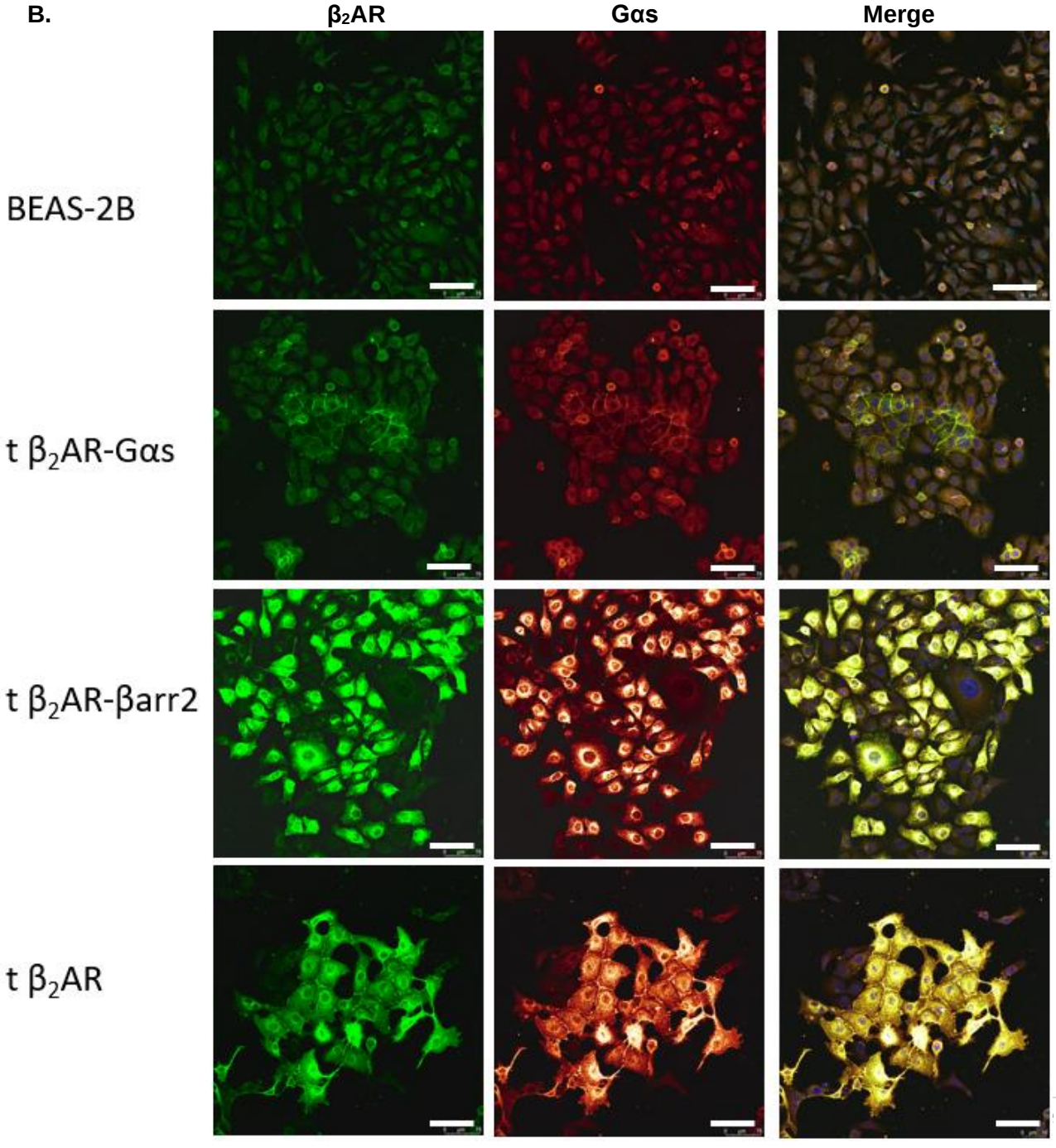
β2AR
Gαs
Merge
BEAS-2B
t β2AR-Gαs
t β2AR-βarr2
t β2AR

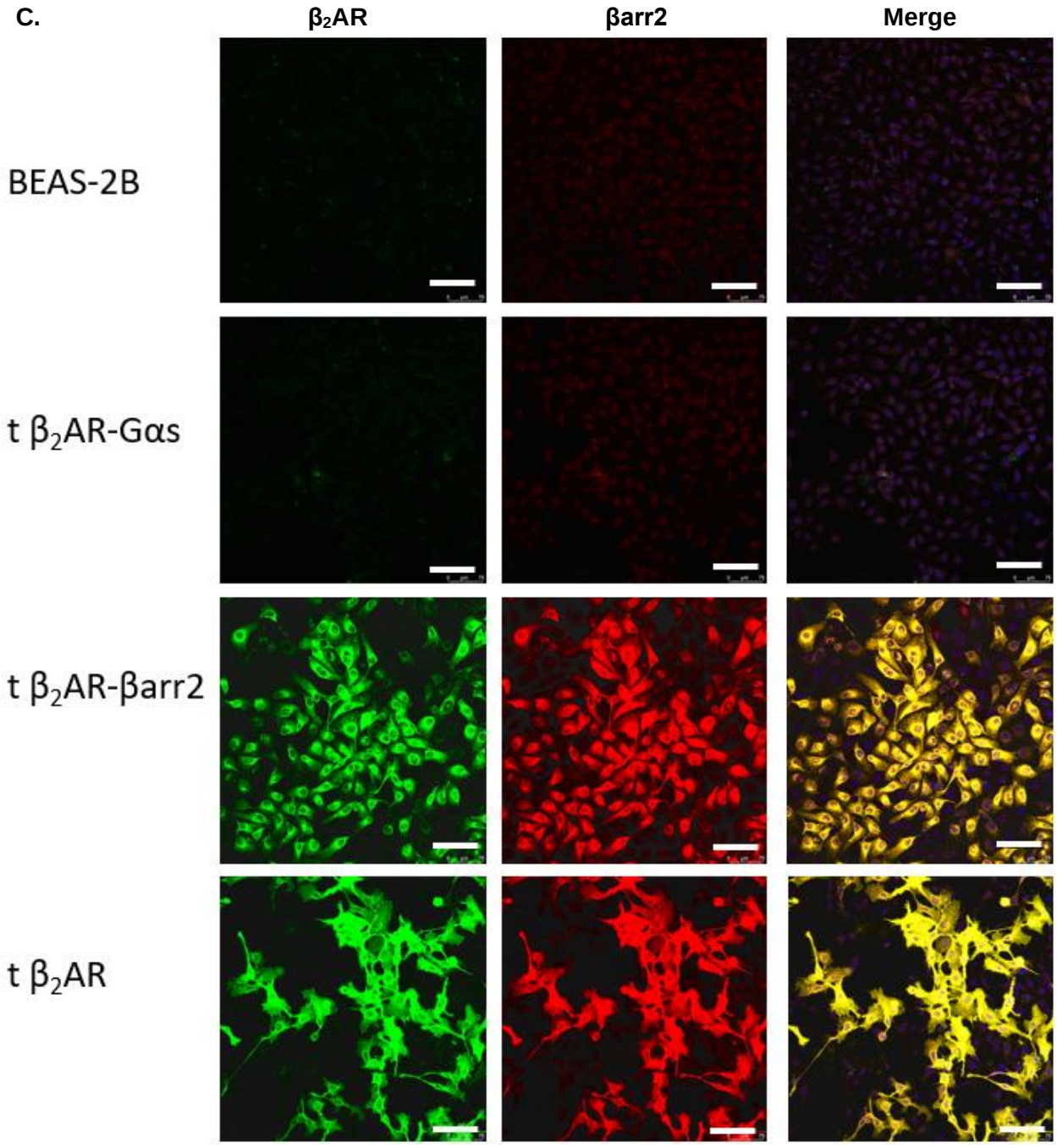

Figure 12. Expression of the fusion proteins β_2AR-Gαs and β_2AR-βarr2 in BEAS-2B cells.

(A) Reverse transcriptase-PCR shows the gene expression of the β_2AR alone (lane-2 and lane-5) and when fused to either Gαs or βarr2 (lane-3 and lane-4, respectively). The first lane shows the molecular weight (MW) ladder for base-pair quantification. (B)

Representative images of protein expression of either β_2AR (green) or Gαs (orange). Both proteins are observed together in the merged image (yellow) showing colocalization for β_2AR and Gαs at the cellular membrane for t β_2AR-Gαs whereas a cytoplasmic colocalization is observed for t β_2AR-βarr2. The expression of t β_2AR showed a mixed pattern of colocalization at the membrane, and cytoplasm whereas no pattern was observed for the non-transfected BEAS-2B group (low signal). (C) Representative images of the protein expression of either β_2AR (green) or βarr2 (red). Both proteins are observed together in the merged image (yellow) showing colocalization for β_2AR and βarr2 at the cytoplasm of the t β_2AR-βarr2, a mixed expression pattern for the t β_2AR, and no expression pattern for either non-transfected BEAS-2B or t β_2AR-Gαs (low IF signal). Proteins were detected by immunofluorescence at a lens magnification of 20x using confocal microscopy. Scale bars represent 100μm.

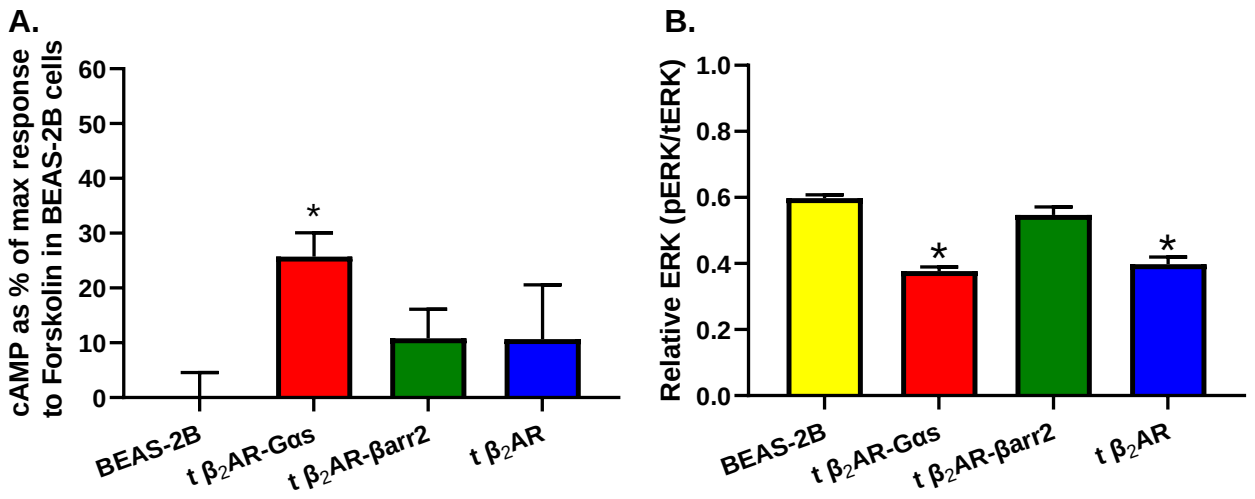

Figure 13. Constitutive activity for Gαs and βarr2 signaling pathways in BEAS-2B cells transfected with the fusion proteins.

(A) cAMP measurements represent the Gαs pathway using a scale based on the adenylate cyclase activator, Forskolin (10μM). Forskolin was used to define 100% of the response whereas the basal response of the untransfected BEAS-2B cells was used to define 0% of the response in all groups. The constitutive activity of the t β_2AR-Gαs group (red) was significantly increased compared to the untransfected BEAS-2B cells. Conversely, the t β_2AR-βarr2 group (green) and t β_2AR group (blue) had similar basal activity when compared with the untransfected BEAS-2B cells. (B) ERK1/2 phosphorylation (pERK) relative to total ERK1/2 (tERK) as the surrogate measurement of the βarr2 pathway. Constitutively high pERK was observed for the untransfected BEAS-2B (yellow) similar to the basal activity of the t β_2AR-βarr2 group. The t β_2AR-Gαs and t β_2AR had a lower constitutive activity when compared to the control BEAS-2B group. Data are the means ± S.E.M. from at least 3 independent experiments. *$P<0.05$ was considered significant by one-way ANOVA and Tukey was used as the post hoc test.

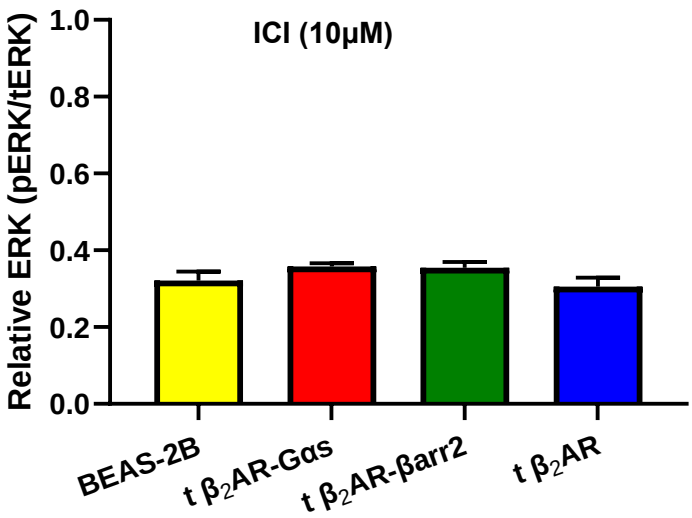

Figure 14. The high ERK phosphorylation observed in BEAS-2B cells is elicited by the constitutive activity of the βarr2 pathway.

ERK1/2 phosphorylation (pERK) relative to total ERK1/2 (tERK) as the surrogate measurement of the βarr2 pathway. The constitutive activity of the BEAS-2B (yellow) and the t β_2AR-βarr2 (green) groups were comparable to the basal activity of the t β_2AR-Gαs (red) and t β_2AR (blue) groups after 90 mins of treatment with the selective β_2AR inverse agonist ICI 118,551 (10μM). Data are the means ± S.E.M. of at least 3 independent experiments. *P<0.05 was considered significant by one-way ANOVA and Tukey was used as the post hoc test.

The cytokine profile and cell size change depending on the fusion protein expressed in BEAS-2B cells.

After stable transfection, we noted the cytokine secretion profile changed depending on the fusion protein expressed by the transfected BEAS-2B cells. From the 15 cytokines analyzed (see methods), five were not detected in the supernatant of any group (IL-2, IL-4, IL-5, IL-10 and, IL-12p70) and, thus, were not included in the present analysis. For the remaining cytokines, a heatmap was used as a visual representation of normalized percentile changes in cytokine secretion by each group (Fig. 15A). Specifically, the non-transfected BEAS-2B group showed a high secretion pattern for 7 out of 10 cytokines measured. The secretion of cytokines modulating a Th1 (IL-12p40, IFN-γ) or Th2 (IL-13, IL-6) cellular response was reduced in all transfected groups when compared to the control BEAS-2B group (Fig. 15B). Conversely, TNFα secretion was increased in the t β_2AR group only, while IL-1β and IL-1Ra were increased in the t β_2AR-βarr2 group only (Fig. 15C; upper panel). For the fusion proteins, the cytokine profile of the t β_2AR-Gαs group showed a constitutively decreased secretion of GM-CSF and IL-8, and a similar high secretion of CCL2 when compared to the control BEAS-2B group. Conversely, the t β_2AR-βarr2 group had constitutively reduced CCL2 secretion and a similar high GM-CSF and IL-8 secretion when compared to the control BEAS-2B group (Fig. 15C; lower panel). When comparing the cytokine profile between fusion proteins, there was a reciprocal regulation of the chemoattractants CCL2, GM-CSF and IL-8. The former was highly secreted in the t β_2AR-Gαs group when compared to the t β_2AR-βarr2 group, whereas GM-CSF and IL-8 were increased in the t β_2AR-βarr2 group when compared to the t β_2AR-Gαs group (Fig. 15C; lower panel). These results indicate that there is differential regulation of cytokine/chemokine secretion by each signaling pathway of the β_2AR.

Finally, morphological evidence of differential regulation between fusion proteins was observed in the average diameter of detached cells. The t β_2AR-βarr2 group showed a larger diameter than the control groups as well as the t β_2AR-Gαs group (Fig. 16). Additionally, the attached cells from the t β_2AR group further displayed a change in their morphology compared to the other transfected groups at 100x confocal magnification. Particularly, lamellipodia were observed only in the t β_2AR group where

high expression of β_2AR and its cognate transducers, Gαs and βarr2, was also observed (Fig. 17). The mechanisms for the change in cell structure and morphology elicited by the βarr2 signaling pathway and β_2AR overexpression, respectively, were not investigated.

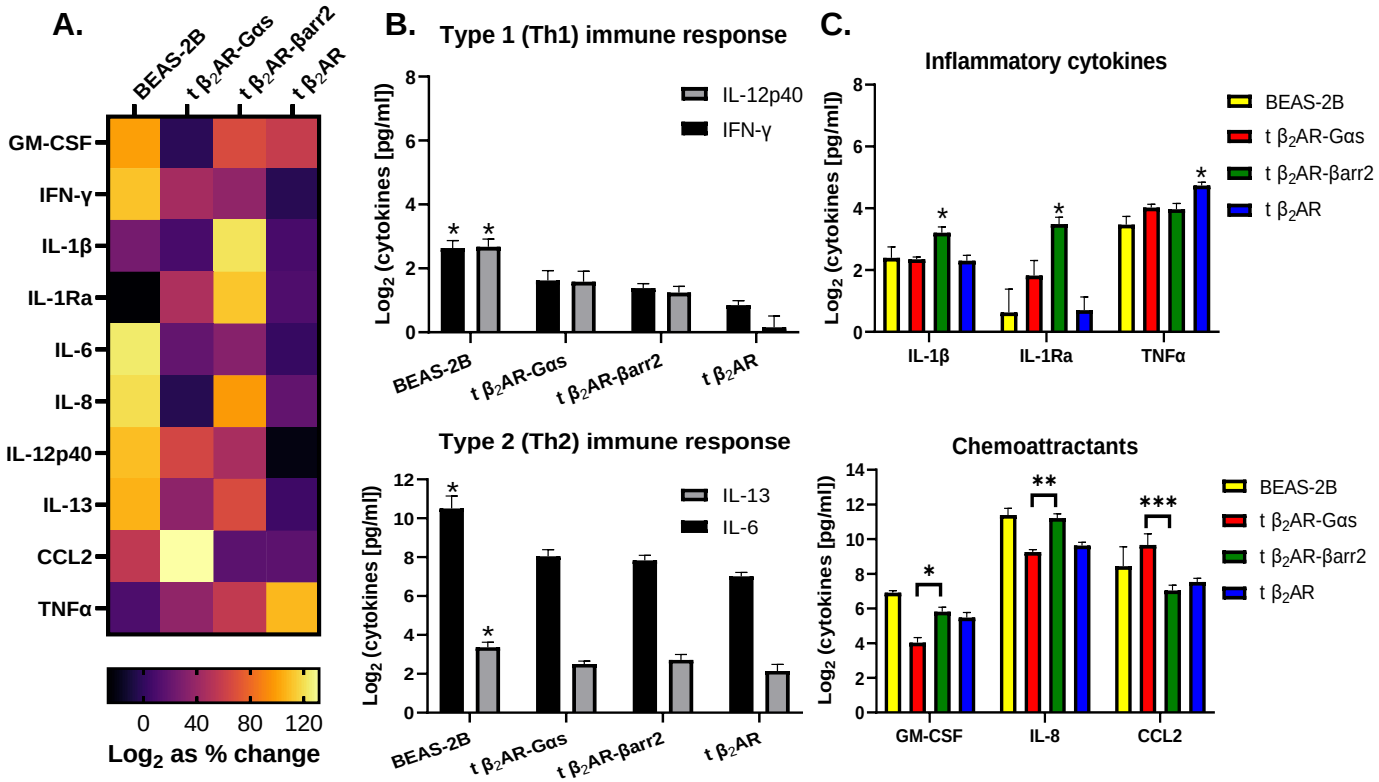

Figure 15. Cytokine profile changes for BEAS-2B cells transfected with the WT β2AR or the fusion proteins.

Changes in the secretion of multiple cytokines were measured as [pg/ml] and transformed to log_2 units for clear visualization. (A) Heatmap of the inflammatory cytokine profile representing the magnitude of secretion relative to each group (percentile change). The cytokine profile of the control BEAS-2B group (high cytokine secretion) was in stark opposition with the profile of the t β_2AR group (low cytokine secretion). Similarly, the fusion proteins showed distinctive profiles favoring a type-1 (e.g., t β_2AR- Gαs group) or type-2 (e.g., t β_2AR-βarr2 group) immune response. (B) Cytokines are known to polarize the differentiation of naïve T cells into type-1 (Th1) (upper panel) or type-2 (Th2) (lower panel) helper T cells. Non-transfected BEAS-2B cells show the highest levels for both immune responses. All transfected groups show lower secretion of Th1 (IL-12, IFN-γ) or Th2 (IL-6, IL-13) polarizing cytokines compared to BEAS-2B cells. (C) The pro-inflammatory cytokines IL-1β and TNFα are elevated for the t β_2AR-βarr2 and t β_2AR group, respectively, when compared to the rest of the groups (*upper panel*). The *lower panel* shows a reciprocal activation of

chemoattractants by each fusion protein. The t β_2AR-Gαs group has constitutively high CCL2 along with low GM-CSF and IL-8 secretion whereas constitutively low CCL2, and high GM-CSF and IL-8 secretion were observed for the t β_2AR-βarr2. The control untransfected BEAS-2B cells were not different from the transfected group with the highest secretion. Data are expressed as the mean ± S.E.M from 3 independent experiments (n=3). *P-value ≤ 0.01 was considered significant by two-way ANOVA and Tukey was used as the post hoc test.

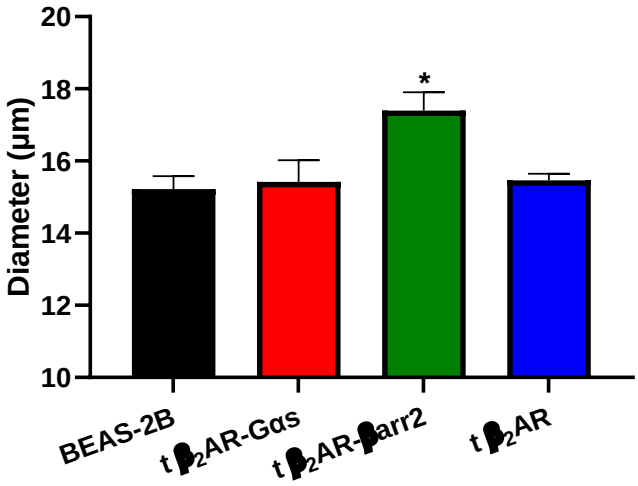

Figure 16. The constitutive activity of the βarr2 pathway modifies the cell size of BEAS-2B cells.

Cell diameter was measured in live detached cells using trypan blue as a die to identify living from dead cells. The wild-type BEAS-2B cells (black) or the cells transfected with the β_2AR alone (blue) or the fusion proteins β_2AR-Gαs (red) show a shorter cell diameter when compared to BEAS-2B cells transfected with the β_2AR-βarr2 fusion (green). Experiments were performed in duplicate at least 3 separate times (n≥3). *P≤0.05 was considered significant by one-way ANOVA and Tukey was used as the post hoc test.

BEAS-2B t β_2AR

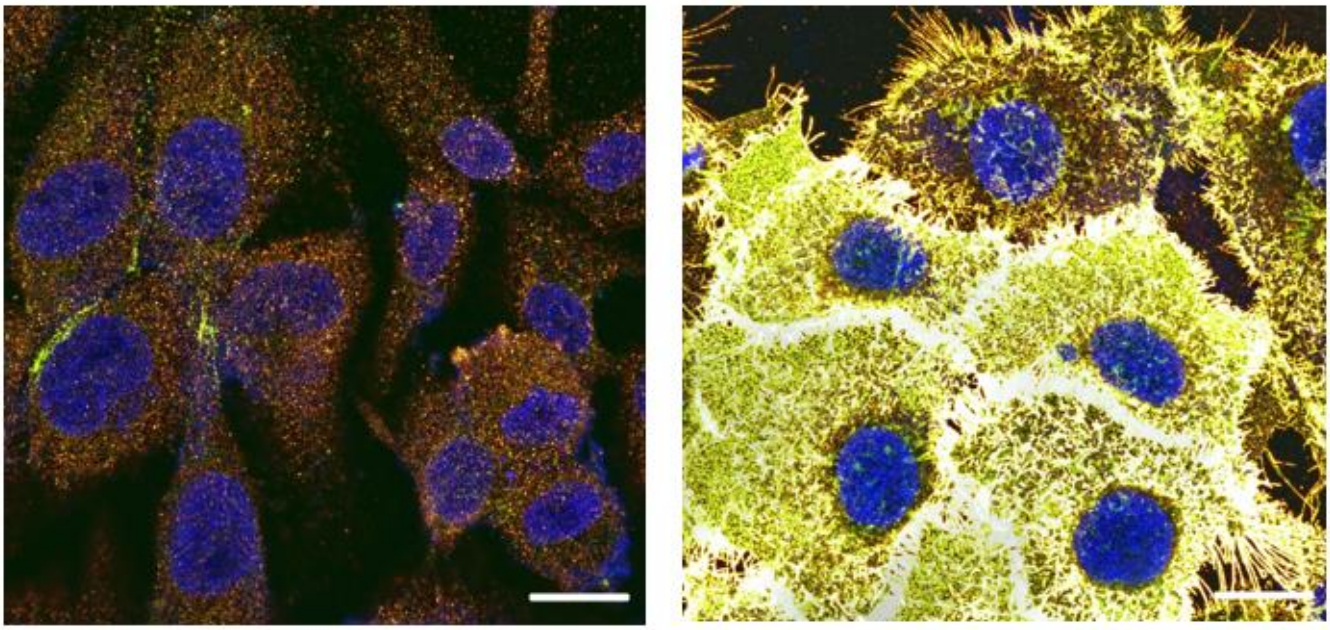

Figure 17. The morphology of BEAS-2B cells changes when the β2AR is overexpressed.

Representative images of the BEAS-2B group (left) with a typical shape characteristic of epithelial cells. Overexpression of the β_2AR (right) altered the morphology of BEAS-2B cells displaying filamentous extensions resembling cilia. The yellow label represents the merged signal between the expression of the β_2AR (green) and Gαs (orange). Signal was detected by immunofluorescence at a lens magnification of 100x using confocal microscopy. Scale bars represent 20μm.

XIII. Discussion

Here, we transfected the β_2AR-Gαs and β_2AR-βarr2 fusions into two different cell lines: HEK 293 and BEAS-2B cells. The expressed fusion proteins in HEK 293 cells allowed us to independently characterize the constitutive activity of two of the most known signaling pathways of the β_2AR: Gαs and βarr2. We also determined that, after receptor activation, the signaling molecule moiety of the fusion protein dampens the recruitment of the endogenous signaling molecules Gαs and βarr2, indicative of steric hindrance. Additionally, the use of the full agonist isoproterenol and the antagonist/inverse agonist ICI 118,551 on our fusion proteins showed that the fusion proteins remain sensitive to pharmacological manipulation. These findings suggest that our novel chimeric proteins of β_2AR fused to either Gαs or βarr2, have a conformational restriction. Therefore, our fusion proteins might predominantly exist as two separate active conformations of the receptor (i.e., R* as the active conformation that favors Gαs signaling and R** as the active conformation that favors βarr2 signaling). Indeed, our findings exploring the pharmacological properties of affinity, potency, and efficacy of selected β_2AR ligands in our fusion proteins are in accordance with the isolation of two different active conformational states of the β_2AR. Based on the previous pharmacological parameters, we quantified the biased signaling of these β_2AR ligands using a modified version of the transducer coefficient ratio under an absolute scale. This approach has the advantage of being independent of a reference ligand and therefore, can represent more closely an absolute measure of the intrinsic power of a ligand to activate a certain pathway. Finally, the experiments with BEAS-2B cells supported the pattern of constitutive signaling by a single pathway that was observed in HEK 293 cells. This unique constitutive activity was related to a different physiological response on cytokine release, as well as an observed change in the average size and shape of cells.

Selective affinity.

The competition binding studies to determine affinity showed that all β_2AR agonists, classically known to stimulate the Gs pathway, had higher affinity for the

active conformation that couples to Gαs (R*) versus the active conformation that couples to βarr2 (R**). Isoproterenol and epinephrine showed the highest degree of preference for a conformational state as they were 4 times more selective for R* over R**. Conversely, none of the beta-blockers showed a binding preference for the R* and only propranolol showed a higher affinity for R** versus R*. Therefore, changes in the binding affinity of ligands for the receptor can reveal a predominant conformational state of the receptor. Additionally, nadolol showed the highest affinity for the receptor alone (not fused with any signaling molecule) suggesting that another conformation of the receptor (likely the inactive conformation expressed as R) is present simultaneously with R* and R** in physiological conditions. Therefore, this data supports a preexisting array of, at least, 3 different conformational states of the receptor that presumably determines the responsiveness of a β_2AR ligand in any system (i.e., different tissues). Other methods that detect small subpopulations of the unliganded receptor (Lerch et al., 2020; Nygaard et al., 2013), as well as the detection of the active and inactive conformations of the β_2AR by X-ray crystallography (Cherezov et al., 2007; Rasmussen, Choi, et al., 2011; Rasmussen et al., 2007), support a preexisting equilibrium between the inactive and multiple active conformations of the β_2AR. Different affinity patterns were also observed for alprenolol (R over R**), carvedilol (R over R*), and ICI 118,551 and metoprolol (no preference) evidencing an “individual” preference among beta-blockers for receptor subpopulations that could be translated into multiple functional responses beyond only “blocking” the receptor. Altogether, these findings fit what is proposed in the current receptor theory where the signaling proteins behave as allosteric components that stabilize the ever-changing structure of the receptor. Hence, a functional affinity is observed between a ligand and the multiple allosterically modified receptor conformations (Kenakin & Christopoulos, 2013a).

Constitutive activity.

The functional data measuring cAMP accumulation as a surrogate of the Gαs pathway, and ERK1/2 phosphorylation as a surrogate of the βarr2 pathway revealed that each fusion protein was constitutively active for their respective pathways. The increased constitutive activity for the canonical pathway, Gαs, was also observed when

the receptor was overexpressed regardless of the moiety tethered to the receptor. For cells expressing the β_2AR-βarr2 fusion protein, there was a small increase in basal cAMP activity. This might be explained by the remnant expression of the endogenous β_2AR in HEK 293 cells that likely couples to the endogenous protein Gs (Kim et al., 2014; Periole et al., 2007), whereas the rest of the transfected receptors remain coupled to βarr2. Further supporting the weakness of this remnant endogenous β_2AR signal is that low concentrations of ICI 118,551 decreased the cAMP in cells predominantly expressing the β_2AR-βarr2 fusion. In contrast, only a small reduction in the cAMP constitutive activity of the β_2AR-Gαs fusion protein is observed even at high ICI 118,551 concentrations (Fig. 3A). This can be also explained based on the mechanistic models of receptor theory. In this case, the crowded conditions elicited by the increased receptor density at the membrane (Kim et al., 2014; Periole et al., 2007), might force the receptor to adopt the thermodynamically favored R* conformation whereas the rest of the transfected receptors keep an R** conformation. Thus, low concentrations of ICI can easily overcome the small R* subpopulation and shift the equilibrium from R* to R which does not start signaling. Comparatively, a small reduction in the constitutive activity of the highly expressed β_2AR-Gαs fusion protein, even at high ICI concentrations, cannot shift the equilibrium back to the inactive state because of the overpopulated R* conformation of the receptor. Beyond receptor theory, another contributing factor for the increased strength of the β_2AR-Gαs fusion protein on cAMP production is the length of the linker between the β_2AR and Gαs. Previous reports on the β_2AR-Gαs fusion proteins have shown a variable degree of constitutive activity presumably by the change in the linker length (Bertin et al., 1994; Molinari et al., 2003; Small et al., 2000). This variability was particularly addressed by exploring multiple lengths between the tethered proteins, demonstrating that the length of the linker is inversely proportional to the basal activity elicited by the fusion protein (Malik et al., 2017; Wenzel-Seifert et al., 1998). Therefore, the small size of the linker in the β_2AR-Gαs fusion is constraining the receptor to couple to the Gαs pathway. This approach has also been used to stabilize the conformation of GPCRs for crystallization (Chun et al., 2012; Zou et al., 2012) supporting the idea of conformational restriction in our fusion proteins. In conformity with this hypothesis is the lack of constitutive activity of the β_2AR-Gαs fusion for the βarr2 pathway (Fig. 3B)

suggesting the receptor is being tightly held in the conformation coupling to Gαs. For the βarr2 pathway, the constitutive activity was observed only when the β_2AR-βarr2 fusion was expressed. This finding corroborates one of the well-established signaling mechanisms of βarr2 (Shenoy et al., 2006). Moreover, the increased basal ERK1/2 phosphorylation elicited by the β_2AR-βarr2 fusion protein was not observed in the β_2AR-Gαs fusion protein. Because these measurements required a starvation step of 24 hours, the constitutive activity observed was in chronic conditions. Therefore, this confirms previous studies showing the lack of chronic ERK1/2 activation by the Gαs pathway (Gesty-Palmer et al., 2006; Goldsmith & Dhanasekaran, 2007). To the best of our knowledge, this is the first study showing increased constitutive activity of the β_2AR-βarr2-dependent ERK1/2 phosphorylation. Therefore, the chimeric β_2AR-βarr2 fusion can be used as a tool for the exploration of the mechanisms involved in the downstream signaling of this pathway.

Steric Hindrance.

The recruitment of the reciprocal signaling molecules Gαs and βarr2 after ISO stimulation is inhibited by the fusion proteins whereas the receptor alone kept the recruitment feature for both signaling proteins. This indicates that each fusion protein excludes the coupling of the alternative signaling pathway, likely by steric hindrance. In contrast with our findings, other studies have shown the formation of a 7TMR-Gαs-βarr2 megacomplex (Nguyen & Lefkowitz, 2021; Thomsen et al., 2016). The discrepancy can be reconciled based on the conformational interaction βarr has with GPCRs. Based on the strength of the interaction between β-arrestins and 7TMR, receptors have been classified in class A (transient interactions) or class B (stable interactions) (Oakley et al., 2001; Oakley et al., 2000). Such interactions are dependent on the conformation of βarr whereby the tail conformation (predominantly observed across class B GPCRs) would allow βarr to remain attached to the C-terminal of the receptor while the intracellular core of the receptor is still accessible to the G protein for canonical signaling. Conversely, the core-engaged βarr (observed in class A GPCRs such as the β_2AR) would not allow G protein interaction with the receptor (Shukla et al., 2014; Thomsen et

al., 2016). Therefore, the core conformation of βarr is most likely present in the β_2AR-βarr2 fusion.

Fusion proteins remain functional.

In addition, both fusion proteins can be functionally manipulated using β_2AR ligands by either increasing or decreasing their constitutive activity. However, the overexpression of the receptor alone increased cAMP to the maximal levels of the system masking the stimulatory effect of isoproterenol. This has been previously observed both *in vitro* and *in vivo.* For example, in mice overexpressing the β_2AR in cardiomyocytes, one of the physiological outcomes was a maximal increase of heart rate with no change after isoproterenol administration (Milano et al., 1994). ICI 118,551, however, markedly reduced heart rate in these transgenic mice (Milano et al., 1994). Accordingly, our data is consistent with the reduction of the maximal cAMP levels in the overexpressed receptor group using ICI 118,551 which allowed for the observation of the stimulatory effect of isoproterenol. Additionally, both fusion proteins generated classical sigmoidal response curves for both signaling pathways. isoproterenol was initially tested showing curves that could be displaced to the right by increasing concentrations of ICI 118,551 showing that both fusion proteins can be selectively modulated by agonists and antagonists/inverse agonists. For the Gs pathway, a Schild regression analysis on the displacement of isoproterenol curves by ICI 118,551 demonstrated higher pA_2 values for both fusion proteins compared to the controls. Further reassessment using a Schild plot due to the Schild slope being different from unity decreased the pA_2 values of ICI 118,551 in all groups. These values were largely similar among all groups and closely resembled the observed values in the affinity binding experiments. The deviations from unity in the slope of our Schild regression analysis might reflect a system that is at semi-equilibrium (Kenakin, 1982). Since for cAMP measurements, the best response window for agonists was 10 minutes, this time frame might not have been enough for the re-equilibration between the preincubated ICI 118,551 and the newly added isoproterenol with all receptors. Thus, a decrease in the maximal activity of isoproterenol was observed in the group with low endogenous expression of the β_2AR (HEK 293 group), and the group expressing the β_2AR-βarr2

fusion protein (Fig 6A and D). However, this was not the case for the other groups; no reduction in the maximal activity of isoproterenol curves pretreated with ICI 118,551 was observed in the cell expressing either the wild type β_2AR or when fused to Gαs (Fig 6B and C). This disparity might be explained in terms of receptor occupancy and the efficiency of the system to produce a response. That is, the sensitivity of a system, reflected as the maximal response measurements, depends on the receptor density and the receptor coupling with other members of the signaling pathway measured (Kenakin, 2019; Seifert et al., 2001; Seifert et al., 1999). Therefore, reducing the number of receptors or decoupling them from the signaling pathway that is being measured can change the maximal response of the system. Accordingly, the already low receptor expression in the untransfected HEK 293 cells is further reduced since some of the receptors occupied by ICI 118,551 would not form part of the observed semi-equilibrium. Likewise, the decoupling of cAMP production by the steric hindrance for the recruitment of Gαs when the β_2AR is fused to βarr2 together with the endogenous receptors functionally reduced by ICI 118,551 also decrease the maximal response of isoproterenol to a similar degree. In both cases, the new equilibrium formed after 10 minutes of isoproterenol administration represents a smaller receptor density that still allows for the parallel rightward shift induced by ICI 118,551 without changes in the new maximal response. For the ERK1/2 phosphorylation measurements, the collapse of the maximal response of isoproterenol under increasing concentrations of ICI was observed for all groups except the t β_2AR-βarr2 group. This is suggestive of a decreased availability of the receptor subpopulation that can preferentially couple to βarr2. Accordingly, the increased availability of the receptor subpopulation that couples to βarr2 by the overexpression of the β_2AR-βarr2 fusion protein show parallel rightward displacements with similar maximal activities of the ISO curves under increasing concentrations of ICI. Thus, the receptor subpopulation that preferentially couples to βarr2 and signals through ERK1/2 phosphorylation is not the predominant species in basal conditions. Taken together, the high degree of responsiveness of our fusion proteins to isoproterenol and ICI 118,551 further allows for the quantification of signaling preference of other β_2AR ligands for the Gαs or the βarr2 pathway.

Potency of β_2AR agonists for the Gs and βarr2 pathways.

The potency measurements of selected β_2AR ligands for two distinct signaling pathways (i.e., cAMP accumulation for Gs pathway, and ERK1/2 phosphorylation for the βarr2 pathway) was analyzed in two separate systems expressing either the β_2AR-Gαs or β_2AR-βarr2 fusion proteins. The potency of all β_2AR agonists on cAMP accumulation was increased by at least a half logarithmic unit when the receptor was overexpressed or fused to Gαs. Conversely, lower receptor expression or fusion of the β_2AR to βarr2 yielded lower potency values. These results are consistent with changes in potency based on the receptor density (Gazi et al., 1999; Hermans et al., 1999) or coupling efficiency (Morfis et al., 2008; Ostrom et al., 2001). For the βarr2 pathway, the data was less homogenous showing only a trend of increased potency in some β_2AR agonists on ERK1/2 phosphorylation when the β_2AR is overexpressed or fused to βarr2. Thus, we cannot conclude with certainty that the receptor behavior observed for the Gs pathway remains consistent at the βarr2 pathway. Nevertheless, the fact that all agonists showed an increased affinity for the β_2AR-Gs fusion protein and had increased potency (either significantly or as a trend) when the receptor is overexpressed or fused to the cognate transducer upstream the measured pathway, strongly argues in favor of the currently described GPCR behavior in receptor theory (Kenakin, 2017b).

Regarding the intrinsic activity of the β_2AR ligands, we observed the expected increase in the maximal response when the receptor was overexpressed for the Gs pathway. Paradoxically, the maximal response was significantly reduced when the receptor was overexpressed in the βarr2 pathway. This behavior is counterintuitive and goes against the current receptor theory based on experimental evidence that increasing the receptor number would increase the probabilities of coupling to its cognate transducers (Kenakin, 2016, 2017b). However, rigorous evidence about the receptor density-intrinsic activity relationship only comes from studies analyzing the canonical pathway (Hermans et al., 1999; Koener et al., 2012). Therefore, no pharmacological explanation can currently fit with our experimental observations. However, as an alternative to explaining this phenomenon pharmacologically, we propose that the decreased coupling efficiency observed with high receptor density in

the βarr2 pathway answers to the physical property of protein crowding (Harada et al., 2012; Stachowiak et al., 2010). We speculate that the crowded environment by the overexpression of the β_2AR (which is at least 100-fold higher compared to the endogenously expressed β_2AR in our settings) induces steric pressure that constrains the receptor conformation ultimately leading to an increase in the energetic barrier for β_2AR-βarr2 coupling. In turn, only a limited receptor population can exist in a conformational state that couples to βarr2 and induce ERK1/2 phosphorylation.

Potency of beta-blockers for the Gs and βarr2 pathways.

We also tested selected beta-blockers for their potential to decrease the previously observed constitutive activity of the β_2AR in our transfected groups. By increasing the cell number and therefore the receptor concentration, all the beta-blockers behaved as inverse agonists for the βarr2 pathway regardless of the receptor quantity or chimeric nature. Similarly, all beta-blockers decreased cAMP accumulation when the receptor was overexpressed (increased density) or fused to βarr2 whereas nadolol was the only one with such effect when the β_2AR was fused to Gαs. This was also observed for the βarr2 pathway whereas nadolol was the only beta-blocker that behave as an inverse agonist when the receptor was fused to Gαs. As expected, the low expression of the β_2AR in the untransfected HEK 293 cells did not show constitutive activity even when we increased the receptor concentration, and therefore no inverse agonism was detected. Our data is consistent with the extensive body of evidence showing that increasing the constitutive activity of a system by increasing the number of receptors uncovers the negative efficacy of multiple antagonists, e.g., beta-blockers (Bond et al., 1995; Costa & Herz, 1989; Wisler et al., 2007). Moreover, the potency of all beta-blockers for ERK1/2 dephosphorylation was decreased when the receptor was fused to Gαs, except for alprenolol which showed increased potency in this group. Similarly, nadolol also show decreased potency for decreasing cAMP accumulation when tested in the transfected β_2AR-Gαs group whereas no potency was detected for the rest of the beta-blockers. Altogether, the detection of differences in potencies by our fusion proteins, in both signaling pathways opens the opportunity to mathematically determine the biased signaling profile of beta-blockers.

Finally, we recognized that for the untransfected control HEK 293 group, the increase in constitutive activity by augmenting the receptor concentration was only observed in the βarr2 pathway and could be decreased by beta-blockers. These results indicate amplification of the β_2AR-βarr2 signaling pathway and suggest that the β_2AR-βarr2 signaling is necessary for the basal functions of starving HEK 293 cells. Conversely, the lack of amplification in the β_2AR-Gαs signaling suggests that this pathway is not fundamental in the basic needs of HEK 293 cells. Indeed, the stimulation of GPCRs in cells lacking both β arrestin isoforms induces apoptosis, whereas GPCR-dependent βarr2 signaling activation also shows antiapoptotic effects (DeFea et al., 2000; Revankar et al., 2004). In an *in vivo* context, there is also evidence of early birth lethality in mice lacking βarr1/2 (Zhang et al., 2011). Altogether, our data is consistent with a fundamental role of the β_2AR-βarr2 signaling pathway in cell survival for the untransfected HEK 293 cells.

Absolute bias for β_2AR ligands.

Currently, the most used method to quantify biased agonism is the transduction coefficient ratios based on the operational model (Black et al., 1985; Kenakin et al., 2012). This method allows for the detection of the preference of a ligand to stimulate a signaling pathway by using simple functional concentration-response curves for the signaling pathways that are under analysis. However, Eq 12 shows that the parameters τ, K_A, and Emax are interdependent when obtained from functional curves only (Jakubik et al., 2019). This means that certain conditions must be met for the accurate prediction of bias in experimental settings. Particularly, the fit of at least two concentration-response curves with shared parameters is needed to fit the operational model (Frigyesi & Hossjer, 2006). Variability on the Emax by using a scale determined on the response of a full agonist might not represent the maximal response of the system and would yield erroneous values for the calculation of τ and K_A of other agonists. The other important issue is the assumption of an 'operational' affinity which means that the parameter K_A for a given receptor has the same value for both active states. If the K_A is different between active states of the receptor, as we have observed in our results, the method becomes invalid. In other words, the operational model skips the dissociation

constants for individual active or inactive states, thus, ignoring the true equilibrium between an agonist and each active state. Furthermore, this model does not include the measure of bias signaling in inverse agonists due to its mathematical nature (Kenakin, 2016) and needs a reference ligand which could be another source of bias in itself.

For these reasons, we decided to take a direct approach and experimentally calculated τ, Ka, and Emax. This way, the interdependence of these parameters is canceled and more accurate measurements reflecting the true nature of affinity and efficacy for each ligand were included in the transduction coefficient ratios. Importantly, we directly calculated efficacy by extrapolating the IC/EC_{50} values to the functional affinity (K_A) values. Therefore, we determined the concentration of ligand-active receptor complex needed to produce the half-maximal response on functional experiments; this concept is represented by the parameter Ke (described in methods) which is necessary for the calculation of τ. Because our calculations yielded two K_A and two IC/EC_{50} values per pathway for each ligand, the reference ligand was not necessary. Thus, each ligand became its own reference for the quantification of bias. This method corroborated the dogmatic assumption that the endogenous ligand is unbiased in equilibrium conditions, which might not be the case in clinical settings (dynamic bias) (Kenakin & Christopoulos, 2013b; Michel et al., 2014). Additionally, isoproterenol showed an absolute bias towards the Gαs pathway. Conversely, carvedilol had a marked absolute bias towards the βarr2 pathway followed by the selective β_1AR antagonist metoprolol. This specific degree of absolute ligand bias can be interpreted as the intrinsic power of the chemical structure of a ligand to elicit a biological response. Therefore, the use of our method to detect absolute ligand bias might be of clinical relevance when modulation of a specific signaling pathway is required. Accordingly, a well-stablished mechanism to induce heart injury and dysfunction is the chronic administration of isoproterenol (Brooks & Conrad, 2009; Teerlink et al., 1994). On the contrary, metoprolol and carvedilol are widely used in the treatment of heart failure due to their clinical benefits of increased contractility and long-term survival (Packer et al., 1996; Ramahi et al., 2001). When compared to metoprolol, carvedilol has shown superiority in the long-term survival of heart failure patients (Poole-Wilson et al., 2003). Furthermore, the bias of carvedilol for the βarr2 pathway has been well documented

(van der Westhuizen et al., 2014; Wisler et al., 2007) corroborating that our method is highly sensitive for detection of bias. Therefore, our absolute bias measurements concur with the (pre)clinical outcomes observed under chronic treatment of biased β_2AR ligands.

Extrapolation of constitutive activity to a physiological system.

For the BEAS-2B cells, the preserved constitutive activity together with the distinctive cytokine profile elicited by each fusion protein demonstrates a gain-of-function mechanism in a physiologically relevant cell line. While activation of the Gs pathway follows the well-described β_2AR behavior in BEAS-2B cells (Williams et al., 2000), there is some controversy on the basal activity of BEAS-2B cells elicited by the β_2AR-βarr2 pathway. A recent study analyzing multiple cell lines of human bronchial epithelial cells, including the BEAS-2B, showed constitutively high ERK1/2 phosphorylation (Hamed et al., 2021). Yet, no clear evidence on the βarr2-dependent ERK1/2 phosphorylation was observed since the βarr2-biased partial agonist, carvedilol, failed to further increase ERK1/2 phosphorylation (Hamed et al., 2021; Peitzman et al., 2015). In the present study, we observed similar high ERK1/2 phosphorylation between non-transfected BEAS-2B cells and transfected with the β_2AR-βarr2 fusion protein. Treatment with the selective β_2AR inverse agonist, ICI 118,551, decreased ERK1/2 phosphorylation in both groups to the basal levels observed in the t β_2AR-Gαs group. Therefore, our data suggest that the high ERK1/2 phosphorylation observed in BEAS-2B cells is mediated by the constitutive activity of the β_2AR-βarr2 pathway.

Independent gain-of-function was observed as alternative cytokine profiles and altered morphology.

Under pathologic states, the epithelium secretes selective cytokines inducing a local inflammatory response that activates and recruits a myriad of immune cells (Weitnauer et al., 2016). The inflammatory response can be divided into 2 types (Th1 and Th2) based on the cytokine-induced polarization of naïve T lymphocytes. Here, we show that the human BEAS-2B cell line has a constitutively high secretion of most cytokines measured, except for the proinflammatory cytokines IL-1 and TNFα. This suggests that under basal conditions, there exists an equilibrium at the epithelial

microenvironment between the two main immune responses, Th1 and Th2 (Del Prete et al., 1991; Mosmann & Coffman, 1989). Additionally, the chemokine profile observed for non-transfected BEAS-2B cells does not suggest a preference of chemoattraction between immune cell types. Overexpression of the β_2AR altered the cytokine profile of BEAS-2B cells showing TNFα as the only elevated cytokine. Together with the change to a ciliated-shaped morphology (Fig 17), our findings suggest that BEAS-2B cells overexpressing the β_2AR became differentiated. Previous observations defining the lack of differentiation of BEAS-2B under similar environmental conditions (Stewart et al., 2012) challenge our observations. Further structural and genetic characterization of BEAS-2B cells overexpressing the β_2AR and comparison with subpopulations of epithelial cells (Vieira Braga et al., 2019) is needed.

Regarding the fusion proteins, the cytokine profile of BEAS-2B cells shifts based on the activated downstream signaling of the β_2AR. When the constitutive activity is high for the Gαs signaling, the cytokine profile shifts to the secretion of the monocyte chemoattractant CCL2 (MCP-1) only. Conversely, the chemokines GM-CSF and IL-8 (CXCL8), known for eosinophil and neutrophil recruitment, respectively, are decreased under the β_2AR-Gαs signaling pathway. Accordingly, manipulation of the Gs pathway with the adenylate cyclase activator, forskolin, or a cAMP analog, 8-Br-cAMP, decreases GM-CSF, IL-6, and IL-8 secretion (Kainuma et al., 2017; Wyatt et al., 2014). A reciprocal shift in the cytokine profile of BEAS-2B cells is observed for the t β_2AR-βarr2 group where the constitutive activity for the β_2AR-βarr2 signaling pathway decreases CCL2 secretion while GM-CSF and IL-8 remain at high concentrations. Furthermore, the proinflammatory cytokine IL-1β, instrumental in the activation and recruitment of eosinophils, mast cells, neutrophils, and dendritic cells (Willart et al., 2012), is increased only in the t β_2AR-βarr2 group. Together with the increase in IL-8 secretion, this cytokine profile suggests that the β_2AR-βarr2 signaling axis mediates the Th2 immune response. This profile is consistent with the immune phenotype of asthma reported in human and animal studies (Baines et al., 2010; Broide et al., 1992; Nguyen et al., 2017). Moreover, β2AR signaling, predominantly through the βarr2 pathway, is necessary for the development of an asthma phenotype (Al-Sawalha et al., 2015; Nguyen et al., 2017; Nguyen et al., 2009). Thus, our results suggest that the β_2AR-βarr2

signaling pathway in human bronchial epithelial cells favors the development of an asthma-like phenotype by generating a biased response towards the Th2 pro-inflammatory profile.

XIV. Summary and Conclusion

Here we show that our fusion proteins can elicit a robust and independent activation of each signaling pathway in multiple cellular systems. We transfected our β_2AR-Gαs and β_2AR-βarr2 fusion constructs separately into HEK 293 cells; cells that are commonly used to characterize the β_2AR behavior and pharmacology. As predicted, the β_2AR-Gαs and β_2AR-βarr2 fusion proteins showed steric hindrance from other non-tethered signaling molecules and selectively increased the constitutive activity of the receptor via the signaling molecule fused to the receptor. The differential affinity of ligands for our fusion proteins also favored the argument that each fusion protein has a distinct active conformation. We also demonstrated that the signaling activity of the receptor for both pathways can still be manipulated by ligands, suggesting that the structure of the receptor fused to any signaling molecule is not locked in its conformational state. This allowed us to measure the potency of all β_2AR ligands and create an integral scale based on the properties of affinity and efficacy of each ligand to quantify their absolute biased signaling independent from a reference ligand. This method might reveal the true intrinsic power of the chemical structure of a ligand. Therefore, our fusion proteins can also facilitate the study and development of biased ligands by the implementation of the absolute ligand bias scale proposed here that could ultimately increase the therapeutic efficacy and/or decrease adverse effects. Finally, by using the immortalized human bronchial epithelial cell line, BEAS-2B cells, we further demonstrated that the selective constitutive activity of our fusion proteins observed in HEK 293 cells is preserved in a more physiologically relevant cell type. Measurements of β_2AR-mediated cytokine release in BEAS-2B cells revealed that the constitutive signaling via each pathway is translated into a unique cellular response that differs between the two pathways. Moreover, the β_2AR-βarr2 signaling pathway induces a strong type 2 immune response not observed for the β_2AR-Gαs signaling pathway. Thus, the fusion proteins can be used to study the pathway-specific pharmacology of

β_2AR ligands and the physiological consequences of inducing a gain-of-function. This mechanism can also be used as a tool to dissect the most well-known signaling pathways of the β_2AR and study other physiological systems.

References

Al-Sawalha, N., Pokkunuri, I., Omoluabi, O., Kim, H., Thanawala, V. J., Hernandez, A., Bond, R. A., & Knoll, B. J. (2015). Epinephrine Activation of the beta2-Adrenoceptor Is Required for IL-13-Induced Mucin Production in Human Bronchial Epithelial Cells. *PLoS One, 10*(7), e0132559. https://doi.org/10.1371/journal.pone.0132559

Alexander, S. P. H., Christopoulos, A., Davenport, A. P., Kelly, E., Mathie, A., Peters, J. A., Veale, E. L., Armstrong, J. F., Faccenda, E., Harding, S. D., Pawson, A. J., Sharman, J. L., Southan, C., Davies, J. A., & Collaborators, C. (2019, Dec). THE CONCISE GUIDE TO PHARMACOLOGY 2019/20: G protein-coupled receptors. *Br J Pharmacol, 176 Suppl 1*, S21-S141. https://doi.org/10.1111/bph.14748

Antos, C. L., Frey, N., Marx, S. O., Reiken, S., Gaburjakova, M., Richardson, J. A., Marks, A. R., & Olson, E. N. (2001, Nov 23). Dilated cardiomyopathy and sudden death resulting from constitutive activation of protein kinase a. *Circ Res, 89*(11), 997-1004. https://doi.org/10.1161/hh2301.100003

Ariens, E. J. (1954, Sep 1). Affinity and intrinsic activity in the theory of competitive inhibition. I. Problems and theory. *Arch Int Pharmacodyn Ther, 99*(1), 32-49. https://www.ncbi.nlm.nih.gov/pubmed/13229418

Arunlakshana, O., & Schild, H. O. (1959, Mar). Some quantitative uses of drug antagonists. *Br J Pharmacol Chemother, 14*(1), 48-58. https://doi.org/10.1111/j.1476-5381.1959.tb00928.x

Atsuta, J., Sterbinsky, S. A., Plitt, J., Schwiebert, L. M., Bochner, B. S., & Schleimer, R. P. (1997, Nov). Phenotyping and cytokine regulation of the BEAS-2B human bronchial epithelial cell: demonstration of inducible expression of the adhesion molecules VCAM-1 and ICAM-1. *Am J Respir Cell Mol Biol, 17*(5), 571-582. https://doi.org/10.1165/ajrcmb.17.5.2685

Attramadal, H., Arriza, J. L., Aoki, C., Dawson, T. M., Codina, J., Kwatra, M. M., Snyder, S. H., Caron, M. G., & Lefkowitz, R. J. (1992, Sep 5). Beta-arrestin2, a novel member of the arrestin/beta-arrestin gene family. *J Biol Chem, 267*(25), 17882-17890. https://www.ncbi.nlm.nih.gov/pubmed/1517224

Azzi, M., Charest, P. G., Angers, S., Rousseau, G., Kohout, T., Bouvier, M., & Pineyro, G. (2003, Sep 30). Beta-arrestin-mediated activation of MAPK by inverse agonists reveals distinct active conformations for G protein-coupled receptors. *Proc Natl Acad Sci U S A, 100*(20), 11406-11411. https://doi.org/10.1073/pnas.1936664100

Baines, K. J., Simpson, J. L., Bowden, N. A., Scott, R. J., & Gibson, P. G. (2010, Mar). Differential gene expression and cytokine production from neutrophils in asthma phenotypes. *Eur Respir J, 35*(3), 522-531. https://doi.org/10.1183/09031936.00027409

Baker, J. G. (2005, Feb). The selectivity of beta-adrenoceptor antagonists at the human beta1, beta2 and beta3 adrenoceptors. *Br J Pharmacol, 144*(3), 317-322. https://doi.org/10.1038/sj.bjp.0706048

Ballesteros, J. A., Jensen, A. D., Liapakis, G., Rasmussen, S. G., Shi, L., Gether, U., & Javitch, J. A. (2001, Aug 3). Activation of the beta 2-adrenergic receptor involves disruption of an ionic lock between the cytoplasmic ends of transmembrane

segments 3 and 6. *J Biol Chem, 276*(31), 29171-29177. https://doi.org/10.1074/jbc.M103747200

Barak, L. S., Menard, L., Ferguson, S. S., Colapietro, A. M., & Caron, M. G. (1995, Nov 28). The conserved seven-transmembrane sequence NP(X)2,3Y of the G-protein-coupled receptor superfamily regulates multiple properties of the beta 2-adrenergic receptor. *Biochemistry, 34*(47), 15407-15414. https://doi.org/10.1021/bi00047a003

Barnes, P. J. (2008, Nov). The cytokine network in asthma and chronic obstructive pulmonary disease. *J Clin Invest, 118*(11), 3546-3556. https://doi.org/10.1172/JCI36130

Benovic, J. L., Kuhn, H., Weyand, I., Codina, J., Caron, M. G., & Lefkowitz, R. J. (1987, Dec). Functional desensitization of the isolated beta-adrenergic receptor by the beta-adrenergic receptor kinase: potential role of an analog of the retinal protein arrestin (48-kDa protein). *Proc Natl Acad Sci U S A, 84*(24), 8879-8882. https://doi.org/10.1073/pnas.84.24.8879

Benovic, J. L., Pike, L. J., Cerione, R. A., Staniszewski, C., Yoshimasa, T., Codina, J., Caron, M. G., & Lefkowitz, R. J. (1985, Jun 10). Phosphorylation of the mammalian beta-adrenergic receptor by cyclic AMP-dependent protein kinase. Regulation of the rate of receptor phosphorylation and dephosphorylation by agonist occupancy and effects on coupling of the receptor to the stimulatory guanine nucleotide regulatory protein. *J Biol Chem, 260*(11), 7094-7101. https://www.ncbi.nlm.nih.gov/pubmed/2987243

Benovic, J. L., Strasser, R. H., Caron, M. G., & Lefkowitz, R. J. (1986, May). Beta-adrenergic receptor kinase: identification of a novel protein kinase that

phosphorylates the agonist-occupied form of the receptor. *Proc Natl Acad Sci U S A, 83*(9), 2797-2801. https://doi.org/10.1073/pnas.83.9.2797

Berg, K. A., Maayani, S., Goldfarb, J., Scaramellini, C., Leff, P., & Clarke, W. P. (1998, Jul). Effector pathway-dependent relative efficacy at serotonin type 2A and 2C receptors: evidence for agonist-directed trafficking of receptor stimulus. *Mol Pharmacol, 54*(1), 94-104. https://www.ncbi.nlm.nih.gov/pubmed/9658194

Bertin, B., Freissmuth, M., Jockers, R., Strosberg, A. D., & Marullo, S. (1994, Sep 13). Cellular signaling by an agonist-activated receptor/Gs alpha fusion protein. *Proc Natl Acad Sci U S A, 91*(19), 8827-8831. https://doi.org/10.1073/pnas.91.19.8827

Bhattacharya, S., Hall, S. E., Li, H., & Vaidehi, N. (2008, Mar 15). Ligand-stabilized conformational states of human beta(2) adrenergic receptor: insight into G-protein-coupled receptor activation. *Biophys J, 94*(6), 2027-2042. https://doi.org/10.1529/biophysj.107.117648

Black, J. W., & Leff, P. (1983, Dec 22). Operational models of pharmacological agonism. *Proc R Soc Lond B Biol Sci, 220*(1219), 141-162. https://doi.org/10.1098/rspb.1983.0093

Black, J. W., Leff, P., Shankley, N. P., & Wood, J. (1985, Feb). An operational model of pharmacological agonism: the effect of E/[A] curve shape on agonist dissociation constant estimation. *Br J Pharmacol, 84*(2), 561-571. https://doi.org/10.1111/j.1476-5381.1985.tb12941.x

Bond, R. A. (2001, Jun). Is paradoxical pharmacology a strategy worth pursuing? *Trends Pharmacol Sci, 22*(6), 273-276. https://doi.org/10.1016/s0165-6147(00)01711-9

Bond, R. A., Leff, P., Johnson, T. D., Milano, C. A., Rockman, H. A., McMinn, T. R., Apparsundaram, S., Hyek, M. F., Kenakin, T. P., Allen, L. F., & et al. (1995, Mar 16). Physiological effects of inverse agonists in transgenic mice with myocardial overexpression of the beta 2-adrenoceptor. *Nature, 374*(6519), 272-276. https://doi.org/10.1038/374272a0

Bond, R. A., Lucero Garcia-Rojas, E. Y., Hegde, A., & Walker, J. K. L. (2019). Therapeutic Potential of Targeting ss-Arrestin. *Front Pharmacol, 10*, 124. https://doi.org/10.3389/fphar.2019.00124

Bouaboula, M., Perrachon, S., Milligan, L., Canat, X., Rinaldi-Carmona, M., Portier, M., Barth, F., Calandra, B., Pecceu, F., Lupker, J., Maffrand, J. P., Le Fur, G., & Casellas, P. (1997, Aug 29). A selective inverse agonist for central cannabinoid receptor inhibits mitogen-activated protein kinase activation stimulated by insulin or insulin-like growth factor 1. Evidence for a new model of receptor/ligand interactions. *J Biol Chem, 272*(35), 22330-22339. https://doi.org/10.1074/jbc.272.35.22330

Bourquard, T., Landomiel, F., Reiter, E., Crepieux, P., Ritchie, D. W., Aze, J., & Poupon, A. (2015, Jun 1). Unraveling the molecular architecture of a G protein-coupled receptor/beta-arrestin/Erk module complex. *Sci Rep, 5*, 10760. https://doi.org/10.1038/srep10760

Bozkurt, B., Bolos, M., Deswal, A., Ather, S., Chan, W., Mann, D. L., & Carabello, B. (2012, Mar). New insights into mechanisms of action of carvedilol treatment in chronic heart failure patients--a matter of time for contractility. *J Card Fail, 18*(3), 183-193. https://doi.org/10.1016/j.cardfail.2011.11.004

Bristow, M. R. (2000, Feb 8). beta-adrenergic receptor blockade in chronic heart failure. *Circulation, 101*(5), 558-569. https://doi.org/10.1161/01.cir.101.5.558

Bristow, M. R. (2011, Oct 28). Treatment of chronic heart failure with beta-adrenergic receptor antagonists: a convergence of receptor pharmacology and clinical cardiology. *Circ Res, 109*(10), 1176-1194. https://doi.org/10.1161/CIRCRESAHA.111.245092

Bristow, M. R., Ginsburg, R., Umans, V., Fowler, M., Minobe, W., Rasmussen, R., Zera, P., Menlove, R., Shah, P., Jamieson, S., & et al. (1986, Sep). Beta 1- and beta 2-adrenergic-receptor subpopulations in nonfailing and failing human ventricular myocardium: coupling of both receptor subtypes to muscle contraction and selective beta 1-receptor down-regulation in heart failure. *Circ Res, 59*(3), 297-309. https://doi.org/10.1161/01.res.59.3.297

Bristow, M. R., Port, J. D., Hershberger, R. E., Gilbert, E. M., & Feldman, A. M. (1989, Jun). The beta-adrenergic receptor-adenylate cyclase complex as a target for therapeutic intervention in heart failure. *Eur Heart J, 10 Suppl B*, 45-54. https://doi.org/10.1093/eurheartj/10.suppl_b.45

Brodde, O. E. (2007, Feb). Beta-adrenoceptor blocker treatment and the cardiac beta-adrenoceptor-G-protein(s)-adenylyl cyclase system in chronic heart failure. *Naunyn Schmiedebergs Arch Pharmacol, 374*(5-6), 361-372. https://doi.org/10.1007/s00210-006-0125-7

Broide, D. H., Lotz, M., Cuomo, A. J., Coburn, D. A., Federman, E. C., & Wasserman, S. I. (1992, May). Cytokines in symptomatic asthma airways. *J Allergy Clin Immunol, 89*(5), 958-967. https://doi.org/10.1016/0091-6749(92)90218-q

Brooks, W. W., & Conrad, C. H. (2009, Aug). Isoproterenol-induced myocardial injury and diastolic dysfunction in mice: structural and functional correlates. *Comp Med, 59*(4), 339-343. https://www.ncbi.nlm.nih.gov/pubmed/19712573

Callaerts-Vegh, Z., Evans, K. L., Dudekula, N., Cuba, D., Knoll, B. J., Callaerts, P. F., Giles, H., Shardonofsky, F. R., & Bond, R. A. (2004, Apr 6). Effects of acute and chronic administration of beta-adrenoceptor ligands on airway function in a murine model of asthma. *Proc Natl Acad Sci U S A, 101*(14), 4948-4953. https://doi.org/10.1073/pnas.0400452101

Capote, A. E., Batra, A., Warren, C. M., Chowdhury, S. A. K., Wolska, B. M., Solaro, R. J., & Rosas, P. C. (2021). B-arrestin-2 Signaling Is Important to Preserve Cardiac Function During Aging. *Front Physiol, 12*, 696852. https://doi.org/10.3389/fphys.2021.696852

Carr, R., 3rd, Du, Y., Quoyer, J., Panettieri, R. A., Jr., Janz, J. M., Bouvier, M., Kobilka, B. K., & Benovic, J. L. (2014, Dec 26). Development and characterization of pepducins as Gs-biased allosteric agonists. *J Biol Chem, 289*(52), 35668-35684. https://doi.org/10.1074/jbc.M114.618819

Carr, R., 3rd, Schilling, J., Song, J., Carter, R. L., Du, Y., Yoo, S. M., Traynham, C. J., Koch, W. J., Cheung, J. Y., Tilley, D. G., & Benovic, J. L. (2016, Jul 12). beta-arrestin-biased signaling through the beta2-adrenergic receptor promotes cardiomyocyte contraction. *Proc Natl Acad Sci U S A, 113*(28), E4107-4116. https://doi.org/10.1073/pnas.1606267113

Casella, I., Ambrosio, C., Gro, M. C., Molinari, P., & Costa, T. (2011, Aug 15). Divergent agonist selectivity in activating beta1- and beta2-adrenoceptors for G-protein and

arrestin coupling. *Biochem J,* *438*(1), 191-202. https://doi.org/10.1042/BJ20110374

Cerione, R. A., Strulovici, B., Benovic, J. L., Strader, C. D., Caron, M. G., & Lefkowitz, R. J. (1983, Aug). Reconstitution of beta-adrenergic receptors in lipid vesicles: affinity chromatography-purified receptors confer catecholamine responsiveness on a heterologous adenylate cyclase system. *Proc Natl Acad Sci U S A, 80*(16), 4899-4903. https://doi.org/10.1073/pnas.80.16.4899

Chen, M., Hegde, A., Choi, Y. H., Theriot, B. S., Premont, R. T., Chen, W., & Walker, J. K. (2015, Sep). Genetic Deletion of beta-Arrestin-2 and the Mitigation of Established Airway Hyperresponsiveness in a Murine Asthma Model. *Am J Respir Cell Mol Biol, 53*(3), 346-354. https://doi.org/10.1165/rcmb.2014-0231OC

Cherezov, V., Rosenbaum, D. M., Hanson, M. A., Rasmussen, S. G., Thian, F. S., Kobilka, T. S., Choi, H. J., Kuhn, P., Weis, W. I., Kobilka, B. K., & Stevens, R. C. (2007, Nov 23). High-resolution crystal structure of an engineered human beta2-adrenergic G protein-coupled receptor. *Science, 318*(5854), 1258-1265. https://doi.org/10.1126/science.1150577

Christopoulos, A., Changeux, J. P., Catterall, W. A., Fabbro, D., Burris, T. P., Cidlowski, J. A., Olsen, R. W., Peters, J. A., Neubig, R. R., Pin, J. P., Sexton, P. M., Kenakin, T. P., Ehlert, F. J., Spedding, M., & Langmead, C. J. (2014, Oct). International Union of Basic and Clinical Pharmacology. XC. multisite pharmacology: recommendations for the nomenclature of receptor allosterism and allosteric ligands. *Pharmacol Rev,* *66*(4), 918-947. https://doi.org/10.1124/pr.114.008862

Chun, E., Thompson, A. A., Liu, W., Roth, C. B., Griffith, M. T., Katritch, V., Kunken, J., Xu, F., Cherezov, V., Hanson, M. A., & Stevens, R. C. (2012, Jun 6). Fusion partner toolchest for the stabilization and crystallization of G protein-coupled receptors. *Structure, 20*(6), 967-976. https://doi.org/10.1016/j.str.2012.04.010

Chung, K. Y., Rasmussen, S. G., Liu, T., Li, S., DeVree, B. T., Chae, P. S., Calinski, D., Kobilka, B. K., Woods, V. L., Jr., & Sunahara, R. K. (2011, Sep 28). Conformational changes in the G protein Gs induced by the beta2 adrenergic receptor. *Nature, 477*(7366), 611-615. https://doi.org/10.1038/nature10488

Clark, A., & Raventos, J. (1937). The antagonism of acetylcholine and of quaternary ammonium salts. *Quarterly Journal of Experimental Physiology: Translation and Integration, 26*(4), 375-392.

Clark, A. J. (1926, Aug 6). The reaction between acetyl choline and muscle cells. *J Physiol, 61*(4), 530-546. https://doi.org/10.1113/jphysiol.1926.sp002314

Clark, A. J. (1927, Nov 21). The reaction between acetyl choline and muscle cells: Part II. *J Physiol, 64*(2), 123-143. https://doi.org/10.1113/jphysiol.1927.sp002424

Clarke, W. P., & Bond, R. A. (1998, Jul). The elusive nature of intrinsic efficacy. *Trends Pharmacol Sci, 19*(7), 270-276. https://doi.org/10.1016/s0165-6147(97)01138-3

Coffa, S., Breitman, M., Hanson, S. M., Callaway, K., Kook, S., Dalby, K. N., & Gurevich, V. V. (2011). The effect of arrestin conformation on the recruitment of c-Raf1, MEK1, and ERK1/2 activation. *PLoS One, 6*(12), e28723. https://doi.org/10.1371/journal.pone.0028723

Cohn, J. N., Levine, T. B., Olivari, M. T., Garberg, V., Lura, D., Francis, G. S., Simon, A. B., & Rector, T. (1984, Sep 27). Plasma norepinephrine as a guide to prognosis in patients with chronic congestive heart failure. *N Engl J Med, 311*(13), 819-823. https://doi.org/10.1056/NEJM198409273111303

Colquhoun, D. (2007, Dec). Why the Schild method is better than Schild realised. *Trends Pharmacol Sci, 28*(12), 608-614. https://doi.org/10.1016/j.tips.2007.09.011

Costa, T., & Herz, A. (1989, Oct). Antagonists with negative intrinsic activity at delta opioid receptors coupled to GTP-binding proteins. *Proc Natl Acad Sci U S A, 86*(19), 7321-7325. https://doi.org/10.1073/pnas.86.19.7321

de Diego, A. M., Gandia, L., & Garcia, A. G. (2008, Feb). A physiological view of the central and peripheral mechanisms that regulate the release of catecholamines at the adrenal medulla. *Acta Physiol (Oxf), 192*(2), 287-301. https://doi.org/10.1111/j.1748-1716.2007.01807.x

De Lean, A., Stadel, J. M., & Lefkowitz, R. J. (1980, Aug 10). A ternary complex model explains the agonist-specific binding properties of the adenylate cyclase-coupled beta-adrenergic receptor. *J Biol Chem, 255*(15), 7108-7117. https://www.ncbi.nlm.nih.gov/pubmed/6248546

de Lucia, C., Eguchi, A., & Koch, W. J. (2018). New Insights in Cardiac beta-Adrenergic Signaling During Heart Failure and Aging. *Front Pharmacol, 9*, 904. https://doi.org/10.3389/fphar.2018.00904

DeFea, K. A., Vaughn, Z. D., O'Bryan, E. M., Nishijima, D., Dery, O., & Bunnett, N. W. (2000, Sep 26). The proliferative and antiapoptotic effects of substance P are

facilitated by formation of a beta -arrestin-dependent scaffolding complex. *Proc Natl Acad Sci U S A, 97*(20), 11086-11091. https://doi.org/10.1073/pnas.190276697

Del Castillo, J., & Katz, B. (1957, May 7). Interaction at end-plate receptors between different choline derivatives. *Proc R Soc Lond B Biol Sci, 146*(924), 369-381. https://doi.org/10.1098/rspb.1957.0018

Del Prete, G. F., De Carli, M., Mastromauro, C., Biagiotti, R., Macchia, D., Falagiani, P., Ricci, M., & Romagnani, S. (1991, Jul). Purified protein derivative of Mycobacterium tuberculosis and excretory-secretory antigen(s) of Toxocara canis expand in vitro human T cells with stable and opposite (type 1 T helper or type 2 T helper) profile of cytokine production. *J Clin Invest, 88*(1), 346-350. https://doi.org/10.1172/JCI115300

Deupi, X., & Kobilka, B. K. (2010, Oct). Energy landscapes as a tool to integrate GPCR structure, dynamics, and function. *Physiology (Bethesda), 25*(5), 293-303. https://doi.org/10.1152/physiol.00002.2010

Dixon, R. A., Kobilka, B. K., Strader, D. J., Benovic, J. L., Dohlman, H. G., Frielle, T., Bolanowski, M. A., Bennett, C. D., Rands, E., Diehl, R. E., Mumford, R. A., Slater, E. E., Sigal, I. S., Caron, M. G., Lefkowitz, R. J., & Strader, C. D. (1986, May 1-7). Cloning of the gene and cDNA for mammalian beta-adrenergic receptor and homology with rhodopsin. *Nature, 321*(6065), 75-79. https://doi.org/10.1038/321075a0

Dixon, R. A., Sigal, I. S., Rands, E., Register, R. B., Candelore, M. R., Blake, A. D., & Strader, C. D. (1987, Mar 5-11). Ligand binding to the beta-adrenergic receptor

involves its rhodopsin-like core. *Nature, 326*(6108), 73-77. https://doi.org/10.1038/326073a0

Dror, R. O., Arlow, D. H., Maragakis, P., Mildorf, T. J., Pan, A. C., Xu, H., Borhani, D. W., & Shaw, D. E. (2011, Nov 15). Activation mechanism of the beta2-adrenergic receptor. *Proc Natl Acad Sci U S A, 108*(46), 18684-18689. https://doi.org/10.1073/pnas.1110499108

Du, X. J., Gao, X. M., Wang, B., Jennings, G. L., Woodcock, E. A., & Dart, A. M. (2000, Dec). Age-dependent cardiomyopathy and heart failure phenotype in mice overexpressing beta(2)-adrenergic receptors in the heart. *Cardiovasc Res, 48*(3), 448-454. https://doi.org/10.1016/s0008-6363(00)00187-5

Du, Y., Duc, N. M., Rasmussen, S. G. F., Hilger, D., Kubiak, X., Wang, L., Bohon, J., Kim, H. R., Wegrecki, M., Asuru, A., Jeong, K. M., Lee, J., Chance, M. R., Lodowski, D. T., Kobilka, B. K., & Chung, K. Y. (2019, May 16). Assembly of a GPCR-G Protein Complex. *Cell, 177*(5), 1232-1242 e1211. https://doi.org/10.1016/j.cell.2019.04.022

Eddy, M. T., Didenko, T., Stevens, R. C., & Wuthrich, K. (2016, Dec 6). beta2-Adrenergic Receptor Conformational Response to Fusion Protein in the Third Intracellular Loop. *Structure, 24*(12), 2190-2197. https://doi.org/10.1016/j.str.2016.09.015

Ehlert, F. J. (2005, Nov). Analysis of allosterism in functional assays. *J Pharmacol Exp Ther, 315*(2), 740-754. https://doi.org/10.1124/jpet.105.090886

Eichel, K., Jullie, D., Barsi-Rhyne, B., Latorraca, N. R., Masureel, M., Sibarita, J. B., Dror, R. O., & von Zastrow, M. (2018, May). Catalytic activation of beta-arrestin

by GPCRs. *Nature, 557*(7705), 381-386. https://doi.org/10.1038/s41586-018-0079-1

El-Armouche, A., Wittkopper, K., Degenhardt, F., Weinberger, F., Didie, M., Melnychenko, I., Grimm, M., Peeck, M., Zimmermann, W. H., Unsold, B., Hasenfuss, G., Dobrev, D., & Eschenhagen, T. (2008, Dec 1). Phosphatase inhibitor-1-deficient mice are protected from catecholamine-induced arrhythmias and myocardial hypertrophy. *Cardiovasc Res, 80*(3), 396-406. https://doi.org/10.1093/cvr/cvn208

Erickson, C. E., Gul, R., Blessing, C. P., Nguyen, J., Liu, T., Pulakat, L., Bastepe, M., Jackson, E. K., & Andresen, B. T. (2013). The beta-blocker Nebivolol Is a GRK/beta-arrestin biased agonist. *PLoS One, 8*(8), e71980. https://doi.org/10.1371/journal.pone.0071980

Fajardo, G., Zhao, M., Urashima, T., Farahani, S., Hu, D. Q., Reddy, S., & Bernstein, D. (2013, Oct). Deletion of the beta2-adrenergic receptor prevents the development of cardiomyopathy in mice. *J Mol Cell Cardiol, 63*, 155-164. https://doi.org/10.1016/j.yjmcc.2013.07.016

Fathy, D. B., Leeb, T., Mathis, S. A., & Leeb-Lundberg, L. M. (1999, Oct 15). Spontaneous human B2 bradykinin receptor activity determines the action of partial agonists as agonists or inverse agonists. Effect of basal desensitization. *J Biol Chem, 274*(42), 29603-29606. https://doi.org/10.1074/jbc.274.42.29603

Ferrara, N., Komici, K., Corbi, G., Pagano, G., Furgi, G., Rengo, C., Femminella, G. D., Leosco, D., & Bonaduce, D. (2014, Jan 9). beta-adrenergic receptor responsiveness in aging heart and clinical implications. *Front Physiol, 4*, 396. https://doi.org/10.3389/fphys.2013.00396

Ferrero, P., Said, M., Sanchez, G., Vittone, L., Valverde, C., Donoso, P., Mattiazzi, A., & Mundina-Weilenmann, C. (2007, Sep). Ca2+/calmodulin kinase II increases ryanodine binding and Ca2+-induced sarcoplasmic reticulum Ca2+ release kinetics during beta-adrenergic stimulation. *J Mol Cell Cardiol, 43*(3), 281-291. https://doi.org/10.1016/j.yjmcc.2007.05.022

Forkuo, G. S., Kim, H., Thanawala, V. J., Al-Sawalha, N., Valdez, D., Joshi, R., Parra, S., Pera, T., Gonnella, P. A., Knoll, B. J., Walker, J. K., Penn, R. B., & Bond, R. A. (2016, Aug). Phosphodiesterase 4 Inhibitors Attenuate the Asthma Phenotype Produced by beta2-Adrenoceptor Agonists in Phenylethanolamine N-Methyltransferase-Knockout Mice. *Am J Respir Cell Mol Biol, 55*(2), 234-242. https://doi.org/10.1165/rcmb.2015-0373OC

Frigyesi, A., & Hossjer, O. (2006, Sep 15). Estimating the parameters of the operational model of pharmacological agonism. *Stat Med, 25*(17), 2932-2945. https://doi.org/10.1002/sim.2448

Furchgott, R. F. (1966, Nov). Metabolic factors that influence contractility of vascular smooth muscle. *Bull N Y Acad Med, 42*(11), 996-1006. https://www.ncbi.nlm.nih.gov/pubmed/5232128

Furchgott, R. F., & Bursztyn, P. (1967). Comparison of dissociation constants and of relative efficacies of selected agonists acting on parasympathetic receptors. *Annals of the New York Academy of Sciences, 144*(2), 882-899.

Gabilondo, A. M., Krasel, C., & Lohse, M. J. (1996, Jun 27). Mutations of Tyr326 in the beta 2-adrenoceptor disrupt multiple receptor functions. *Eur J Pharmacol, 307*(2), 243-250. https://doi.org/10.1016/0014-2999(96)00247-6

Gaddum, J. (1943). Introductory address. Part I. Biological aspects: the antagonism of drugs. *Transactions of the Faraday Society, 39*, 323-332.

Gaddum, J. H. (1937). The quantitative effects of antagonistic drugs. *J. physiol, 89*, 7P-9P.

Galandrin, S., & Bouvier, M. (2006, Nov). Distinct signaling profiles of beta1 and beta2 adrenergic receptor ligands toward adenylyl cyclase and mitogen-activated protein kinase reveals the pluridimensionality of efficacy. *Mol Pharmacol, 70*(5), 1575-1584. https://doi.org/10.1124/mol.106.026716

Gazi, L., Bobirnac, I., Danzeisen, M., Schupbach, E., Langenegger, D., Sommer, B., Hoyer, D., Tricklebank, M., & Schoeffter, P. (1999, Oct). Receptor density as a factor governing the efficacy of the dopamine D4 receptor ligands, L-745,870 and U-101958 at human recombinant D4.4 receptors expressed in CHO cells. *Br J Pharmacol, 128*(3), 613-620. https://doi.org/10.1038/sj.bjp.0702849

Gesty-Palmer, D., Chen, M., Reiter, E., Ahn, S., Nelson, C. D., Wang, S., Eckhardt, A. E., Cowan, C. L., Spurney, R. F., Luttrell, L. M., & Lefkowitz, R. J. (2006, Apr 21). Distinct beta-arrestin- and G protein-dependent pathways for parathyroid hormone receptor-stimulated ERK1/2 activation. *J Biol Chem, 281*(16), 10856-10864. https://doi.org/10.1074/jbc.M513380200

Ghanouni, P., Gryczynski, Z., Steenhuis, J. J., Lee, T. W., Farrens, D. L., Lakowicz, J. R., & Kobilka, B. K. (2001, Jul 6). Functionally different agonists induce distinct conformations in the G protein coupling domain of the beta 2 adrenergic receptor. *J Biol Chem, 276*(27), 24433-24436. https://doi.org/10.1074/jbc.C100162200

Ghanouni, P., Schambye, H., Seifert, R., Lee, T. W., Rasmussen, S. G., Gether, U., & Kobilka, B. K. (2000, Feb 4). The effect of pH on beta(2) adrenoceptor function. Evidence for protonation-dependent activation. *J Biol Chem, 275*(5), 3121-3127. https://doi.org/10.1074/jbc.275.5.3121

Giembycz, M. A., & Newton, R. (2006, Jun). Beyond the dogma: novel beta2-adrenoceptor signalling in the airways. *Eur Respir J, 27*(6), 1286-1306. https://doi.org/10.1183/09031936.06.00112605

Goldsmith, Z. G., & Dhanasekaran, D. N. (2007, May 14). G protein regulation of MAPK networks. *Oncogene, 26*(22), 3122-3142. https://doi.org/10.1038/sj.onc.1210407

Gomes, I., Sierra, S., Lueptow, L., Gupta, A., Gouty, S., Margolis, E. B., Cox, B. M., & Devi, L. A. (2020, May 26). Biased signaling by endogenous opioid peptides. *Proc Natl Acad Sci U S A, 117*(21), 11820-11828. https://doi.org/10.1073/pnas.2000712117

Goodman, O. B., Jr., Krupnick, J. G., Santini, F., Gurevich, V. V., Penn, R. B., Gagnon, A. W., Keen, J. H., & Benovic, J. L. (1996, Oct 3). Beta-arrestin acts as a clathrin adaptor in endocytosis of the beta2-adrenergic receptor. *Nature, 383*(6599), 447-450. https://doi.org/10.1038/383447a0

Granzin, J., Wilden, U., Choe, H. W., Labahn, J., Krafft, B., & Buldt, G. (1998, Feb 26). X-ray crystal structure of arrestin from bovine rod outer segments. *Nature, 391*(6670), 918-921. https://doi.org/10.1038/36147

Gregory, K. J., Hall, N. E., Tobin, A. B., Sexton, P. M., & Christopoulos, A. (2010, Mar 5). Identification of orthosteric and allosteric site mutations in M2 muscarinic

acetylcholine receptors that contribute to ligand-selective signaling bias. *J Biol Chem, 285*(10), 7459-7474. https://doi.org/10.1074/jbc.M109.094011

Grimm, M., & Brown, J. H. (2010, Feb). Beta-adrenergic receptor signaling in the heart: role of CaMKII. *J Mol Cell Cardiol, 48*(2), 322-330. https://doi.org/10.1016/j.yjmcc.2009.10.016

Grisanti, L. A., Thomas, T. P., Carter, R. L., de Lucia, C., Gao, E., Koch, W. J., Benovic, J. L., & Tilley, D. G. (2018). Pepducin-mediated cardioprotection via beta-arrestin-biased beta2-adrenergic receptor-specific signaling. *Theranostics, 8*(17), 4664-4678. https://doi.org/10.7150/thno.26619

Gurevich, V. V., & Gurevich, E. V. (2004, Feb). The molecular acrobatics of arrestin activation. *Trends Pharmacol Sci, 25*(2), 105-111. https://doi.org/10.1016/j.tips.2003.12.008

Gurwitz, D., Haring, R., Heldman, E., Fraser, C. M., Manor, D., & Fisher, A. (1994, Mar 15). Discrete activation of transduction pathways associated with acetylcholine m1 receptor by several muscarinic ligands. *Eur J Pharmacol, 267*(1), 21-31. https://doi.org/10.1016/0922-4106(94)90220-8

Hall, S. A., Cigarroa, C. G., Marcoux, L., Risser, R. C., Grayburn, P. A., & Eichhorn, E. J. (1995, Apr). Time course of improvement in left ventricular function, mass and geometry in patients with congestive heart failure treated with beta-adrenergic blockade. *J Am Coll Cardiol, 25*(5), 1154-1161. https://doi.org/10.1016/0735-1097(94)00543-y

Hamed, O., Joshi, R., Michi, A. N., Kooi, C., & Giembycz, M. A. (2021, Oct). beta 2-Adrenoceptor Agonists Promote Extracellular Signal-Regulated Kinase 1/2

Dephosphorylation in Human Airway Epithelial Cells by Canonical, cAMP-Driven Signaling Independently of beta-Arrestin 2. *Mol Pharmacol, 100*(4), 388-405. https://doi.org/10.1124/molpharm.121.000294

Hanania, N. A., Mannava, B., Franklin, A. E., Lipworth, B. J., Williamson, P. A., Garner, W. J., Dickey, B. F., & Bond, R. A. (2010, Oct). Response to salbutamol in patients with mild asthma treated with nadolol. *Eur Respir J, 36*(4), 963-965. https://doi.org/10.1183/09031936.00003210

Hanania, N. A., Singh, S., El-Wali, R., Flashner, M., Franklin, A. E., Garner, W. J., Dickey, B. F., Parra, S., Ruoss, S., Shardonofsky, F., O'Connor, B. J., Page, C., & Bond, R. A. (2008). The safety and effects of the beta-blocker, nadolol, in mild asthma: an open-label pilot study. *Pulm Pharmacol Ther, 21*(1), 134-141. https://doi.org/10.1016/j.pupt.2007.07.002

Hanson, M. A., Cherezov, V., Griffith, M. T., Roth, C. B., Jaakola, V. P., Chien, E. Y., Velasquez, J., Kuhn, P., & Stevens, R. C. (2008, Jun). A specific cholesterol binding site is established by the 2.8 A structure of the human beta2-adrenergic receptor. *Structure, 16*(6), 897-905. https://doi.org/10.1016/j.str.2008.05.001

Harada, R., Sugita, Y., & Feig, M. (2012, Mar 14). Protein crowding affects hydration structure and dynamics. *J Am Chem Soc, 134*(10), 4842-4849. https://doi.org/10.1021/ja211115q

Hargrave, P. A., McDowell, J. H., Curtis, D. R., Wang, J. K., Juszczak, E., Fong, S. L., Rao, J. K., & Argos, P. (1983). The structure of bovine rhodopsin. *Biophys Struct Mech, 9*(4), 235-244. https://doi.org/10.1007/BF00535659

Hasford, J., & Virchow, J. C. (2006, Nov). Excess mortality in patients with asthma on long-acting beta2-agonists. *Eur Respir J, 28*(5), 900-902. https://doi.org/10.1183/09031936.00085606

Hauser, A. S., Attwood, M. M., Rask-Andersen, M., Schioth, H. B., & Gloriam, D. E. (2017, Dec). Trends in GPCR drug discovery: new agents, targets and indications. *Nat Rev Drug Discov, 16*(12), 829-842. https://doi.org/10.1038/nrd.2017.178

Hermans, E., Challiss, R. A., & Nahorski, S. R. (1999, Feb). Effects of varying the expression level of recombinant human mGlu1alpha receptors on the pharmacological properties of agonists and antagonists. *Br J Pharmacol, 126*(4), 873-882. https://doi.org/10.1038/sj.bjp.0702359

Higgins, J. B., & Casey, P. J. (1994, Mar 25). In vitro processing of recombinant G protein gamma subunits. Requirements for assembly of an active beta gamma complex. *J Biol Chem, 269*(12), 9067-9073. https://www.ncbi.nlm.nih.gov/pubmed/8132644

Hill, A. V. (1913). The combinations of haemoglobin with oxygen and with carbon monoxide. I. *Biochemical Journal, 7*(5), 471.

Hoffmann, C., Leitz, M. R., Oberdorf-Maass, S., Lohse, M. J., & Klotz, K. N. (2004, Feb). Comparative pharmacology of human beta-adrenergic receptor subtypes--characterization of stably transfected receptors in CHO cells. *Naunyn Schmiedebergs Arch Pharmacol, 369*(2), 151-159. https://doi.org/10.1007/s00210-003-0860-y

Ippolito, M., & Benovic, J. L. (2021, Apr). Biased agonism at beta-adrenergic receptors. *Cell Signal, 80*, 109905. https://doi.org/10.1016/j.cellsig.2020.109905

Isin, B., Estiu, G., Wiest, O., & Oltvai, Z. N. (2012). Identifying ligand binding conformations of the beta2-adrenergic receptor by using its agonists as computational probes. *PLoS One, 7*(12), e50186. https://doi.org/10.1371/journal.pone.0050186

Iwase, M., Uechi, M., Vatner, D. E., Asai, K., Shannon, R. P., Kudej, R. K., Wagner, T. E., Wight, D. C., Patrick, T. A., Ishikawa, Y., Homcy, C. J., & Vatner, S. F. (1997, Jan). Cardiomyopathy induced by cardiac Gs alpha overexpression. *Am J Physiol, 272*(1 Pt 2), H585-589. https://doi.org/10.1152/ajpheart.1997.272.1.H585

Jakubik, J., Randakova, A., Rudajev, V., Zimcik, P., El-Fakahany, E. E., & Dolezal, V. (2019, Mar 15). Applications and limitations of fitting of the operational model to determine relative efficacies of agonists. *Sci Rep, 9*(1), 4637. https://doi.org/10.1038/s41598-019-40993-w

Jung, G., Fajardo, G., Ribeiro, A. J., Kooiker, K. B., Coronado, M., Zhao, M., Hu, D. Q., Reddy, S., Kodo, K., Sriram, K., Insel, P. A., Wu, J. C., Pruitt, B. L., & Bernstein, D. (2016, Apr). Time-dependent evolution of functional vs. remodeling signaling in induced pluripotent stem cell-derived cardiomyocytes and induced maturation with biomechanical stimulation. *FASEB J, 30*(4), 1464-1479. https://doi.org/10.1096/fj.15-280982

Kainuma, K., Kobayashi, T., D'Alessandro-Gabazza, C. N., Toda, M., Yasuma, T., Nishihama, K., Fujimoto, H., Kuwabara, Y., Hosoki, K., Nagao, M., Fujisawa, T., & Gabazza, E. C. (2017, May 2). beta2 adrenergic agonist suppresses

eosinophil-induced epithelial-to-mesenchymal transition of bronchial epithelial cells. *Respir Res, 18*(1), 79. https://doi.org/10.1186/s12931-017-0563-4

Katz, B., & Thesleff, S. (1957, Aug 29). A study of the desensitization produced by acetylcholine at the motor end-plate. *J Physiol, 138*(1), 63-80. https://doi.org/10.1113/jphysiol.1957.sp005838

Kaye, D. M., Lefkovits, J., Jennings, G. L., Bergin, P., Broughton, A., & Esler, M. D. (1995, Nov 1). Adverse consequences of high sympathetic nervous activity in the failing human heart. *J Am Coll Cardiol, 26*(5), 1257-1263. https://doi.org/10.1016/0735-1097(95)00332-0

Kenakin, T. (1995, Jul). Agonist-receptor efficacy. II. Agonist trafficking of receptor signals. *Trends Pharmacol Sci, 16*(7), 232-238. https://doi.org/10.1016/s0165-6147(00)89032-x

Kenakin, T. (2011, Feb). Functional selectivity and biased receptor signaling. *J Pharmacol Exp Ther, 336*(2), 296-302. https://doi.org/10.1124/jpet.110.173948

Kenakin, T. (2016, Jan). The mass action equation in pharmacology. *Br J Clin Pharmacol, 81*(1), 41-51. https://doi.org/10.1111/bcp.12810

Kenakin, T. (2017a, Oct). A Scale of Agonism and Allosteric Modulation for Assessment of Selectivity, Bias, and Receptor Mutation. *Mol Pharmacol, 92*(4), 414-424. https://doi.org/10.1124/mol.117.108787

Kenakin, T. (2017b, Jan 11). Theoretical Aspects of GPCR-Ligand Complex Pharmacology. *Chem Rev, 117*(1), 4-20. https://doi.org/10.1021/acs.chemrev.5b00561

Kenakin, T. (2019, Apr). Biased Receptor Signaling in Drug Discovery. *Pharmacol Rev, 71*(2), 267-315. https://doi.org/10.1124/pr.118.016790

Kenakin, T., & Christopoulos, A. (2013a, Jun). Measurements of ligand bias and functional affinity. *Nat Rev Drug Discov, 12*(6), 483. https://doi.org/10.1038/nrd3954-c2

Kenakin, T., & Christopoulos, A. (2013b, Mar). Signalling bias in new drug discovery: detection, quantification and therapeutic impact. *Nat Rev Drug Discov, 12*(3), 205-216. https://doi.org/10.1038/nrd3954

Kenakin, T., & Strachan, R. T. (2018, Aug). PAM-Antagonists: A Better Way to Block Pathological Receptor Signaling? *Trends Pharmacol Sci, 39*(8), 748-765. https://doi.org/10.1016/j.tips.2018.05.001

Kenakin, T., Watson, C., Muniz-Medina, V., Christopoulos, A., & Novick, S. (2012, Mar 21). A simple method for quantifying functional selectivity and agonist bias. *ACS Chem Neurosci, 3*(3), 193-203. https://doi.org/10.1021/cn200111m

Kenakin, T. P. (1982, Mar). The Schild regression in the process of receptor classification. *Can J Physiol Pharmacol, 60*(3), 249-265. https://doi.org/10.1139/y82-036

Kenakin, T. P., & Boselli, C. (1991, Aug). Biphasic dose-response curves to arecoline in rat atria-mediation by a single promiscuous receptor or two receptor subtypes? *Naunyn Schmiedebergs Arch Pharmacol, 344*(2), 201-205. https://doi.org/10.1007/BF00167219

Kim, T. J., Sun, J., Lu, S., Zhang, J., & Wang, Y. (2014, Sep). The regulation of beta-adrenergic receptor-mediated PKA activation by substrate stiffness via microtubule dynamics in human MSCs. *Biomaterials, 35*(29), 8348-8356. https://doi.org/10.1016/j.biomaterials.2014.06.018

Kim, Y. J., Hofmann, K. P., Ernst, O. P., Scheerer, P., Choe, H. W., & Sommer, M. E. (2013, May 2). Crystal structure of pre-activated arrestin p44. *Nature, 497*(7447), 142-146. https://doi.org/10.1038/nature12133

Kobilka, B. K. (2011, Apr). Structural insights into adrenergic receptor function and pharmacology. *Trends Pharmacol Sci, 32*(4), 213-218. https://doi.org/10.1016/j.tips.2011.02.005

Koener, B., Focant, M. C., Bosier, B., Maloteaux, J. M., & Hermans, E. (2012, Jan 10). Increasing the density of the D2L receptor and manipulating the receptor environment are required to evidence the partial agonist properties of aripiprazole. *Prog Neuropsychopharmacol Biol Psychiatry, 36*(1), 60-70. https://doi.org/10.1016/j.pnpbp.2011.08.007

Kohout, T. A., Lin, F. S., Perry, S. J., Conner, D. A., & Lefkowitz, R. J. (2001, Feb 13). beta-Arrestin 1 and 2 differentially regulate heptahelical receptor signaling and trafficking. *Proc Natl Acad Sci U S A, 98*(4), 1601-1606. https://doi.org/10.1073/pnas.041608198

Kovoor, A., Celver, J., Abdryashitov, R. I., Chavkin, C., & Gurevich, V. V. (1999, Mar 12). Targeted construction of phosphorylation-independent beta-arrestin mutants with constitutive activity in cells. *J Biol Chem, 274*(11), 6831-6834. https://doi.org/10.1074/jbc.274.11.6831

Lambrecht, B. N., & Hammad, H. (2015, Jan). The immunology of asthma. *Nat Immunol, 16*(1), 45-56. https://doi.org/10.1038/ni.3049

Langley, J. N. (1905, Dec 30). On the reaction of cells and of nerve-endings to certain poisons, chiefly as regards the reaction of striated muscle to nicotine and to curari. *J Physiol, 33*(4-5), 374-413. https://doi.org/10.1113/jphysiol.1905.sp001128

Langmuir, I. (1918). The adsorption of gases on plane surfaces of glass, mica and platinum. *Journal of the American Chemical society, 40*(9), 1361-1403.

Lee, M. H., Appleton, K. M., Strungs, E. G., Kwon, J. Y., Morinelli, T. A., Peterson, Y. K., Laporte, S. A., & Luttrell, L. M. (2016, Mar 31). The conformational signature of beta-arrestin2 predicts its trafficking and signalling functions. *Nature, 531*(7596), 665-668. https://doi.org/10.1038/nature17154

Lerch, M. T., Matt, R. A., Masureel, M., Elgeti, M., Kumar, K. K., Hilger, D., Foys, B., Kobilka, B. K., & Hubbell, W. L. (2020, Dec 15). Viewing rare conformations of the beta2 adrenergic receptor with pressure-resolved DEER spectroscopy. *Proc Natl Acad Sci U S A, 117*(50), 31824-31831. https://doi.org/10.1073/pnas.2013904117

Liggett, S. B., Tepe, N. M., Lorenz, J. N., Canning, A. M., Jantz, T. D., Mitarai, S., Yatani, A., & Dorn, G. W., 2nd. (2000, Apr 11). Early and delayed consequences

of beta(2)-adrenergic receptor overexpression in mouse hearts: critical role for expression level. *Circulation, 101*(14), 1707-1714. https://doi.org/10.1161/01.cir.101.14.1707

Liu, J. J., Horst, R., Katritch, V., Stevens, R. C., & Wuthrich, K. (2012, Mar 2). Biased signaling pathways in beta2-adrenergic receptor characterized by 19F-NMR. *Science, 335*(6072), 1106-1110. https://doi.org/10.1126/science.1215802

Liu, X., Ahn, S., Kahsai, A. W., Meng, K. C., Latorraca, N. R., Pani, B., Venkatakrishnan, A. J., Masoudi, A., Weis, W. I., Dror, R. O., Chen, X., Lefkowitz, R. J., & Kobilka, B. K. (2017, Aug 24). Mechanism of intracellular allosteric beta2AR antagonist revealed by X-ray crystal structure. *Nature, 548*(7668), 480-484. https://doi.org/10.1038/nature23652

Liu, X., Kaindl, J., Korczynska, M., Stossel, A., Dengler, D., Stanek, M., Hubner, H., Clark, M. J., Mahoney, J., Matt, R. A., Xu, X., Hirata, K., Shoichet, B. K., Sunahara, R. K., Kobilka, B. K., & Gmeiner, P. (2020, Jul). An allosteric modulator binds to a conformational hub in the beta2 adrenergic receptor. *Nat Chem Biol, 16*(7), 749-755. https://doi.org/10.1038/s41589-020-0549-2

Liu, X., Xu, X., Hilger, D., Aschauer, P., Tiemann, J. K. S., Du, Y., Liu, H., Hirata, K., Sun, X., Guixa-Gonzalez, R., Mathiesen, J. M., Hildebrand, P. W., & Kobilka, B. K. (2019, May 16). Structural Insights into the Process of GPCR-G Protein Complex Formation. *Cell, 177*(5), 1243-1251 e1212. https://doi.org/10.1016/j.cell.2019.04.021

Louis, S. N., Nero, T. L., Iakovidis, D., Jackman, G. P., & Louis, W. J. (1999, Feb 19). LK 204-545, a highly selective beta1-adrenoceptor antagonist at human beta-

adrenoceptors. *Eur J Pharmacol, 367*(2-3), 431-435. https://doi.org/10.1016/s0014-2999(99)00019-9

Luo, J., Yang, L., Yang, J., Yang, D., Liu, B. C., Liu, D., Liang, B. M., & Liu, C. T. (2018, May). Efficacy and safety of phosphodiesterase 4 inhibitors in patients with asthma: A systematic review and meta-analysis. *Respirology, 23*(5), 467-477. https://doi.org/10.1111/resp.13276

Luttrell, L. M., Ferguson, S. S., Daaka, Y., Miller, W. E., Maudsley, S., Della Rocca, G. J., Lin, F., Kawakatsu, H., Owada, K., Luttrell, D. K., Caron, M. G., & Lefkowitz, R. J. (1999, Jan 29). Beta-arrestin-dependent formation of beta2 adrenergic receptor-Src protein kinase complexes. *Science, 283*(5402), 655-661. https://doi.org/10.1126/science.283.5402.655

Luttrell, L. M., Roudabush, F. L., Choy, E. W., Miller, W. E., Field, M. E., Pierce, K. L., & Lefkowitz, R. J. (2001, Feb 27). Activation and targeting of extracellular signal-regulated kinases by beta-arrestin scaffolds. *Proc Natl Acad Sci U S A, 98*(5), 2449-2454. https://doi.org/10.1073/pnas.041604898

Malik, R. U., Dysthe, M., Ritt, M., Sunahara, R. K., & Sivaramakrishnan, S. (2017, Aug 10). ER/K linked GPCR-G protein fusions systematically modulate second messenger response in cells. *Sci Rep, 7*(1), 7749. https://doi.org/10.1038/s41598-017-08029-3

Malik, R. U., Ritt, M., DeVree, B. T., Neubig, R. R., Sunahara, R. K., & Sivaramakrishnan, S. (2013, Jun 14). Detection of G protein-selective G protein-coupled receptor (GPCR) conformations in live cells. *J Biol Chem, 288*(24), 17167-17178. https://doi.org/10.1074/jbc.M113.464065

Manglik, A., Kim, T. H., Masureel, M., Altenbach, C., Yang, Z., Hilger, D., Lerch, M. T., Kobilka, T. S., Thian, F. S., Hubbell, W. L., Prosser, R. S., & Kobilka, B. K. (2015, May 21). Structural Insights into the Dynamic Process of beta2-Adrenergic Receptor Signaling. *Cell, 161*(5), 1101-1111. https://doi.org/10.1016/j.cell.2015.04.043

Mann, D. L., & Young, J. B. (1994, Mar). Basic mechanisms in congestive heart failure. Recognizing the role of proinflammatory cytokines. *Chest, 105*(3), 897-904. https://doi.org/10.1378/chest.105.3.897

Manning, D. R. (2002, Sep). Measures of efficacy using G proteins as endpoints: differential engagement of G proteins through single receptors. *Mol Pharmacol, 62*(3), 451-452. https://doi.org/10.1124/mol.62.3.451

Masureel, M., Zou, Y., Picard, L. P., van der Westhuizen, E., Mahoney, J. P., Rodrigues, J., Mildorf, T. J., Dror, R. O., Shaw, D. E., Bouvier, M., Pardon, E., Steyaert, J., Sunahara, R. K., Weis, W. I., Zhang, C., & Kobilka, B. K. (2018, Nov). Structural insights into binding specificity, efficacy and bias of a beta2AR partial agonist. *Nat Chem Biol, 14*(11), 1059-1066. https://doi.org/10.1038/s41589-018-0145-x

Matera, M. G., Ora, J., Cavalli, F., Rogliani, P., & Cazzola, M. (2021). New Avenues for Phosphodiesterase Inhibitors in Asthma. *J Exp Pharmacol, 13*, 291-302. https://doi.org/10.2147/JEP.S242961

McKee, E. E., Bentley, A. T., Smith, R. M., Jr., & Ciaccio, C. E. (1999, Apr 13). Origin of guanine nucleotides in isolated heart mitochondria. *Biochem Biophys Res Commun, 257*(2), 466-472. https://doi.org/10.1006/bbrc.1999.0489

Michel, M. C., Seifert, R., & Bond, R. A. (2014, Nov). Dynamic bias and its implications for GPCR drug discovery. *Nat Rev Drug Discov, 13*(11), 869. https://doi.org/10.1038/nrd3954-c3

Milano, C. A., Allen, L. F., Rockman, H. A., Dolber, P. C., McMinn, T. R., Chien, K. R., Johnson, T. D., Bond, R. A., & Lefkowitz, R. J. (1994, Apr 22). Enhanced myocardial function in transgenic mice overexpressing the beta 2-adrenergic receptor. *Science, 264*(5158), 582-586. https://doi.org/10.1126/science.8160017

Molinari, P., Ambrosio, C., Riitano, D., Sbraccia, M., Gro, M. C., & Costa, T. (2003, May 2). Promiscuous coupling at receptor-Galpha fusion proteins. The receptor of one covalent complex interacts with the alpha-subunit of another. *J Biol Chem, 278*(18), 15778-15788. https://doi.org/10.1074/jbc.M300731200

Morfis, M., Tilakaratne, N., Furness, S. G., Christopoulos, G., Werry, T. D., Christopoulos, A., & Sexton, P. M. (2008, Nov). Receptor activity-modifying proteins differentially modulate the G protein-coupling efficiency of amylin receptors. *Endocrinology, 149*(11), 5423-5431. https://doi.org/10.1210/en.2007-1735

Mosmann, T. R., & Coffman, R. L. (1989). TH1 and TH2 cells: different patterns of lymphokine secretion lead to different functional properties. *Annu Rev Immunol, 7*, 145-173. https://doi.org/10.1146/annurev.iy.07.040189.001045

Mougenot, N., Mika, D., Czibik, G., Marcos, E., Abid, S., Houssaini, A., Vallin, B., Guellich, A., Mehel, H., Sawaki, D., Vandecasteele, G., Fischmeister, R., Hajjar, R. J., Dubois-Rande, J. L., Limon, I., Adnot, S., Derumeaux, G., & Lipskaia, L. (2019, Oct 1). Cardiac adenylyl cyclase overexpression precipitates and

aggravates age-related myocardial dysfunction. *Cardiovasc Res, 115*(12), 1778-1790. https://doi.org/10.1093/cvr/cvy306

Murphy, D. M., & O'Byrne, P. M. (2010, Jun). Recent advances in the pathophysiology of asthma. *Chest, 137*(6), 1417-1426. https://doi.org/10.1378/chest.09-1895

Nabhan, J. F., Pan, H., & Lu, Q. (2010, Aug). Arrestin domain-containing protein 3 recruits the NEDD4 E3 ligase to mediate ubiquitination of the beta2-adrenergic receptor. *EMBO Rep, 11*(8), 605-611. https://doi.org/10.1038/embor.2010.80

Nelson, H. S., Weiss, S. T., Bleecker, E. R., Yancey, S. W., Dorinsky, P. M., & Group, S. S. (2006, Jan). The Salmeterol Multicenter Asthma Research Trial: a comparison of usual pharmacotherapy for asthma or usual pharmacotherapy plus salmeterol. *Chest, 129*(1), 15-26. https://doi.org/10.1378/chest.129.1.15

Neubig, R. R., Spedding, M., Kenakin, T., Christopoulos, A., International Union of Pharmacology Committee on Receptor, N., & Drug, C. (2003, Dec). International Union of Pharmacology Committee on Receptor Nomenclature and Drug Classification. XXXVIII. Update on terms and symbols in quantitative pharmacology. *Pharmacol Rev, 55*(4), 597-606. https://doi.org/10.1124/pr.55.4.4

Nguyen, A. H., & Lefkowitz, R. J. (2021, Apr). Signaling at the endosome: cryo-EM structure of a GPCR-G protein-beta-arrestin megacomplex. *FEBS J, 288*(8), 2562-2569. https://doi.org/10.1111/febs.15773

Nguyen, L. P., Al-Sawalha, N. A., Parra, S., Pokkunuri, I., Omoluabi, O., Okulate, A. A., Windham Li, E., Hazen, M., Gonzalez-Granado, J. M., Daly, C. J., McGrath, J. C., Tuvim, M. J., Knoll, B. J., Dickey, B. F., & Bond, R. A. (2017, Oct 24). beta2-Adrenoceptor signaling in airway epithelial cells promotes eosinophilic

inflammation, mucous metaplasia, and airway contractility. *Proc Natl Acad Sci U S A, 114*(43), E9163-E9171. https://doi.org/10.1073/pnas.1710196114

Nguyen, L. P., Lin, R., Parra, S., Omoluabi, O., Hanania, N. A., Tuvim, M. J., Knoll, B. J., Dickey, B. F., & Bond, R. A. (2009, Feb 17). Beta2-adrenoceptor signaling is required for the development of an asthma phenotype in a murine model. *Proc Natl Acad Sci U S A, 106*(7), 2435-2440. https://doi.org/10.1073/pnas.0810902106

Nguyen, L. P., Omoluabi, O., Parra, S., Frieske, J. M., Clement, C., Ammar-Aouchiche, Z., Ho, S. B., Ehre, C., Kesimer, M., Knoll, B. J., Tuvim, M. J., Dickey, B. F., & Bond, R. A. (2008, Mar). Chronic exposure to beta-blockers attenuates inflammation and mucin content in a murine asthma model. *Am J Respir Cell Mol Biol, 38*(3), 256-262. https://doi.org/10.1165/rcmb.2007-0279RC

Nobles, K. N., Xiao, K., Ahn, S., Shukla, A. K., Lam, C. M., Rajagopal, S., Strachan, R. T., Huang, T. Y., Bressler, E. A., Hara, M. R., Shenoy, S. K., Gygi, S. P., & Lefkowitz, R. J. (2011, Aug 9). Distinct phosphorylation sites on the beta(2)-adrenergic receptor establish a barcode that encodes differential functions of beta-arrestin. *Sci Signal, 4*(185), ra51. https://doi.org/10.1126/scisignal.2001707

Nuber, S., Zabel, U., Lorenz, K., Nuber, A., Milligan, G., Tobin, A. B., Lohse, M. J., & Hoffmann, C. (2016, Mar 31). beta-Arrestin biosensors reveal a rapid, receptor-dependent activation/deactivation cycle. *Nature, 531*(7596), 661-664. https://doi.org/10.1038/nature17198

Nygaard, R., Zou, Y., Dror, R. O., Mildorf, T. J., Arlow, D. H., Manglik, A., Pan, A. C., Liu, C. W., Fung, J. J., Bokoch, M. P., Thian, F. S., Kobilka, T. S., Shaw, D. E., Mueller, L., Prosser, R. S., & Kobilka, B. K. (2013, Jan 31). The dynamic process

of beta(2)-adrenergic receptor activation. *Cell, 152*(3), 532-542. https://doi.org/10.1016/j.cell.2013.01.008

Oakley, R. H., Laporte, S. A., Holt, J. A., Barak, L. S., & Caron, M. G. (2001, Jun 1). Molecular determinants underlying the formation of stable intracellular G protein-coupled receptor-beta-arrestin complexes after receptor endocytosis*. *J Biol Chem, 276*(22), 19452-19460. https://doi.org/10.1074/jbc.M101450200

Oakley, R. H., Laporte, S. A., Holt, J. A., Caron, M. G., & Barak, L. S. (2000, Jun 2). Differential affinities of visual arrestin, beta arrestin1, and beta arrestin2 for G protein-coupled receptors delineate two major classes of receptors. *J Biol Chem, 275*(22), 17201-17210. https://doi.org/10.1074/jbc.M910348199

Ostrom, R. S., Gregorian, C., Drenan, R. M., Xiang, Y., Regan, J. W., & Insel, P. A. (2001, Nov 9). Receptor number and caveolar co-localization determine receptor coupling efficiency to adenylyl cyclase. *J Biol Chem, 276*(45), 42063-42069. https://doi.org/10.1074/jbc.M105348200

Packer, M., Colucci, W. S., Sackner-Bernstein, J. D., Liang, C. S., Goldscher, D. A., Freeman, I., Kukin, M. L., Kinhal, V., Udelson, J. E., Klapholz, M., Gottlieb, S. S., Pearle, D., Cody, R. J., Gregory, J. J., Kantrowitz, N. E., LeJemtel, T. H., Young, S. T., Lukas, M. A., & Shusterman, N. H. (1996, Dec 1). Double-blind, placebo-controlled study of the effects of carvedilol in patients with moderate to severe heart failure. The PRECISE Trial. Prospective Randomized Evaluation of Carvedilol on Symptoms and Exercise. *Circulation, 94*(11), 2793-2799. https://doi.org/10.1161/01.cir.94.11.2793

Palczewski, K., Kumasaka, T., Hori, T., Behnke, C. A., Motoshima, H., Fox, B. A., Le Trong, I., Teller, D. C., Okada, T., Stenkamp, R. E., Yamamoto, M., & Miyano, M.

(2000, Aug 4). Crystal structure of rhodopsin: A G protein-coupled receptor. *Science, 289*(5480), 739-745. https://doi.org/10.1126/science.289.5480.739

Pascual, R. M., & Peters, S. P. (2005, Sep). Airway remodeling contributes to the progressive loss of lung function in asthma: an overview. *J Allergy Clin Immunol, 116*(3), 477-486; quiz 487. https://doi.org/10.1016/j.jaci.2005.07.011

Paton, W. D. M., & Rang, H. (1965). The uptake of atropine and related drugs by intestinal smooth muscle of the guinea-pig in relation to acetylcholine receptors. *Proceedings of the Royal Society of London. Series B. Biological sciences, 163*(990), 1-44.

Peitzman, E. R., Zaidman, N. A., Maniak, P. J., & O'Grady, S. M. (2015, Dec 15). Agonist binding to beta-adrenergic receptors on human airway epithelial cells inhibits migration and wound repair. *Am J Physiol Cell Physiol, 309*(12), C847-855. https://doi.org/10.1152/ajpcell.00159.2015

Peng, H., Bond, R. A., & Knoll, B. J. (2011, Feb). The effects of acute and chronic nadolol treatment on beta2AR signaling in HEK293 cells. *Naunyn Schmiedebergs Arch Pharmacol, 383*(2), 209-216. https://doi.org/10.1007/s00210-010-0591-9

Periole, X., Huber, T., Marrink, S. J., & Sakmar, T. P. (2007, Aug 22). G protein-coupled receptors self-assemble in dynamics simulations of model bilayers. *J Am Chem Soc, 129*(33), 10126-10132. https://doi.org/10.1021/ja0706246

Picard, L. P., Schonegge, A. M., & Bouvier, M. (2019, Jun 14). Structural Insight into G Protein-Coupled Receptor Signaling Efficacy and Bias between Gs and beta-

Arrestin. *ACS Pharmacol Transl Sci, 2*(3), 148-154. https://doi.org/10.1021/acsptsci.9b00012

Pierce, K. L., Luttrell, L. M., & Lefkowitz, R. J. (2001, Mar 26). New mechanisms in heptahelical receptor signaling to mitogen activated protein kinase cascades. *Oncogene, 20*(13), 1532-1539. https://doi.org/10.1038/sj.onc.1204184

Plazinska, A., Plazinski, W., Luchowski, R., Wnorowski, A., Grudzinski, W., & Gruszecki, W. I. (2017, Dec 20). Ligand-induced action of the W286(6.48) rotamer toggle switch in the beta2-adrenergic receptor. *Phys Chem Chem Phys, 20*(1), 581-594. https://doi.org/10.1039/c7cp04808d

Poole-Wilson, P. A., Swedberg, K., Cleland, J. G., Di Lenarda, A., Hanrath, P., Komajda, M., Lubsen, J., Lutiger, B., Metra, M., Remme, W. J., Torp-Pedersen, C., Scherhag, A., Skene, A., & Carvedilol Or Metoprolol European Trial, I. (2003, Jul 5). Comparison of carvedilol and metoprolol on clinical outcomes in patients with chronic heart failure in the Carvedilol Or Metoprolol European Trial (COMET): randomised controlled trial. *Lancet, 362*(9377), 7-13. https://doi.org/10.1016/S0140-6736(03)13800-7

Ragnarsson, L., Andersson, A., Thomas, W. G., & Lewis, R. J. (2019, Mar 12). Mutations in the NPxxY motif stabilize pharmacologically distinct conformational states of the alpha1B- and beta2-adrenoceptors. *Sci Signal, 12*(572). https://doi.org/10.1126/scisignal.aas9485

Ramahi, T. M., Longo, M. D., Cadariu, A. R., Rohlfs, K., Carolan, S. A., Engle, K. M., Samady, H., & Wackers, F. J. (2001, Mar 1). Left ventricular inotropic reserve and right ventricular function predict increase of left ventricular ejection fraction

after beta-blocker therapy in nonischemic cardiomyopathy. *J Am Coll Cardiol, 37*(3), 818-824. https://doi.org/10.1016/s0735-1097(00)01162-1

Rang, H. (1966). The kinetics of action of acetylcholine antagonists in smooth muscle. *Proceedings of the Royal Society of London. Series B. Biological sciences, 164*(996), 488-510.

Rasmussen, S. G., Choi, H. J., Fung, J. J., Pardon, E., Casarosa, P., Chae, P. S., Devree, B. T., Rosenbaum, D. M., Thian, F. S., Kobilka, T. S., Schnapp, A., Konetzki, I., Sunahara, R. K., Gellman, S. H., Pautsch, A., Steyaert, J., Weis, W. I., & Kobilka, B. K. (2011, Jan 13). Structure of a nanobody-stabilized active state of the beta(2) adrenoceptor. *Nature, 469*(7329), 175-180. https://doi.org/10.1038/nature09648

Rasmussen, S. G., Choi, H. J., Rosenbaum, D. M., Kobilka, T. S., Thian, F. S., Edwards, P. C., Burghammer, M., Ratnala, V. R., Sanishvili, R., Fischetti, R. F., Schertler, G. F., Weis, W. I., & Kobilka, B. K. (2007, Nov 15). Crystal structure of the human beta2 adrenergic G-protein-coupled receptor. *Nature, 450*(7168), 383-387. https://doi.org/10.1038/nature06325

Rasmussen, S. G., DeVree, B. T., Zou, Y., Kruse, A. C., Chung, K. Y., Kobilka, T. S., Thian, F. S., Chae, P. S., Pardon, E., Calinski, D., Mathiesen, J. M., Shah, S. T., Lyons, J. A., Caffrey, M., Gellman, S. H., Steyaert, J., Skiniotis, G., Weis, W. I., Sunahara, R. K., & Kobilka, B. K. (2011, Jul 19). Crystal structure of the beta2 adrenergic receptor-Gs protein complex. *Nature, 477*(7366), 549-555. https://doi.org/10.1038/nature10361

Rasmussen, S. G., Jensen, A. D., Liapakis, G., Ghanouni, P., Javitch, J. A., & Gether, U. (1999, Jul). Mutation of a highly conserved aspartic acid in the beta2

adrenergic receptor: constitutive activation, structural instability, and conformational rearrangement of transmembrane segment 6. *Mol Pharmacol, 56*(1), 175-184. https://doi.org/10.1124/mol.56.1.175

Revankar, C. M., Vines, C. M., Cimino, D. F., & Prossnitz, E. R. (2004, Jun 4). Arrestins block G protein-coupled receptor-mediated apoptosis. *J Biol Chem, 279*(23), 24578-24584. https://doi.org/10.1074/jbc.M402121200

Reyes-Alcaraz, A., Lee, Y. N., Yun, S., Hwang, J. I., & Seong, J. Y. (2018). Conformational signatures in beta-arrestin2 reveal natural biased agonism at a G-protein-coupled receptor. *Commun Biol, 1*, 128. https://doi.org/10.1038/s42003-018-0134-3

Ring, A. M., Manglik, A., Kruse, A. C., Enos, M. D., Weis, W. I., Garcia, K. C., & Kobilka, B. K. (2013, Oct 24). Adrenaline-activated structure of beta2-adrenoceptor stabilized by an engineered nanobody. *Nature, 502*(7472), 575-579. https://doi.org/10.1038/nature12572

Robichaux, W. G., 3rd, & Cheng, X. (2018, Apr 1). Intracellular cAMP Sensor EPAC: Physiology, Pathophysiology, and Therapeutics Development. *Physiol Rev, 98*(2), 919-1053. https://doi.org/10.1152/physrev.00025.2017

Rockman, H. A., Chien, K. R., Choi, D. J., Iaccarino, G., Hunter, J. J., Ross, J., Jr., Lefkowitz, R. J., & Koch, W. J. (1998, Jun 9). Expression of a beta-adrenergic receptor kinase 1 inhibitor prevents the development of myocardial failure in gene-targeted mice. *Proc Natl Acad Sci U S A, 95*(12), 7000-7005. https://doi.org/10.1073/pnas.95.12.7000

Rosenbaum, D. M., Cherezov, V., Hanson, M. A., Rasmussen, S. G., Thian, F. S., Kobilka, T. S., Choi, H. J., Yao, X. J., Weis, W. I., Stevens, R. C., & Kobilka, B. K. (2007, Nov 23). GPCR engineering yields high-resolution structural insights into beta2-adrenergic receptor function. *Science, 318*(5854), 1266-1273. https://doi.org/10.1126/science.1150609

Rosenbaum, D. M., Rasmussen, S. G., & Kobilka, B. K. (2009, May 21). The structure and function of G-protein-coupled receptors. *Nature, 459*(7245), 356-363. https://doi.org/10.1038/nature08144

Rosenbaum, D. M., Zhang, C., Lyons, J. A., Holl, R., Aragao, D., Arlow, D. H., Rasmussen, S. G., Choi, H. J., Devree, B. T., Sunahara, R. K., Chae, P. S., Gellman, S. H., Dror, R. O., Shaw, D. E., Weis, W. I., Caffrey, M., Gmeiner, P., & Kobilka, B. K. (2011, Jan 13). Structure and function of an irreversible agonist-beta(2) adrenoceptor complex. *Nature, 469*(7329), 236-240. https://doi.org/10.1038/nature09665

Rovati, G. E., Capra, V., Shaw, V. S., Malik, R. U., Sivaramakrishnan, S., & Neubig, R. R. (2017, Jul). The DRY motif and the four corners of the cubic ternary complex model. *Cell Signal, 35*, 16-23. https://doi.org/10.1016/j.cellsig.2017.03.020

Salpeter, S. R., Buckley, N. S., Ormiston, T. M., & Salpeter, E. E. (2006, Jun 20). Meta-analysis: effect of long-acting beta-agonists on severe asthma exacerbations and asthma-related deaths. *Ann Intern Med, 144*(12), 904-912. https://doi.org/10.7326/0003-4819-144-12-200606200-00126

Samama, P., Cotecchia, S., Costa, T., & Lefkowitz, R. J. (1993, Mar 5). A mutation-induced activated state of the beta 2-adrenergic receptor. Extending the ternary

complex model. *J Biol Chem, 268*(7), 4625-4636. https://www.ncbi.nlm.nih.gov/pubmed/8095262

Schild, H. O. (1949, Sep). pAx and competitive drug antagonism. *Br J Pharmacol Chemother, 4*(3), 277-280. https://doi.org/10.1111/j.1476-5381.1949.tb00548.x

Schonegge, A. M., Gallion, J., Picard, L. P., Wilkins, A. D., Le Gouill, C., Audet, M., Stallaert, W., Lohse, M. J., Kimmel, M., Lichtarge, O., & Bouvier, M. (2017, Dec 18). Evolutionary action and structural basis of the allosteric switch controlling beta2AR functional selectivity. *Nat Commun, 8*(1), 2169. https://doi.org/10.1038/s41467-017-02257-x

Seifert, R., Wenzel-Seifert, K., Gether, U., & Kobilka, B. K. (2001, Jun). Functional differences between full and partial agonists: evidence for ligand-specific receptor conformations. *J Pharmacol Exp Ther, 297*(3), 1218-1226. https://www.ncbi.nlm.nih.gov/pubmed/11356949

Seifert, R., Wenzel-Seifert, K., Gether, U., Lam, V. T., & Kobilka, B. K. (1999, Mar). Examining the efficiency of receptor/G-protein coupling with a cleavable beta2-adrenoceptor-gsalpha fusion protein. *Eur J Biochem, 260*(3), 661-666. https://doi.org/10.1046/j.1432-1327.1999.00161.x

Shenoy, S. K., Drake, M. T., Nelson, C. D., Houtz, D. A., Xiao, K., Madabushi, S., Reiter, E., Premont, R. T., Lichtarge, O., & Lefkowitz, R. J. (2006, Jan 13). beta-arrestin-dependent, G protein-independent ERK1/2 activation by the beta2 adrenergic receptor. *J Biol Chem, 281*(2), 1261-1273. https://doi.org/10.1074/jbc.M506576200

Shenoy, S. K., McDonald, P. H., Kohout, T. A., & Lefkowitz, R. J. (2001, Nov 9). Regulation of receptor fate by ubiquitination of activated beta 2-adrenergic receptor and beta-arrestin. *Science, 294*(5545), 1307-1313. https://doi.org/10.1126/science.1063866

Shenoy, S. K., Modi, A. S., Shukla, A. K., Xiao, K., Berthouze, M., Ahn, S., Wilkinson, K. D., Miller, W. E., & Lefkowitz, R. J. (2009, Apr 21). Beta-arrestin-dependent signaling and trafficking of 7-transmembrane receptors is reciprocally regulated by the deubiquitinase USP33 and the E3 ligase Mdm2. *Proc Natl Acad Sci U S A, 106*(16), 6650-6655. https://doi.org/10.1073/pnas.0901083106

Shenoy, S. K., Xiao, K., Venkataramanan, V., Snyder, P. M., Freedman, N. J., & Weissman, A. M. (2008, Aug 8). Nedd4 mediates agonist-dependent ubiquitination, lysosomal targeting, and degradation of the beta2-adrenergic receptor. *J Biol Chem, 283*(32), 22166-22176. https://doi.org/10.1074/jbc.M709668200

Shi, L., Liapakis, G., Xu, R., Guarnieri, F., Ballesteros, J. A., & Javitch, J. A. (2002, Oct 25). Beta2 adrenergic receptor activation. Modulation of the proline kink in transmembrane 6 by a rotamer toggle switch. *J Biol Chem, 277*(43), 40989-40996. https://doi.org/10.1074/jbc.M206801200

Short, P. M., Williamson, P. A., Anderson, W. J., & Lipworth, B. J. (2013, Jun 15). Randomized placebo-controlled trial to evaluate chronic dosing effects of propranolol in asthma. *Am J Respir Crit Care Med, 187*(12), 1308-1314. https://doi.org/10.1164/rccm.201212-2206OC

Shukla, A. K., Manglik, A., Kruse, A. C., Xiao, K., Reis, R. I., Tseng, W. C., Staus, D. P., Hilger, D., Uysal, S., Huang, L. Y., Paduch, M., Tripathi-Shukla, P., Koide, A.,

Koide, S., Weis, W. I., Kossiakoff, A. A., Kobilka, B. K., & Lefkowitz, R. J. (2013, May 2). Structure of active beta-arrestin-1 bound to a G-protein-coupled receptor phosphopeptide. *Nature, 497*(7447), 137-141. https://doi.org/10.1038/nature12120

Shukla, A. K., Violin, J. D., Whalen, E. J., Gesty-Palmer, D., Shenoy, S. K., & Lefkowitz, R. J. (2008, Jul 22). Distinct conformational changes in beta-arrestin report biased agonism at seven-transmembrane receptors. *Proc Natl Acad Sci U S A, 105*(29), 9988-9993. https://doi.org/10.1073/pnas.0804246105

Shukla, A. K., Westfield, G. H., Xiao, K., Reis, R. I., Huang, L. Y., Tripathi-Shukla, P., Qian, J., Li, S., Blanc, A., Oleskie, A. N., Dosey, A. M., Su, M., Liang, C. R., Gu, L. L., Shan, J. M., Chen, X., Hanna, R., Choi, M., Yao, X. J., Klink, B. U., Kahsai, A. W., Sidhu, S. S., Koide, S., Penczek, P. A., Kossiakoff, A. A., Woods, V. L., Jr., Kobilka, B. K., Skiniotis, G., & Lefkowitz, R. J. (2014, Aug 14). Visualization of arrestin recruitment by a G-protein-coupled receptor. *Nature, 512*(7513), 218-222. https://doi.org/10.1038/nature13430

Small, K. M., Forbes, S. L., Rahman, F. F., & Liggett, S. B. (2000, Mar 14). Fusion of beta 2-adrenergic receptor to G alpha s in mammalian cells: identification of a specific signal transduction species not characteristic of constitutive activation or precoupling. *Biochemistry, 39*(10), 2815-2821. https://doi.org/10.1021/bi992497z

Smith, J. S., Lefkowitz, R. J., & Rajagopal, S. (2018, Apr). Biased signalling: from simple switches to allosteric microprocessors. *Nat Rev Drug Discov, 17*(4), 243-260. https://doi.org/10.1038/nrd.2017.229

Song, X., Coffa, S., Fu, H., & Gurevich, V. V. (2009, Jan 2). How does arrestin assemble MAPKs into a signaling complex? *J Biol Chem, 284*(1), 685-695. https://doi.org/10.1074/jbc.M806124200

Sprang, S. R. (1997). G protein mechanisms: insights from structural analysis. *Annu Rev Biochem, 66*, 639-678. https://doi.org/10.1146/annurev.biochem.66.1.639

Stachowiak, J. C., Hayden, C. C., & Sasaki, D. Y. (2010, Apr 27). Steric confinement of proteins on lipid membranes can drive curvature and tubulation. *Proc Natl Acad Sci U S A, 107*(17), 7781-7786. https://doi.org/10.1073/pnas.0913306107

Stadel, J. M., DeLean, A., & Lefkowitz, R. J. (1980, Feb 25). A high affinity agonist . beta-adrenergic receptor complex is an intermediate for catecholamine stimulation of adenylate cyclase in turkey and frog erythrocyte membranes. *J Biol Chem, 255*(4), 1436-1441. https://www.ncbi.nlm.nih.gov/pubmed/6243637

Stephenson, R. P. (1956, Dec). A modification of receptor theory. *Br J Pharmacol Chemother, 11*(4), 379-393. https://doi.org/10.1111/j.1476-5381.1956.tb00006.x

Stewart, C. E., Torr, E. E., Mohd Jamili, N. H., Bosquillon, C., & Sayers, I. (2012). Evaluation of differentiated human bronchial epithelial cell culture systems for asthma research. *J Allergy (Cairo), 2012*, 943982. https://doi.org/10.1155/2012/943982

Strasser, R. H., Sibley, D. R., & Lefkowitz, R. J. (1986, Mar 25). A novel catecholamine-activated adenosine cyclic 3',5'-phosphate independent pathway for beta-adrenergic receptor phosphorylation in wild-type and mutant S49 lymphoma cells: mechanism of homologous desensitization of adenylate cyclase. *Biochemistry, 25*(6), 1371-1377. https://doi.org/10.1021/bi00354a027

Strebhardt, K., & Ullrich, A. (2008, Jun). Paul Ehrlich's magic bullet concept: 100 years of progress. *Nat Rev Cancer, 8*(6), 473-480. https://doi.org/10.1038/nrc2394

Strohman, M. J., Maeda, S., Hilger, D., Masureel, M., Du, Y., & Kobilka, B. K. (2019, May 20). Local membrane charge regulates beta2 adrenergic receptor coupling to Gi3. *Nat Commun, 10*(1), 2234. https://doi.org/10.1038/s41467-019-10108-0

Sutton, R. B., Vishnivetskiy, S. A., Robert, J., Hanson, S. M., Raman, D., Knox, B. E., Kono, M., Navarro, J., & Gurevich, V. V. (2005, Dec 16). Crystal structure of cone arrestin at 2.3A: evolution of receptor specificity. *J Mol Biol, 354*(5), 1069-1080. https://doi.org/10.1016/j.jmb.2005.10.023

Swaminath, G., Deupi, X., Lee, T. W., Zhu, W., Thian, F. S., Kobilka, T. S., & Kobilka, B. (2005, Jun 10). Probing the beta2 adrenoceptor binding site with catechol reveals differences in binding and activation by agonists and partial agonists. *J Biol Chem, 280*(23), 22165-22171. https://doi.org/10.1074/jbc.M502352200

Swedberg, K., Viquerat, C., Rouleau, J. L., Roizen, M., Atherton, B., Parmley, W. W., & Chatterjee, K. (1984, Oct 1). Comparison of myocardial catecholamine balance in chronic congestive heart failure and in angina pectoris without failure. *Am J Cardiol, 54*(7), 783-786. https://doi.org/10.1016/s0002-9149(84)80208-8

Tandale, A., Joshi, M., & Sengupta, D. (2016, Apr 14). Structural insights and functional implications of inter-individual variability in beta2-adrenergic receptor. *Sci Rep, 6*, 24379. https://doi.org/10.1038/srep24379

Tattersfield, A. E. (2006, Oct-Dec). Current issues with beta2-adrenoceptor agonists: historical background. *Clin Rev Allergy Immunol, 31*(2-3), 107-118. https://doi.org/10.1385/CRIAI:31:2:107

Teerlink, J. R., Pfeffer, J. M., & Pfeffer, M. A. (1994, Jul). Progressive ventricular remodeling in response to diffuse isoproterenol-induced myocardial necrosis in rats. *Circ Res, 75*(1), 105-113. https://doi.org/10.1161/01.res.75.1.105

Thanawala, V. J., Forkuo, G. S., Al-Sawalha, N., Azzegagh, Z., Nguyen, L. P., Eriksen, J. L., Tuvim, M. J., Lowder, T. W., Dickey, B. F., Knoll, B. J., Walker, J. K., & Bond, R. A. (2013, Feb). beta2-Adrenoceptor agonists are required for development of the asthma phenotype in a murine model. *Am J Respir Cell Mol Biol, 48*(2), 220-229. https://doi.org/10.1165/rcmb.2012-0364OC

Thanawala, V. J., Forkuo, G. S., Stallaert, W., Leff, P., Bouvier, M., & Bond, R. (2014, Jun). Ligand bias prevents class equality among beta-blockers. *Curr Opin Pharmacol, 16*, 50-57. https://doi.org/10.1016/j.coph.2014.03.002

Thanawala, V. J., Valdez, D. J., Joshi, R., Forkuo, G. S., Parra, S., Knoll, B. J., Bouvier, M., Leff, P., & Bond, R. A. (2015, Oct). beta-Blockers have differential effects on the murine asthma phenotype. *Br J Pharmacol, 172*(20), 4833-4846. https://doi.org/10.1111/bph.13253

Thomsen, A. R. B., Plouffe, B., Cahill, T. J., 3rd, Shukla, A. K., Tarrasch, J. T., Dosey, A. M., Kahsai, A. W., Strachan, R. T., Pani, B., Mahoney, J. P., Huang, L., Breton, B., Heydenreich, F. M., Sunahara, R. K., Skiniotis, G., Bouvier, M., & Lefkowitz, R. J. (2016, Aug 11). GPCR-G Protein-beta-Arrestin Super-Complex Mediates Sustained G Protein Signaling. *Cell, 166*(4), 907-919. https://doi.org/10.1016/j.cell.2016.07.004

Tovar, O. H., & Jones, J. L. (1997, May). Epinephrine facilitates cardiac fibrillation by shortening action potential refractoriness. *J Mol Cell Cardiol, 29*(5), 1447-1455. https://doi.org/10.1006/jmcc.1997.0387

Urban, J. D., Clarke, W. P., von Zastrow, M., Nichols, D. E., Kobilka, B., Weinstein, H., Javitch, J. A., Roth, B. L., Christopoulos, A., Sexton, P. M., Miller, K. J., Spedding, M., & Mailman, R. B. (2007, Jan). Functional selectivity and classical concepts of quantitative pharmacology. *J Pharmacol Exp Ther, 320*(1), 1-13. https://doi.org/10.1124/jpet.106.104463

Valentin-Hansen, L., Groenen, M., Nygaard, R., Frimurer, T. M., Holliday, N. D., & Schwartz, T. W. (2012, Sep 14). The arginine of the DRY motif in transmembrane segment III functions as a balancing micro-switch in the activation of the beta2-adrenergic receptor. *J Biol Chem, 287*(38), 31973-31982. https://doi.org/10.1074/jbc.M112.348565

van der Westhuizen, E. T., Breton, B., Christopoulos, A., & Bouvier, M. (2014, Mar). Quantification of ligand bias for clinically relevant beta2-adrenergic receptor ligands: implications for drug taxonomy. *Mol Pharmacol, 85*(3), 492-509. https://doi.org/10.1124/mol.113.088880

Venkatakrishnan, A. J., Deupi, X., Lebon, G., Heydenreich, F. M., Flock, T., Miljus, T., Balaji, S., Bouvier, M., Veprintsev, D. B., Tate, C. G., Schertler, G. F., & Babu, M. M. (2016, Aug 25). Diverse activation pathways in class A GPCRs converge near the G-protein-coupling region. *Nature, 536*(7617), 484-487. https://doi.org/10.1038/nature19107

Vieira Braga, F. A., Kar, G., Berg, M., Carpaij, O. A., Polanski, K., Simon, L. M., Brouwer, S., Gomes, T., Hesse, L., Jiang, J., Fasouli, E. S., Efremova, M., Vento-Tormo, R., Talavera-Lopez, C., Jonker, M. R., Affleck, K., Palit, S., Strzelecka, P. M., Firth, H. V., Mahbubani, K. T., Cvejic, A., Meyer, K. B., Saeb-Parsy, K., Luinge, M., Brandsma, C. A., Timens, W., Angelidis, I., Strunz, M., Koppelman, G. H., van Oosterhout, A. J., Schiller, H. B., Theis, F. J., van den Berge, M., Nawijn, M. C., & Teichmann, S. A. (2019, Jul). A cellular census of human lungs identifies novel cell states in health and in asthma. *Nat Med, 25*(7), 1153-1163. https://doi.org/10.1038/s41591-019-0468-5

Violin, J. D., Ren, X. R., & Lefkowitz, R. J. (2006, Jul 21). G-protein-coupled receptor kinase specificity for beta-arrestin recruitment to the beta2-adrenergic receptor revealed by fluorescence resonance energy transfer. *J Biol Chem, 281*(29), 20577-20588. https://doi.org/10.1074/jbc.M513605200

Virion, Z., Doly, S., Saha, K., Lambert, M., Guillonneau, F., Bied, C., Duke, R. M., Rudd, P. M., Robbe-Masselot, C., Nassif, X., Coureuil, M., & Marullo, S. (2019, Oct 18). Sialic acid mediated mechanical activation of beta2 adrenergic receptors by bacterial pili. *Nat Commun, 10*(1), 4752. https://doi.org/10.1038/s41467-019-12685-6

Vishnivetskiy, S. A., Hirsch, J. A., Velez, M. G., Gurevich, Y. V., & Gurevich, V. V. (2002, Nov 15). Transition of arrestin into the active receptor-binding state requires an extended interdomain hinge. *J Biol Chem, 277*(46), 43961-43967. https://doi.org/10.1074/jbc.M206951200

Waagstein, F. (1993). Beta blockers in heart failure. *Cardiology, 82 Suppl 3*, 13-18. https://doi.org/10.1159/000175929

Walker, J. K., Fong, A. M., Lawson, B. L., Savov, J. D., Patel, D. D., Schwartz, D. A., & Lefkowitz, R. J. (2003, Aug). Beta-arrestin-2 regulates the development of allergic asthma. *J Clin Invest, 112*(4), 566-574. https://doi.org/10.1172/JCI17265

Wang, H., Chen, Y., Zhu, H., Wang, S., Zhang, X., Xu, D., Cao, K., & Zou, J. (2012). Increased response to beta(2)-adrenoreceptor stimulation augments inhibition of IKr in heart failure ventricular myocytes. *PLoS One, 7*(9), e46186. https://doi.org/10.1371/journal.pone.0046186

Wang, Y., Yuan, J., Qian, Z., Zhang, X., Chen, Y., Hou, X., & Zou, J. (2015, Jan 8). beta2 adrenergic receptor activation governs cardiac repolarization and arrhythmogenesis in a guinea pig model of heart failure. *Sci Rep, 5*, 7681. https://doi.org/10.1038/srep07681

Watson, C., Chen, G., Irving, P., Way, J., Chen, W. J., & Kenakin, T. (2000, Dec). The use of stimulus-biased assay systems to detect agonist-specific receptor active states: implications for the trafficking of receptor stimulus by agonists. *Mol Pharmacol, 58*(6), 1230-1238. https://doi.org/10.1124/mol.58.6.1230

Wedegaertner, P. B., Chu, D. H., Wilson, P. T., Levis, M. J., & Bourne, H. R. (1993, Nov 25). Palmitoylation is required for signaling functions and membrane attachment of Gq alpha and Gs alpha. *J Biol Chem, 268*(33), 25001-25008. https://www.ncbi.nlm.nih.gov/pubmed/8227063

Weiss, J. M., Morgan, P. H., Lutz, M. W., & Kenakin, T. P. (1996, Aug 21). The cubic ternary complex receptor-occupancy model. III. resurrecting efficacy. *J Theor Biol, 181*(4), 381-397. https://doi.org/10.1006/jtbi.1996.0139

Weitnauer, M., Mijosek, V., & Dalpke, A. H. (2016, Mar). Control of local immunity by airway epithelial cells. *Mucosal Immunol, 9*(2), 287-298. https://doi.org/10.1038/mi.2015.126

Wenzel-Seifert, K., Lee, T. W., Seifert, R., & Kobilka, B. K. (1998, Sep 15). Restricting mobility of Gsalpha relative to the beta2-adrenoceptor enhances adenylate cyclase activity by reducing Gsalpha GTPase activity. *Biochem J, 334 (Pt 3)*, 519-524. https://doi.org/10.1042/bj3340519

West, G. M., Chien, E. Y., Katritch, V., Gatchalian, J., Chalmers, M. J., Stevens, R. C., & Griffin, P. R. (2011, Oct 12). Ligand-dependent perturbation of the conformational ensemble for the GPCR beta2 adrenergic receptor revealed by HDX. *Structure, 19*(10), 1424-1432. https://doi.org/10.1016/j.str.2011.08.001

Whistler, J. L., Chuang, H. H., Chu, P., Jan, L. Y., & von Zastrow, M. (1999, Aug). Functional dissociation of mu opioid receptor signaling and endocytosis: implications for the biology of opiate tolerance and addiction. *Neuron, 23*(4), 737-746. https://doi.org/10.1016/s0896-6273(01)80032-5

Whorton, M. R., Bokoch, M. P., Rasmussen, S. G., Huang, B., Zare, R. N., Kobilka, B., & Sunahara, R. K. (2007, May 1). A monomeric G protein-coupled receptor isolated in a high-density lipoprotein particle efficiently activates its G protein. *Proc Natl Acad Sci U S A, 104*(18), 7682-7687. https://doi.org/10.1073/pnas.0611448104

Willart, M. A., Deswarte, K., Pouliot, P., Braun, H., Beyaert, R., Lambrecht, B. N., & Hammad, H. (2012, Jul 30). Interleukin-1alpha controls allergic sensitization to inhaled house dust mite via the epithelial release of GM-CSF and IL-33. *J Exp Med, 209*(8), 1505-1517. https://doi.org/10.1084/jem.20112691

Williams, B. R., Barber, R., & Clark, R. B. (2000, Aug). Kinetic analysis of agonist-induced down-regulation of the beta(2)-adrenergic receptor in BEAS-2B cells reveals high- and low-affinity components. *Mol Pharmacol, 58*(2), 421-430. https://doi.org/10.1124/mol.58.2.421

Wisler, J. W., DeWire, S. M., Whalen, E. J., Violin, J. D., Drake, M. T., Ahn, S., Shenoy, S. K., & Lefkowitz, R. J. (2007, Oct 16). A unique mechanism of beta-blocker action: carvedilol stimulates beta-arrestin signaling. *Proc Natl Acad Sci U S A, 104*(42), 16657-16662. https://doi.org/10.1073/pnas.0707936104

Wootten, D., Christopoulos, A., Marti-Solano, M., Babu, M. M., & Sexton, P. M. (2018, Oct). Mechanisms of signalling and biased agonism in G protein-coupled receptors. *Nat Rev Mol Cell Biol, 19*(10), 638-653. https://doi.org/10.1038/s41580-018-0049-3

Wyatt, T. A., Poole, J. A., Nordgren, T. M., DeVasure, J. M., Heires, A. J., Bailey, K. L., & Romberger, D. J. (2014, Oct 15). cAMP-dependent protein kinase activation decreases cytokine release in bronchial epithelial cells. *Am J Physiol Lung Cell Mol Physiol, 307*(8), L643-651. https://doi.org/10.1152/ajplung.00373.2013

Yao, X. J., Velez Ruiz, G., Whorton, M. R., Rasmussen, S. G., DeVree, B. T., Deupi, X., Sunahara, R. K., & Kobilka, B. (2009, Jun 9). The effect of ligand efficacy on the formation and stability of a GPCR-G protein complex. *Proc Natl Acad Sci U S A, 106*(23), 9501-9506. https://doi.org/10.1073/pnas.0811437106

Zhang, M., Teng, H., Shi, J., & Zhang, Y. (2011, Sep-Dec). Disruption of beta-arrestins blocks glucocorticoid receptor and severely retards lung and liver development in mice. *Mech Dev, 128*(7-10), 368-375. https://doi.org/10.1016/j.mod.2011.07.003

Zheng, C., Tholen, J., & Gurevich, V. V. (2019). Critical role of the finger loop in arrestin binding to the receptors. *PLoS One, 14*(3), e0213792. https://doi.org/10.1371/journal.pone.0213792

Zou, Y., Akazawa, H., Qin, Y., Sano, M., Takano, H., Minamino, T., Makita, N., Iwanaga, K., Zhu, W., Kudoh, S., Toko, H., Tamura, K., Kihara, M., Nagai, T., Fukamizu, A., Umemura, S., Iiri, T., Fujita, T., & Komuro, I. (2004, Jun). Mechanical stress activates angiotensin II type 1 receptor without the involvement of angiotensin II. *Nat Cell Biol, 6*(6), 499-506. https://doi.org/10.1038/ncb1137

Zou, Y., Weis, W. I., & Kobilka, B. K. (2012). N-terminal T4 lysozyme fusion facilitates crystallization of a G protein coupled receptor. *PLoS One, 7*(10), e46039. https://doi.org/10.1371/journal.pone.0046039